UNIVERSITY OF CALIFORNIA, SAN DIEGO

Parkin Is Critical For Mitochondrial Clearance And Adaptation In Response To Myocardial Stress

A dissertation submitted in partial satisfaction of the requirements for the degree Doctor of Philosophy

in

Biomedical Science

by

Dieter Andre Kubli

Committee in charge:

Professor Åsa Gustafsson, Chair
Professor Laurence Brunton
Professor Albert La Spada
Professor Anne Murphy
Professor Deborah Yelon

2013

The Thesis of Dieter Andre Kubli is approved and it is acceptable in quality and form for publication on microfilm and electronically:

Chair

University of California, San Diego

2013

DEDICATION

To my mother, who gives everything she has for my sister and me.

To my father, who I hope is proud of who I have become.

And to my wife Corinne, who will always be a better rock climber than I am, for patiently listening to my scientific ranting and always belaying me through life's most challenging routes.

EPIGRAPH

Cmdr. William Riker: Someone once said, "Don't try to be a great man. Just be a man, and let history make its own judgments."

Dr. Zefram Cochrane: That's rhetorical nonsense. Who said that?

Cmdr. William Riker: [*smiles at Cochrane*] You did, ten years from now.

Star Trek: First Contact, 2063

TABLE OF CONTENTS

LIST OF ABBREVIATIONS

AAR – area at risk

AIF – apoptosis inducing factor

AKT – v-akt murine thymoma viral oncogene homolog

ANF – atrial natriuretic factor

ATG – autophagy-related protein

α-MHC – alpha myosin heavy chain

Bcl-2 – B-cell CLL/lymphoma 2

Bnip3 – BCL2/adenovirus E1B 19 kDa protein-interacting protein 3

Bnip3L/NIX – BCL2/adenovirus E1B 19 kDa protein-interacting protein 3-like

BPM – beats per minute

BW – body weight

β-MHC – beta myosin heavy chain

CD36 – Cluster of Differentiation 36

COX III – mitochondrial complex III

COX IV – mitochondrial complex IV

CVD – cardiovascular disease

DA – dopaminergic

Drp1 – Dynamin related protein 1

$\Delta\Psi$m – mitochondrial membrane potential

EF – ejection fraction

EGFR – epidermal growth factor receptor

Eps15 – epidermal growth factor receptor pathway substrate 15

ERK – extracellular signal-regulated kinase

ETC – electron transport chain

FCCP – Carbonyl cyanide-*4*-(trifluoromethoxy)phenylhydrazone

Fis1 – fission protein 1

FS – fractional shortening

GAPDH – glyceraldehyde-3-phosphate dehydrogenase

HKI – mitochondrial hexokinase I

HR – heart rate

HW – heart weight

IKKγ – inhibitor of nuclear factor kappa-B kinase subunit gamma

IPC – ischemic preconditioning

I/R – ischemia/reperfusion

IVSd – interventricular septal thickness at diastole

IVSs – interventricular septal thickness at systole

LAD – left anterior descending coronary artery

LC3 – microtubule-associated protein 1 light chain 3

LIR – LC3 interacting region

LV – left ventricle

LVEDD – left ventricular end diastolic dimension

LVESD – left ventricular end systolic dimension

LVPWd – left ventricular posterior wall thickness at diastole

LVPWs – left ventricular posterior wall thickness at systole

LW – lung weight

MAPK – mitogen-activated protein kinase

MARF – mitochondrial assembly regulatory factor

MDA – malondialdehyde

MEF – mouse embryonic fibroblast

Mfn – Mitofusin

MI – myocardial infarction

MPT – mitochondria permeability transition

MPTP – mitochondria permeability transition pore

NF-κB – nuclear factor kappa-light-chain-enhancer of activated B cells

OCR – oxygen consumption rate

OPA1 – optic atrophy 1

Parkin-/- – Parkin knockout

Parkin-TG – Parkin transgenic

PINK1 – PTEN-induced putative kinase 1

PGC-1α – peroxisome proliferator-activated receptor gamma coactivator 1-alpha

qPCR – quantitative PCR

RCR – respiratory control ratio

ROS – reactive oxygen species

SMA – skeletal muscle actin

TAC – transverse aortic constriction

TEM – transmission electron microscopy

TIM23 – translocase of inner mitochondrial membrane 23

TL – tibia length

TOM20 – translocase of outer mitochondrial membrane 20

TRAF2 – TNF receptor-associated factor 2

UBA – ubiquitin-associated domain

VDAC1 – voltage dependent anion channel 1

WT – wild type

LIST OF FIGURES

LIST OF TABLES

ACKNOWLEDGEMENTS

I would like to acknowledge Dr. Åsa Gustafsson for all her support as my mentor and as chair of my committee. She was kind enough to give me the opportunity to join her lab after my departure from a previous lab, and has pushed me to do my best work.

I would also like to acknowledge Dr. Laurence Brunton who encouraged me to pursue a better learning environment and who has always been supportive.

All current and past members of the Gustafsson lab deserve immense thanks and praise, especially Xiaoxue Zhang who taught me so much more than just microsurgical techniques. She showed us the real meaning of strength and courage. Melissa Quinsay-Cortez is the hardest working and most overqualified technician I have ever known, and she is an unstoppable force. Dr. Youngil Lee deserves all the credit for teaching me how to isolate cardiac myocytes and mitochondria. Everyone else, especially Robert Thomas, thanks for all the help, support, and laughs.

Parts of Chapter 1 and Chapter 7 were originally published in Circulation Research. Kubli, D. A., & Gustafsson, A. B. Mitochondria and Mitophagy: The Yin and Yang of Cell Death Control. *Circulation Research*, *111*(9), 1208–1221. doi:10.1161/CIRCRESAHA.112.265819 © 2012 Wolters Kluwer Health. The dissertation author was the primary investigator and author of this paper.

Parts of Chapter 3, Chapter 4, and Chapter 5 were originally published in the *Journal of Biological Chemistry*. Kubli, D.A., Zhang, X., Lee, Y., Hanna, R.A.,

Quinsay, M.N., Nguyen, C.K., Jimenez, R., Petrosyan, S., Murphy, A.N., Gustafsson, A.B. Parkin Protein Deficiency Exacerbates Cardiac Injury and Reduces Survival following Myocardial Infarction. *The Journal of Biological Chemistry*. 2013; *288*(2), 915–926. © 2013 The American Society for Biochemistry and Molecular Biology. The dissertation author was the primary investigator and author of this paper.

Part of Chapter 3 was also originally published in *Communicative and Integrative Biology*. Kubli, D.A., Quinsay, M.N., & Gustafsson, A.B. Parkin Deficiency Results in Accumulation of Abnormal Mitochondria in Aging Myocytes. *Communicative & Integrative Biology*. 2013; *6*(4), e24511. doi:10.4161/cib.24511. © 2013 Landes Bioscience. The dissertation author was the primary investigator and author of this paper.

VITA

2006	Bachelor of Science, University of California, San Diego
2007	Master of Science, University of California, San Diego
2013	Doctor of Philosophy, University of California, San Diego

FIRST AUTHOR PUBLICATIONS

Kubli, D.A., Ycaza, J.E., and Gustafsson, A.B. Bnip3 Mediates Mitochondrial Dysfunction and Cell Death Through Bax and Bak. Biochem. J. *405*, 407–415, 2007

Kubli, D.A., Quinsay, M.N., Huang, C., Lee, Y., and Gustafsson, A.B. Bnip3 Functions as a Mitochondrial Sensor of Oxidative Stress During Myocardial Ischemia and Reperfusion. Am J Physiol Heart Circ Physiol *295*, H2025–H2031, 2008

Kubli, D.A., and Gustafsson, A.B. Mitochondria and Mitophagy: The Yin and Yang of Cell Death Control. Circulation Research *111*, 1208–1221, 2012

Kubli, D.A., Zhang, X., Lee, Y., Hanna, R.A., Quinsay, M.N., Nguyen, C.K., Jimenez, R., Petrosyan, S., Murphy, A.N., and Gustafsson, A.B. Parkin Protein Deficiency Exacerbates Cardiac Injury and Reduces Survival Following Myocardial Infarction. J Biol Chem *288*, 915–926, 2013

Kubli, D.A., Quinsay, M.N., and Gustafsson, A.B. Parkin Deficiency Results in Accumulation of Abnormal Mitochondria in Aging Myocytes. Commun Integr Biol *6*, e24511, 2013

Kubli, D.A. and Gustafsson, A.B. Cardiomyocyte Health: Adapting to Metabolic Changes Through Autophagy. Trends in Endocrinology & Metabolism, in press 2013

FIELDS OF STUDY

Field: Molecular and Cellular Cardiology

M.S. Thesis: *Bnip3 Functions as a Mitochondrial Sensor of Oxidative Stress in Myocardial Ischemia/Reperfusion*

Dr. Roberta Gottlieb and Dr. Åsa Gustafsson

Field: Diabetic Neuropathy

Dr. Nigel Calcutt

ABSTRACT OF THE DISSERTATION

Parkin Is Critical For Mitochondrial Clearance

And Adaptation In Response To Myocardial Stress

by

Dieter Andre Kubli

Doctor of Philosophy in Biomedical Science

University of California, San Diego, 2013

Professor Åsa Gustafsson, Chair

The lysosomal degradation of misfolded proteins and dysfunctional organelles by the process of autophagy is critical for the maintenance of heart function. Parkin is an E3 ubiquitin ligase that participates in the removal of dysfunctional mitochondria via mitochondrial autophagy (mitophagy). Mutations in the *PARK2* gene encoding Parkin are linked to juvenile recessive forms of

Parkinson's disease. As a result, Parkin has mainly been studied in the context of neurodegenerative disease. However, Parkin is highly expressed in the heart, an organ that is rich in mitochondria and therefore susceptible to cell death caused by mitochondrial dysfunction. The functional role of Parkin in the heart remains largely unexplored. While characterizing the cardiac phenotype of Parkin knockout (Parkin-/-) mice, I found that Parkin was not essential for the normal turnover of mitochondria in the heart. Instead, I determined that Parkin was a critical component in the response to acute cardiac stress such as a myocardial infarction (MI). I found that Parkin supported the adaption to MI stress by enabling mitophagy in the infarction border zone for the clearance of dysfunctional mitochondria. Further, I determined that the mechanism of Parkin function in the heart was dependent on the activity of the mitochondrial fission protein Drp1, but did not depend on the mitochondrial kinase PINK1. Lastly, I investigated the role of Parkin in response to chronic pathophysiological stresses that cause cardiac hypertrophy. Parkin-/- mice had impairments in both physiological hypertrophy in response to exercise and pathological hypertrophy in response to transverse aortic constriction. In contrast, cardiac-specific Parkin transgenic mice (Parkin-TG) had a normal hypertrophic response to pressure overload, but rapidly developed heart failure. Thus, I conclude that Parkin is crucial for the development of cardiac hypertrophy in response to chronic stress in addition to its role in adaptation to acute stress. Parkin may be a viable therapeutic target to promote autophagic clearance of dysfunctional

mitochondria, but excessive Parkin may be detrimental and can result in a predisposition to heart failure in response to chronic stress.

CHAPTER 1: INTRODUCTION

1.1 The Current State of Heart Disease

Cardiovascular disease (CVD) is the number one cause of death in the United States, with almost 600,000 deaths per year (Hoyert and Xu, 2012). Although advances in treatment options have lowered the death rate for CVD by more than 30% over the last decade, it still accounts for one third of the deaths in the U.S. (Go et al., 2013). Thus, there is a continuing need for new options to treat the hundreds of thousands of patients hospitalized each year with new coronary attacks. A high incidence of obesity caused by poor diet and sedentary lifestyle is largely responsible for the increasing number of affected individuals. While the gold standard of preventive treatment has always been improvements to diet and exercise, advances in therapies to reduce cholesterol and blood pressure have contributed immensely to improved outcomes.

Statins and antihypertensive treatments can help control the risk of experiencing an adverse cardiac event such as a myocardial infarction (MI) (Ray and Cannon, 2005), but treatment options to restore cardiac function after an MI are limited. Balloon angioplasty and stent technology restore blood flow to ischemic regions, but until regenerative medicine is clinically available, the functional cardiac tissue that can be lost during an MI cannot currently be replaced. Tissue damage occurs both during ischemia and reperfusion (Gottlieb et al., 1994; Reimer and Jennings, 1979). Restoration of blood flow is critical, yet

the influx of oxygen causes widespread generation of reactive oxygen species (ROS) and mitochondrial damage (Becker, 2004; Braunwald and Kloner, 1985). With its high density of mitochondria, the heart is particularly susceptible to mitochondria-induced cell damage or death. Therapies that focus on restoring or maintaining mitochondrial integrity after a cardiac event are therefore highly desirable but currently unavailable.

1.2 Mitochondria in the Heart

The heart relies on its high mitochondrial density to supply the ATP necessary for continuous contraction over the course of one's life. Mitochondria generate ATP via oxidative phosphorylation, a process that involves the generation of a proton gradient by the electron transport chain (ETC) comprised of multi-protein respiration complexes. As electrons are delivered down the chain, the proton gradient that is generated in the mitochondrial intermembrane space is then used to power the ATP synthase protein complex. Although low levels of ROS generation are normal (Liu et al., 2002; St-Pierre et al., 2002), mitochondria that are not functioning properly can generate amounts of ROS that are beyond the cell's innate antioxidant capacity. Excessive ROS generation can cause further damage and promote cell death through the release of cell death-initiating factors (Simon et al., 2000).

Damaged mitochondria can initiate cell death pathways of apoptosis and necrosis in response to many different stress signals, including loss of growth factors, hypoxia, oxidative stress, and DNA damage. The switch to a cell death

program is mediated by permeabilization of the outer mitochondrial membrane via the pro-apoptotic proteins Bax and Bak, or by opening of the mitochondrial permeability transition pore (MPTP) in the inner mitochondrial membrane. The MPTP is an inner membrane channel that allows for passage of molecules up to 1.5 kDa (Zoratti and Szabò, 1995). Opening of the pore causes a collapse of the proton gradient and electrical potential across the inner mitochondrial membrane, leading to disruption of oxidative phosphorylation (i.e. ATP synthesis). Opening of the MPTP also causes influx of water and subsequent swelling of the inner membrane. The outer mitochondrial membrane is unable to expand, resulting in rupture and release of pro-apoptotic proteins into the cytosol, culminating in necrotic cell death. The MPTP is known to be a major contributor to myocardial ischemia/reperfusion (I/R) injury. Inhibitors of the MPTP protect against cell death and reduce infarct size in *ex vivo* I/R (Clarke et al., 2002; Griffiths and Halestrap, 1993).

Alternatively, permeabilization of the outer membrane by Bax and Bak results in the release of proapoptotic proteins such as cytochrome *c*, Smac/Diablo, and apoptosis-inducing factor (AIF) to activate apoptosis (Gustafsson and Gottlieb, 2003). Upon activation, Bax and Bak form pores in the outer mitochondrial membrane large enough to allow passage of proteins from the intermembrane space to the cytosol (Kuwana et al., 2002). Moreover, Bax is activated in myocytes in response to oxidative stress (Gustafsson et al., 2004) and during ischemia (Capano and Crompton, 2006). Hearts from Bax-deficient mice have reduced mitochondrial damage and decreased infarct size after I/R

compared to wild type mice, implicating Bax as a major player in mitochondrial dysfunction in I/R (Hochhauser et al., 2003). Interestingly, several of the mitochondrial proteins that are essential for mitochondrial respiration, such as cytochrome *c* and AIF, function to promote cell death once released into the cytosol. Both necrotic and apoptotic forms of cell death are therefore highly regulated and activated by mitochondria, and have been implicated in loss of myocardial cells in pathologies such as I/R, cardiomyopathy, and congestive heart failure. Damaged mitochondria must therefore be removed before they can cause myocyte damage or death.

1.3 The Importance of Autophagy in the Heart

Autophagy is an evolutionarily conserved process that is responsible for the degradation of long-lived proteins in the cytoplasm via the lysosomal pathway (Mizushima et al., 2008). Autophagy also plays an important role in intracellular quality control by removing protein aggregates and damaged organelles that can cause harm to the cell (Mizushima et al., 2008). Upon initiation of autophagy, a double-membrane autophagosome forms in the cytosol and engulfs the material to be degraded. Nucleation of the initial phagophore membrane requires assembly of a complex consisting of BECLIN1, vacuolar protein sorting 34 (VPS34), and VPS15 (Kang et al., 2011). Subsequent expansion of the membrane is mediated by two ubiquitin-like conjugation systems, LC3 and ATG12-ATG5, that promote assembly of the ATG16L complex and the conjugation of LC3 with phosphatidylethanolamine (Kabeya et al., 2004;

Mizushima et al., 1999). The phagophore expands until its edges fuse around its target(s), forming a double-membrane structure called the autophagosome. Next, the autophagosome fuses with a lysosome and the contents are degraded by lysosomal enzymes (Huynh et al., 2007).

Autophagy was initially believed to be a non-selective process whereby autophagosomes randomly engulf cytosolic material. However, it is now clear that autophagy specifically targets invading bacteria (Knodler and Celli, 2011), protein aggregates (Tannous et al., 2008), and organelles such as mitochondria (Quinsay et al., 2010b) and the endoplasmic reticulum (Hanna et al., 2012). Thus, autophagy constitutes a very important quality control mechanism in cells, particularly in post-mitotic cells such as cardiac myocytes. Autophagy is also very important in the normal turnover of mitochondria in the myocardium. Disruption of autophagy by conditional deletion of *Atg5* in the adult heart leads to rapid accumulation of dysfunctional mitochondria and development of cardiac dysfunction (Nakai et al., 2007). Maintaining a basal level of autophagy is therefore crucial to overall heart health.

Autophagy in the heart is rapidly upregulated in response to stress conditions, and it is thought that this upregulation is generally a cardioprotective mechanism. During a myocardial infarction, for instance, upregulation of autophagy is important for minimizing myocardial damage, and inhibition of autophagy significantly increases the size of the infarction (Kanamori et al., 2011). Similarly, enhancing autophagy in cardiac myocytes protects against cell death from simulated I/R (Hamacher-Brady et al., 2006). Further, autophagy is

an important component of ischemic preconditioning (IPC), a cardioprotective phenomenon in which brief periods of ischemia prior to a prolonged ischemic period yields less extensive tissue damage compared to prolonged ischemia alone (Huang et al., 2010a; Yitzhaki et al., 2009). However, overactivation of autophagy can be detrimental and can lead to cardiac atrophy (Schips et al., 2011). It is therefore crucial to maintain tight control over autophagy regulation and a high degree of specificity in targeting organelles for degradation by autophagy.

1.4 Mechanisms of Selective Mitophagy

Damage to mitochondria often results in activation of both mitophagy and mitochondrial apoptosis/permeabilization in the same cell. In an effort to prevent cell death, damaged mitochondria are sequestered by autophagosomes and degraded before apoptosis or necrosis can be triggered. Mitophagy allows for the selective removal of only dysfunctional mitochondria by autophagosomes, and mechanisms are in place to ensure a high degree of specificity in targeting only dysfunctional mitochondria.

1.4.1 Adaptor Proteins Mediate Mitophagy

One mechanism of mitochondrial clearance involves autophagy adaptor proteins and ubiquitin, in which specific proteins are ubiquitinated on dysfunctional mitochondria. Ubiquitination serves as a signal for mitophagy (Kirkin et al., 2009; Pankiv et al., 2007). The identification of the autophagy

adaptor protein p62/SQSTM1 (hereafter referred to as p62) has provided important insights into this process (Pankiv et al., 2007). The p62 protein binds to ubiquitinated proteins via its ubiquitin-associated (UBA) domain (Seibenhener et al., 2004), and to LC3 on the phagophore membrane via its LC3 Interacting Region (LIR) (Pankiv et al., 2007). Thus, the recruitment and binding of p62 to ubiquitinated mitochondrial proteins docks the mitochondrion to the LC3-positive phagophore for engulfment. Knockdown of p62 substantially inhibits mitophagy in HeLa and HEK293 cells (Ding et al., 2010; Geisler et al., 2010), although others have found that depletion of p62 by RNAi has little effect on mitophagy in HeLa cells (Narendra et al., 2010b). Additionally, although p62 can be recruited to mitochondria by a mitochondrion-anchored ubiquitin fusion protein, this recruitment does not induce mitophagy (Narendra et al., 2010b). Taken together, these studies suggest that p62 recruitment to mitochondria alone is not sufficient for mitophagy to ensue. Other proteins have been proposed as putative mitophagy scaffolding molecules. NBR1 (neighbor of BRCA1 gene) also contains both LIR and UBA motifs, and has been identified to act as an autophagy adaptor protein (Kirkin et al., 2009). However, it is currently unknown if NBR1 plays a role in mitophagy. Thus, more studies are needed to discern the molecular mechanisms required for highly specific mitophagy.

1.4.2 Selective Mitophagy via Parkin and PINK1

Parkin is an E3 ubiquitin ligase that is predominantly cytosolic under basal conditions. Upon loss of mitochondrial membrane potential ($\Delta\Psi m$), Parkin rapidly

translocates to mitochondria (Narendra et al., 2008; Suen et al., 2010), where it then promotes ubiquitination of mitochondrial proteins to serve as a signal for mitophagy (Geisler et al., 2010). Parkin was initially identified because loss of function mutations in its gene (*PARK2*) were common in autosomal recessive juvenile forms of Parkinsonism (Kitada et al., 1998; Periquet et al., 2003). As such, the majority of studies on mammalian Parkin have been limited to investigating its role in the brain and in neuronal cell cultures (Goldberg et al., 2003; Narendra et al., 2008). However, Parkin also highly expressed in the heart (Kitada et al., 1998), yet its functional importance in the myocardium remains largely unexplored.

A limited number of Parkin ubiquitination substrates on mitochondria have thus far been identified. To date, only five Parkin substrates have been identified on mitochondria: VDAC1 (Geisler et al., 2010), Mitofusin (Mfn)1 and Mfn2 (Gegg et al., 2010), Miro (Wang et al., 2011b), and mitochondrial hexokinase I (HKI) (Okatsu et al., 2012). The physiological relevance of Parkin-mediated ubiquitination and degradation of HKI has yet to be determined. VDAC1 is unnecessary for mitophagy, as Parkin-dependent mitophagy still occurs in VDAC1 and VDAC3-deficient mouse embryonic fibroblasts (MEFs) treated with the mitochondrial uncoupler FCCP (Narendra et al., 2010b). Ubiquitination of Miro to halt trafficking of mitochondria may be an important prerequisite for mitophagy (Wang et al., 2011b), but this has yet to be confirmed.

Mounting evidence suggests that Parkin-mediated ubiquitination of the Mfn proteins is particularly important for mitophagy. Mfn1 and Mfn2 participate in

the fusion of mitochondria, which can have the effect of dispersing dysfunctional respiratory chain components from dysfunctional mitochondria, in essence diluting the compromised components. Ubiquitination of Mfn1/2 by Parkin leads to their rapid proteasomal degradation and inhibition of mitochondrial fusion, thereby preventing dysfunctional mitochondria from refusing with the rest of the mitochondrial network and priming them for mitophagy (Tanaka et al., 2010). Additionally, a recent study by Chen and Dorn implicates Mfn2 as a mitochondrial receptor for Parkin (Chen and Dorn, 2013). The authors confirmed that Parkin binds to Mfn2, and that Mfn2 is necessary for Parkin translocation to uncoupled mitochondria. Mfn2-deficient mouse cardiomyocytes have decreased mitochondrial ubiquitination and impaired mitophagy after treatment with FCCP compared to wild-type cells (Chen and Dorn, 2013). These results demonstrate the importance of Mfn2 in Parkin-dependent mitophagy. The authors also examined the function of *Drosophila* heart tubes in flies lacking Parkin and found contractile dysfunction and impairments in cardiomyocyte mitochondrial respiration (Chen and Dorn, 2013). However, mammalian models of Parkin deficiency were not examined, and heart function in Parkin-/- mouse models needs further exploration.

The serine/threonine kinase PTEN-induced putative kinase 1 (PINK1) plays a central role in communicating the collapse of the $\Delta\Psi m$ to Parkin. PINK1 is a mitochondrial protein that is normally found at very low levels at mitochondria due to its constitutive degradation in the presence of an intact $\Delta\Psi m$ (Matsuda et al., 2010; Narendra et al., 2010a). PINK1 is rapidly imported into mitochondria

and cleaved by mitochondrial proteases before being exported to the cytosol and degraded by the proteasome (Greene et al., 2012; Jin et al., 2010; Narendra et al., 2010a). Upon collapse of the $\Delta\Psi m$, the import and degradation of PINK1 is blocked, and PINK1 accumulates on the outer mitochondrial membrane. It has been suggested that expression of PINK1 is necessary for the recruitment of Parkin to depolarized mitochondria (Matsuda et al., 2010; Narendra et al., 2010a). However, exactly how accumulation of PINK1 on the outer mitochondrial membrane results in recruitment and activation of Parkin is currently unclear. Based on experimental findings, three different models have been proposed. First, it has been suggested that PINK1 directly interacts with Parkin, thereby anchoring it to the mitochondria (Sha et al., 2010; Xiong et al., 2009). Another model suggests that PINK1 directly phosphorylates Parkin, resulting in its activation (Kim et al., 2008; Sha et al., 2010). Alternatively, PINK1 may phosphorylate Parkin substrates on the mitochondria, thereby increasing their affinity for Parkin (Chen and Dorn, 2013). For instance, Mfn2 must be phosphorylated by PINK1 prior to Parkin translocation and Mfn-2 ubiquitination (Chen and Dorn, 2013). In contrast, other studies in *Drosophila* and SH-SY5Y neuroblastoma cells have found that Parkin does not require PINK1 for its function (Clark et al., 2006; Dagda et al., 2009; Park et al., 2006). Additional studies are therefore needed to elucidate the relationship between PINK1 and Parkin in mitophagy, particularly in mammalian cell systems.

PINK1 and Parkin are both found in the heart (Billia et al., 2011; Kitada et al., 1998), and recent studies have provided some insights into their functional

role in the myocardium. Billia et al. reported that PINK1 protein levels are markedly reduced in end-stage human heart failure, and that PINK1-deficient mitochondria have reduced oxidative capacity, which correlates with the development of cardiac dysfunction and hypertrophy by two months of age (Billia et al., 2011). Moreover, Parkin has been found to play an important role in clearing mitochondria in ischemic preconditioning (IPC), and mice deficient in Parkin are resistant to IPC and develop tissue damage to the same extent as control mice without IPC (Huang et al., 2011). Prior results from my lab also show that mitophagy stimulated by the pro-autophagic Bcl-2 family protein Bnip3 is associated with translocation of Parkin to mitochondria in mouse cardiac myocytes (Lee et al., 2011). A more thorough investigation into the functional role of Parkin in the heart would contribute substantially to the understanding of its relevance in normal mitochondrial turnover and to the development of novel therapeutics aimed at minimizing cardiac tissue damage after an ischemic event through the modulation of mitophagy.

1.5 Mitochondrial Dynamics Impact Mitophagy

Several different GTPases regulate mitochondrial fission and fusion. As previously mentioned, Mfn1 and Mfn2 regulate fusion of the outer mitochondrial membrane, whereas optic atrophy protein 1 (OPA1) promotes fusion of the inner membrane (Chen et al., 2003; Cipolat et al., 2004). By contrast, mitochondrial fission is regulated by dynamin-related protein 1 (Drp1) and fission protein 1 (FIS1) (Smirnova et al., 2001; Yoon et al., 2003). All of these proteins are highly

expressed in the heart (Delettre et al., 2000; Ong et al., 2010; Papanicolaou et al., 2011; Parra et al., 2008). Deletion of the *Drp1* gene is embryonic lethal, and cardiac myocytes from *Drp1*-null embryos have reduced contractility (Wakabayashi et al., 2009). Defects in Drp1 function are also associated with early infant mortality and cardiomyopathy (Ashrafian et al., 2010; Waterham et al., 2007). Likewise, knockdown of the fusion proteins mitochondrial assembly regulatory factor (MARF) or OPA1 leads to the development of cardiomyopathy in *Drosophila* (Dorn et al., 2011). These studies demonstrate that functional mitochondrial dynamics are important for normal heart and mitochondrial function.

Mitochondrial dynamics are closely integrated with mitophagy. Mitophagy is consistently attenuated in cells with reduced mitochondrial fission, suggesting that fission is a prerequisite for mitophagy to occur (Lee et al., 2011; Twig et al., 2008). For instance, Drp1-deficient MEFs have significantly reduced Parkin-mediated mitophagy compared with wild-type MEFs (Tanaka et al., 2010). Further, my lab has also found that Drp1-mediated fission is a prerequisite for mitophagy in cardiac myocytes (Lee et al., 2011). However, why mitochondrial fission must occur prior to mitophagy currently remains unclear. One possibility could be that fission produces smaller mitochondrial fragments that are more readily engulfed by autophagosomes. Mitochondria usually have an elongated shape and can be up to 5 μm long (Cereghetti and Scorrano, 2006), whereas autophagosomes are spherical in shape with a diameter of about 1 μm (Komatsu

and Ichimura, 2010). Thus, breaking up larger mitochondria into smaller fragments may be a requirement for mitophagy.

Recent studies have connected the PINK1/Parkin mitophagy pathway with mitochondrial dynamics. I previously discussed how Mfn1 and Mfn2 are substrates for Parkin (Gegg et al., 2010; Tanaka et al., 2010). Mfn1 and Mfn2 ubiquitination also leads to their proteasomal degradation prior to mitophagy (Gegg et al., 2010; Tanaka et al., 2010), which may serve to switch the balance of mitochondrial dynamics towards fission to facilitate mitochondrial fragmentation and autophagocytosis. The loss of Mfn proteins may prevent damaged mitochondria from fusing with healthy mitochondria in the cell. Additionally, mitochondrial size plays a role in regulating mitophagy. Nutrient deprivation induces formation of hyperfused mitochondrial networks that protect mitochondria from elimination by autophagosomes (Gomes et al., 2011; Rambold et al., 2011). Lastly, fission can segregate dysfunctional components of mitochondria for removal by mitophagy by yielding two fragments with different $\Delta\Psi m$ (Twig et al., 2008) to be targeted by PINK1 and Parkin. Mitochondrial fragments with low $\Delta\Psi m$ are targeted for mitophagy, whereas fragments with high $\Delta\Psi m$ have a higher probability of fusing with the mitochondrial network. However, the relationship between mitochondrial dynamics and Parkin/PINK1 function is not yet fully elucidated. Additional studies are necessary to examine the interplay between mitochondrial fission/fusion and Parkin-mediated mitophagy in the heart.

1.6 Rationale and Specific Aims of the Thesis

Parkin is widely expressed in many tissues, and its important role in mitophagy has been well documented in neuronal cells and in neurodegenerative disease. Parkin is found at particularly high levels in the myocardium, a tissue with a high density of mitochondria that is also subject to severe mitochondrial stress after a myocardial infarction. It is likely that Parkin plays a crucial role in the maintenance of mitochondrial integrity in the heart, yet its functional role in this tissue remains largely unstudied. I hypothesize that Parkin plays a critical role in clearing dysfunctional mitochondria via mitophagy in response to cardiac stress. To investigate this hypothesis, I propose the following specific aims.

Aim 1: Characterize the effects of Parkin deficiency on heart function. *Hypothesis: Since Parkin is important for mitochondrial turnover by mitophagy, Parkin-deficient mice will be more susceptible to stress such as myocardial infarction (MI).*

Aim 2: Investigate the role of Parkin in mitophagy in cardiomyocytes. *Hypothesis: Parkin is important for clearing dysfunctional mitochondria via autophagy.*

Parts of Chapter 1 were originally published in Circulation Research. Kubli, D. A., & Gustafsson, A. B. Mitochondria and Mitophagy: The Yin and Yang of Cell Death Control. *Circulation Research*, *111*(9), 1208–1221.

doi:10.1161/CIRCRESAHA.112.265819 The dissertation author was the primary investigator and author of this paper.

CHAPTER 2: EXPERIMENTAL METHODS AND MATERIALS

Animals

All animal protocols were in accordance with institutional guidelines and approved by the Institutional Animal Care and Use Committee of the University of California San Diego. Adult cardiac myocytes were isolated from 250-300 g male Sprague Dawley rats (Harlan) as previously described (Kubli et al., 2008). *Park2* and *Pink1* knockout mice were obtained from Jackson Laboratories (B6.129S4-*Park2*^{tm1Shn}/J, stock number 006582; B6;129-*Pink1*^{tmAub}/J, stock number 013050) and have been described previously (Gispert et al., 2009; Goldberg et al., 2003).

Myocardial Infarction

Mice were subjected to myocardial infarction by permanently ligating the left anterior descending (LAD) coronary artery as described previously (Huang et al., 2010b). Briefly, 12-week-old WT and Parkin-/- mice were anesthetized with isoflurane, intubated, and ventilated. Pressure-controlled ventilation (Harvard Apparatus) was maintained at 9 cm H_2O. An 8-0 silk suture was placed around the LAD coronary artery and then tightened. The suture was left in place, and the incision was immediately closed.

Transverse Aortic Constriction

Transverse aortic constriction was performed on mice anesthetized with isoflurane. Mice were intubated and ventilated, and the aortic arch accessed by

partial upper sternotomy. A 7-0 silk suture was tied around a 27G blunt-tipped needle and the aortic arch between the left carotid and brachiocephalic arteries. The needle was then removed, leaving a constriction in the aorta. The ribs were then sutured together with 3-0 silk suture and the chest was massaged to reduce the chance of pneumothorax before closure of the incision site.

Histology and Measurement of Ventricular Remodeling

Mice were anesthetized with 100 mg/kg sodium pentobarbital and hearts were perfused with 200 mmol/L KCl to induce diastolic arrest prior to harvesting. Hearts were fixed in 10% formalin for 20-24 hours and then transferred to 70% ethanol for an additional 20 hours before embedding in paraffin. The percent of the total left ventricle that had undergone remodeling was calculated according to Takagawa et al. (Takagawa et al., 2007). 10 μm-thick heart cross-sections were cut at 300 μm intervals through the left ventricle and stained with Masson's Trichrome (Sigma-Aldrich). Percent remodeling was determined by dividing the total midline length of all fibrotic remodeled regions by the total midline length of all left ventricle sections. The remodeled region was defined as the region in which ≥50% of the total wall thickness had increased collagen deposition. Measurements were performed using ImageJ software.

Determination of Myocyte Area

Hearts were paraffin embedded as described above, and 10 μm-thick heart cross-sections were cut from a central region of the heart. Sections were

stained with Alexa Fluor 488-conjugated wheat germ agglutinin (Life Technologies) to label plasma membranes and counterstained with Hoechst 33342 (Life Technologies) to label nuclei. Measurements of myocyte area were performed using Photoshop CS5 software. Only myocytes with roughly circular profiles and large, centrally-located nuclei were quantified.

Determination of Area At Risk

Area at risk (AAR) was determined 24 hours after MI. Mice were anesthetized by intraperitoneal injection of 100 mg/kg sodium pentobarbital. Hearts were excised and perfused with 1% Evans blue in PBS to delineate the non-perfused area before freezing at -20˚C. Hearts were then cut into 1 mm-thick sections and fixed in 10% formalin for 2 hours before imaging. Adobe Photoshop CS5 software was used to quantitate the relative areas of blue and white regions. AAR was defined as the percent of the left ventricle that was not stained blue.

Echocardiography

Echocardiography was performed using a Vevo 770 equipped with an RMV707B 15 – 45-MHz imaging transducer (VisualSonics). Prior to the procedure, thoracic hair was removed with a depilatory cream. Mice were maintained under light inhalable anesthesia (2% isoflurane for induction, 0.5 – 1% isoflurane for maintenance, 98 – 99.5% oxygen) through a nose cone and secured in a supine position to a circulating water warming pad maintained at 42˚C. Conductivity gel that had been prewarmed to 40˚C was applied to the

thorax of the mouse. Recordings of the parasternal long-axis (B-mode), parasternal short axis (M-mode), apical 4-chamber (pulsed wave Doppler), and aortic arch (pulsed wave Doppler) views were taken. All measurements were collected using VisualSonics software. Only data with heart rates > 450bpm were accepted.

Mouse Swimming Studies

Mice were swum in a heated tank (34˚C). For acute swimming studies, mice received 2 days of swim training comprised of twice-daily 10 min sessions, followed by one 90 min session. Tissue was harvested immediately after the final swim. For chronic swimming studies, mice received 8 days of training comprised of twice-daily sessions increasing in duration by 10 minutes each day. Thus, on day one, mice swam twice for 10 minutes, and on day two they swam twice for 20 minutes, etc. The experimental sessions began on day 9, at which time mice began swimming twice per day for 90 minutes, for 14 additional days. Echocardiography was performed within 24 hours of the final swim. Tissue was collected as described above.

FCCP Perfusion of Mouse Hearts

Mice were anesthetized with 100 mg/kg sodium pentobarbital via intraperitoneal injection. Hearts were rapidly excised, cannulated via the aorta, and perfused with Krebs Henseleit (KH) buffer for 5 minutes for stabilization. DMSO or FCCP was then added to the KH buffer to a final concentration of 100

nM. Control hearts were then perfused for 15 min with DMSO, and experimental hearts were perfused with FCCP for 5 or 15 min. Immediately after each perfusion, hearts were removed from the cannula, and mitochondria were isolated for Western blotting as per the Swelling Assay procedure described below.

Mitochondrial Respiration Measurements

The procedure used for mitochondrial isolation has been described previously (Sayen et al., 2003). Hearts were removed while still contracting from mice anesthetized with ketamine/xylazine (50 mg/kg and 10 mg/kg, respectively) via intraperitoneal injection. Individual mouse hearts were rapidly minced in ice-cold isolation buffer (100 mmol/L KCl, 50 mmol/L MOPS pH 7.4, 1 mmol/L EGTA, 5 mmol/L MgSO4, 1 mmol/L ATP, 0.2% essentially fatty acid free BSA). Henceforth, all steps were performed at 0˚C on wet ice. Tissue was homogenized in isolation buffer with a Polytron tissue grinder at 11,000 RPM for 2.5 s, followed by 3 strokes at 500 RPM with a Potter-Elvehjem PTFE tissue grinder. The homogenate was centrifuged at 600×g twice for 5 min and the supernatant was saved. Mitochondria were pelleted from the supernatant by centrifugation at 3,000×g twice, and the pellet was rinsed with isolation buffer. The final mitochondrial pellet was resuspended in 100 µl of resuspension buffer (220 mmol/L mannitol, 70 mmol/L sucrose, 2 mmol/L Tris base, and 20 mmol/L HEPES pH 7.4). Protein concentration was determined by Bradford assay using BSA standards. Oxygen consumption measurements were performed with an

Oxygraph Clark type electrode (Hansatech Instruments) in respiration buffer (10 mmol/L MgCl2, 100 mmol/L KCl, 50 mmol/L MOPS pH 7.0, 1 mmol/L EGTA, 5 mmol/L KH_2PO_4, 0.2% essentially fatty acid free BSA). 200 µg of mitochondria were added to a final volume of 1 ml respiration buffer at 30˚C. Complex I activity was measured using 2 mmol/L pyruvate and 2 mmol/L malate as substrates. Complex II activity was measured using 5 µmol/L rotenone with 5 mmol/L succinate as substrate.

For measurements of mitochondrial respiration in intact adult mouse cardiomyocytes, cells were isolated as described in the Isolation of Cardiomyocytes section below. Aliquots of cells were centrifuged at 240×g at room temperature for 1 min. The pellet was resuspended in either 250 or 500 ml of plating medium (containing 5.56 mmol/L glucose) supplemented with 10 mmol/L pyruvate, and cells were transferred directly into the 37°C Oxytherm apparatus (Hansatech Instruments) for oxygen consumption measurements. The chamber was calibrated with air-equilibrated water to 228 µmol/L O2 and $Na_2S_2O_5$-saturated water to zero. Baseline respiration was evaluated before any additions. Sequential additions of 10ug/ml oligomycin followed by titration with either 200 or 400 nmol/L FCCP were made to inhibit ATP-synthase and to measure maximal rates of uncoupled mitochondria, respectively.

Mitochondrial Swelling Assay

Mitochondria were isolated using a procedure previously established in our laboratory (Gustafsson et al., 2004; Quinsay et al., 2010a). Mice were

anesthetized with 100 mg/kg sodium pentobarbital via intraperitoneal injection. Hearts were rapidly excised, minced, and homogenized with a Polytron tissue grinder in ice-cold homogenization buffer (10 mmol/L MOPS pH 7.4, 250 mmol/L sucrose, 5 mmol/L KH_2PO_4, 2 mmol/L $MgCl_2$, 1 mmol/L EGTA, 0.1% BSA). Lysates were centrifuged for 5 min at 600×g, and the supernatants were centrifuged for 10 min at 3,000×g to pellet mitochondria. The mitochondrial pellets were resuspended in swelling buffer (10 mmol/L MOPS pH 7.4, 250 mmol/L sucrose, 5 mmol/L KH_2PO_4, 2 mmol/L $MgCl_2$, 5 μmol/L EGTA, 5 mmol/L pyruvate, and 5 mmol/L malate). Sixty micrograms of mitochondria in a volume of 200 μl was added per well in a 96-well plate. Ca^{2+} was rapidly added to a final concentration of 250 μmol/L. Mitochondrial swelling was monitored by measuring absorbance on a plate reader at 520 nm for 60 min. The amplitude of each curve was obtained by subtracting the endpoint absorbance from the maximal absorbance obtained from the swelling assay. Maximum rate of change in amplitude (V_{max}) was obtained by calculating the slope of the linear segment of the swelling curve.

Subcellular Fractionation of Border Zone Samples

At the indicated study endpoints, mice were anesthetized with 100 mg/kg sodium pentobarbital via intraperitoneal injection, and the chest cavity was opened. The infarct border zone was visualized under a dissecting microscope and dissected out from the contracting heart. The border zone was immediately placed into a cryovial, snap-frozen in liquid nitrogen, and stored at -80˚C. For

subcellular fractionation, 350-500 µl of ice-cold homogenization buffer (10 mmol/L MOPS pH 7.4, 250 mmol/L sucrose, 5 mmol/L KH_2PO_4, 2 mmol/L $MgCl_2$, 1 mmol/L EGTA, 0.1% BSA) was added to the cryovial, and the border zone was resuspended and transferred to a Potter-Elvehjem PTFE homogenizer. Sample material and tools were kept at 0˚C on wet ice throughout the procedure. Tissue was homogenized at 2000 RPM with 10 strokes of the pestle before centrifuging twice at 600×g for 5 min. After each spin, the supernatant was saved. Mitochondria were then pelleted out of the supernatant by centrifugation at 3000×g for 10 min. The supernatant was saved as the cytosolic fraction. Mitochondria were washed twice by gently resuspending in 1 ml homogenization buffer followed by centrifugation at 3000×g for 10 min. The final mitochondrial pellet was resuspended in 25 µl of homogenization buffer, and the protein concentration was determined by Bradford assay using BSA standards before proceeding with SDS-PAGE and immunoblotting.

Western Blotting Analysis

Lysates were prepared as previously described (Lee et al., 2011) in buffer containing 50 mmol/L Tris-HCl (pH 7.4), 150 mmol/L NaCl, 1 mmol/L EGTA, 1 mmol/L EDTA, 1% Triton X-100, and cOmplete protease inhibitor cocktail (Roche Applied Bioscience). Tissue was homogenized with a Polytron tissue grinder at 20,000 RPM, then cleared by centrifugation at 20,000×g for 20 min. Protein concentration was determined by Bradford assay using BSA standards. Proteins were separated by SDS-PAGE, transferred to nitrocellulose, and immunoblotted

with antibodies against Parkin (Cell Signaling, 1:1000), LC3 (Cell Signaling, 1:1000), GAPDH (Cell Signaling, 1:1000), PINK1 (Cayman Chemical, 1:500), ubiquitin (Santa Cruz, 1:200), TOM20 (Santa Cruz, 1:1000), TIM23 (BD Biosciences, 1:1000), Mfn1 (Santa Cruz, 1:200), Mfn2 (Sigma-Aldrich, 1:1000), Opa1 (BD Biosciences, 1:1000), Drp1 (BD Biosciences, BD Biosciences, 1:1000), or Fis1 (Enzo Life Sciences, 1:500), OxPhos Complex III Core 2 (Invitrogen, 1:1000), OxPhos Complex IV subunit 4 (Invitrogen, 1:1000), or p62 (American Research Products, 1:1000). Quantitation was performed using BioRad Quantity One software.

Oxidation Assessments

Protein carbonyls were detected with the Oxyblot Protein Oxidation Detection Kit (Millipore). Malondialdehyde content was determined using the OxiSelect TBARS Assay Kit (Cell Biolabs, Inc). Lysates for oxidation assessments were prepared in lysis buffer in the absence of Triton X-100 as described above.

Transmission Electron Microscopy and Morphometric Analysis

Adult mouse hearts were fixed in 2.5% glutaraldehyde in 0.1 mmol/L cacodylate buffer, post-fixed in 1% osmium tetroxide, and then treated with 0.5% tannic acid, 1% sodium sulfate, cleared in 2-hydroxypropyl methacrylate and embedded in LX112 (Ladd Research, Williston, VT). Sections were mounted on copper slot grids coated with parlodion and stained with uranyl acetate and lead

citrate for examination on a Philips CM100 electron microscope (FEI, Hillsbrough OR). Mitochondrial morphometric measurements were performed using Adobe Photoshop CS5 software. A total of 298 mitochondria from WT mice and 272 mitochondria from Parkin-/- mice were analyzed from 5 electron micrographs taken at 7900X magnification.

Isolation of Cardiomyocytes

Adult rat cardiomyocytes were isolated as previously described (Kubli et al., 2008). Rats were anesthetized with 100 mg/kg sodium pentobarbital via intraperitoneal injection. Hearts were quickly excised, cannulated via the aorta, and perfused with heart medium [Joklik Minimal Essential Medium (Sigma) supplemented with 10 mmol/L HEPES pH 7.4 at 37˚C, 30 mmol/L taurine, 2 mmol/L carnitine, and 2 mmol/L creatine] for 5 min. Hearts were then digested by perfusion with 0.1% Collagenase II (Worthington Biochemicals) plus 0.1% BSA and 25 μmol/L $CaCl_2$ in heart medium. The ventricles were then minced, and myocytes were dissociated by pipetting. Cells were filtered through a 100 μm nylon cell strainer into an equal volume of stop buffer (heart medium supplemented with 5% newborn calf serum) and allowed to sediment for 10 minutes. The supernatant was removed, and cells were washed by resuspending in stop buffer, followed by 10 minutes of sedimentation. Calcium was slowly reintroduced to isolated cells to a final concentration of 1 mmol/L. Cells were then collected by centrifugation at 100×g for 1 minute, and finally resuspended in plating medium [Medium 199 (Invitrogen) supplemented with 10 mmol/L HEPES

pH 7.4 at 37˚C, 5 mmol/L taurine, 5 mmol/L creatine, 2 mmol/L carnitine, 0.2% essentially fatty acid free BSA, 100 U/ml penicillin] for plating on laminin-coated dishes.

Adult mouse cardiomyocytes were isolated as described previously (Carreira et al., 2010; Hilal-Dandan et al., 2000). Mice were anesthetized with 50 mg/kg sodium pentobarbital via intraperitoneal injection and also injected with heparin (350 U/kg, i.p.). Hearts were rapidly excised and placed in ice-cold perfusion solution (113 mmol/L NaCl, 4.7 mmol/L KCl, 0.6 mmol/L KH_2PO_4, 0.6 mmol/L Na_2HPO_4, 1.2 mmol/L $MgSO_4 \cdot 7H_2O$, 0.032 phenol red, 12 mmol/L $NaHCO_3$, 10 mmol/L $KHCO_3$, 10 mmol/L HEPES pH 7.4 at 37˚C, 30 mmol/L taurine, 5.5 mmol/L glucose, 10 mmol/L 2,3-butanedione monoxime). The aorta was quickly cannulated and the heart was perfused retrogradely with perfusion solution followed by digestion buffer [perfusion buffer supplemented with 0.25 mg/mL Liberase Blendzyme 1 (Roche Applied Science), 0.14 mg/mL Trypsin (Invitrogen), and 12.5 μmol/L $CaCl_2$]. After tissue digestion, the ventricles were minced in digestion buffer and then filtered through a 100 μm nylon cell strainer. Stop solution 1 (perfusion buffer supplemented with 10% bovine calf serum and 12.5 μmol/L $CaCl_2$) was added to the cardiomyocytes, and cells were pelleted by gravity for 10 minutes. The resulting cell pellet was resuspended in stop solution 2 (perfusion buffer supplemented with 5% bovine calf serum and 12.5 μmol/L $CaCl_2$), and calcium was gradually reintroduced up to a concentration of 1 mmol/L. The cells were centrifuged at 100×g for 1 min before resuspending in plating medium [Hank’s Minimum Essential Medium (Invitrogen), 5% bovine calf

serum, 10 mmol/L 2,3-butanedione monoxime, 100 U/mL penicillin, and 2 mmol/L L-glutamine].

Hypoxia and Cell Death Assay

After isolation, adult rat or mouse cardiomyocytes were allowed to plate on laminin-coated dishes for 2 hours before infection with adenoviruses encoding mCherry, mCherry-Parkin, mCherry-Parkin-R42P, and mCherry-Parkin-G430D at a multiplicity of infection (MOI) of 25 (for mouse) or 50 (for rat), or β-Gal and Drp1K38E at an MOI of 150 in plating medium plus 2% heat-inactivated serum. Eighteen hours later, myocytes were subjected to hypoxia by incubation in DMEM without glucose (Invitrogen) in hypoxic pouches (GasPak EZ, BD Biosciences) for 4 – 8 hours at 37°C. Cell death was assessed by measuring increased plasma membrane permeability to YoPro-1 (Invitrogen) as previously described (Hamacher-Brady et al., 2007). Cells were examined by fluorescence microscopy using a Carl Zeiss AxioObserver Z1 at 10X magnification.

Preparation of Parkin Mutants and Adenoviral Constructs

mCherry-Parkin was obtained from Dr. Richard Youle (National Institute of Neurological Disorders and Stroke, National Institutes of Health, Bethesda, MD) (Narendra et al., 2008). mCherry-ParkinR42P and mCherry-ParkinG430D were generated by site-directed mutagenesis as previously described (Kubli et al., 2008) using mCherry-Parkin as a template. Parkin adenoviruses were generated

using the pENTR Directional TOPO cloning kit (Invitrogen) followed by recombination into the pAd/CMV/V5-DEST Gateway vector (Invitrogen).

Fluorescence Microscopy

For visualizing Parkin translocation to mitochondria, adult rat cardiomyocytes infected with mCherry-Parkin were fixed with 4% paraformaldehyde (Ted Pella Inc., 18505) in PBS pH 7.4, permeabilized with 0.2% Triton X-100 in PBS, and blocked in 5% normal goat serum before incubation with anti-COXIV antibody (Invitrogen, 1:100). Cells were then rinsed and incubated with goat anti-mouse AlexaFluor-488 secondary antibody (Invitrogen). For induction of autophagy by nutrient deprivation, isolated cardiac myocytes from Parkin-/- mice were infected with Ad-LC3-GFP for 24 hours before incubation in plating medium (nonstarved) or starvation media (20 mmol/L HEPES pH 7.4 at 37˚C, 110 mmol/L NaCl, 4.7 mmol/L KCl, 1.2 mmol/L KH2PO4, 1.25 mmol/L MgSO4, 1.2 mmol/L CaCl2, 25 mmol/L NaHCO3) at 37°C in an atmosphere of 2% CO_2 as previously described (Quinsay et al., 2010b). After 4 hrs, cells were stained for COXIV and analyzed by fluorescence microscopy for the presence of autophagosomes. Fluorescence micrographs were captured using a Carl Zeiss AxioObserver Z1 fitted with a motorized Z-stage and an Apotome for optical sectioning. Z-stacks were acquired in ApoTome mode using a high-resolution AxioCam MRm digital camera, a 63X Plan-Apochromat Oil-immersion) objective and Zeiss AxioVision 4.8 software (Carl Zeiss) (Quinsay et al., 2010b). Pseudo-linescans were performed using ImageJ software.

Quantitative PCR

Centrally-located 10 mg slices of heart tissue were collected into RNAlater solution (Ambion). Total RNA was extracted RNeasy Fibrous Tissue Mini Kit (Qiagen) according to the manufacturer's instructions. First strand cDNA synthesis from total RNA was performed using High Capacity RNA-to-cDNA Master Mix (Applied Biosystems). TaqMan primers and probes for real-time PCR were designed by Applied Biosystems. Real-time PCR was performed using a BIO-RAD CFX96 Real Time System on a C1000 thermal cycler, and relative quantification of RNA amount was accomplished by using the comparative *Ct* method ($2^{-\Delta\Delta Ct}$). Relative amounts of mRNA for genes of interest were normalized to housekeeping gene GAPDH and expressed relative to the calibrator.

Statistical Analyses

All values are expressed as mean ± standard error of mean (SEM). Statistical analyses were performed using Student's t-test or ANOVA followed by Tukey's or Student-Newman-Keul's Multiple Comparison test. Survival was assessed using the Kaplan-Meier method and logrank test. $p<0.05$ was considered significant.

CHAPTER 3: THE BASELINE CARDIAC PHENOTYPE OF PARKIN-/- AND PARKIN-TG MICE

3.1 Abstract

Parkin plays an important role in the removal of dysfunctional mitochondria via autophagy. Although Parkin is expressed in the heart, its functional role in this tissue is largely unexplored. Here, I investigated the functional role of Parkin in the myocardium under normal physiological conditions. Parkin deficient (Parkin-/-) mice showed normal cardiac function for up to 12 months of age as determined by echocardiographic analysis. Although ultrastructural analysis revealed that Parkin-/- hearts had disorganized mitochondrial networks and significantly smaller mitochondria, mitochondrial function was normal. Parkin-/- mice also showed no signs of oxidative stress, as both malondialdehyde (MDA) content and protein carbonylation were unchanged compared to wild type (WT) mice. In contrast, cardiac-specific overexpression of Parkin in Parkin transgenic (Parkin-TG) mice resulted in a modest but significant impairment on baseline cardiac function and morphology. These results suggest that Parkin is not critical to the maintenance of cardiac mitochondria under baseline conditions, suggesting that the role of Parkin in normal cell function is nonessential. In contrast, overexpression of Parkin is sufficient to cause cardiac functional deficits, indicating that excessive levels of Parkin are detrimental to myocyte health.

3.2 Introduction

Autophagy plays an important role in intracellular quality control by removing protein aggregates and damaged organelles that can cause harm to the cell (Okamoto et al., 2009). Recent studies have demonstrated that organelles can be specifically targeted for removal by autophagy under certain conditions (Kim et al., 2007; Twig et al., 2008). Autophagy is very important in the normal turnover of mitochondria in the myocardium. The PTEN-induced putative kinase 1 (PINK1) and Parkin pathway has been reported to regulate mitochondrial autophagy (mitophagy) in cells (Narendra et al., 2008; 2010a). The E3 ubiquitin ligase Parkin translocates to damaged mitochondria, where it ubiquitinates proteins to serve as a signal for autophagic degradation of the mitochondrion (Narendra et al., 2010b; Pankiv et al., 2007; Tanaka et al., 2010).

Parkin has been extensively studied with regards to its role in mitophagy in neurons. Loss of function mutations in the gene encoding Parkin were initially identified to be involved in the development of Parkinson's disease (PD) (Kitada et al., 1998), and to date, the majority of studies on Parkin have been limited to investigating its role in the brain (Goldberg et al., 2003; Narendra et al., 2008). Although Parkin is highly expressed in the heart (Kitada et al., 1998), its functional importance in this tissue is essentially unexplored. In the present study, I investigated the functional role of Parkin in the myocardium. I report that Parkin deficiency had no effect on mitochondria or cardiac function in mice under normal conditions, suggesting that Parkin is not required for the baseline turnover of mitochondria. However, cardiac-specific overexpression of Parkin led to

deficits in cardiac function in mice by 3 months of age. Excessive Parkin was therefore disadvantageous to the heart under baseline conditions.

3.3 Results

3.3.1 Parkin Deficient Mice Have Normal Cardiac Function

First, I examined the expression of Parkin in different mouse tissues by Western blotting. I found that Parkin was highly expressed in several tissues, including the heart (Figure 3.1A). To investigate the functional importance of Parkin in the heart, I characterized the cardiac phenotype in mice deficient for Parkin (Parkin-/-) (Figure 3.1B). Although Parkin-/- mice were smaller than WT mice as previously reported (Goldberg et al., 2003), there were no significant differences in heart weight/body weight or lung weight/body weight ratios between WT and Parkin-/- mice (Figures 3.2A-3.2D). To assess the effect of Parkin deficiency on cardiac function, I analyzed mice by echocardiography. I found that at 12 weeks of age, WT and Parkin-/- mice had similar fractional shortening (%FS), ejection fractions (%EF), and left ventricular internal end-diastolic and systolic dimensions (Table 1). To investigate if Parkin deficiency would affect cardiac function in aging mice, I also evaluated cardiac function and structure in 6- and 12-month old mice. However, I observed no significant differences in cardiac function or in diastolic or systolic dimensions between aged WT and Parkin-/- mice (Table 1).

3.3.2 Parkin Transgenic Mice Have Impaired Cardiac Function

Parkin transgenic mice that overexpress the Parkin gene under the control of the α-myosin heavy chain (α-MHC) promoter and therefore specifically in cardiac tissue were developed to study the effects of Parkin at above-normal levels. Parkin transgenic (Parkin-TG) mice expressed Parkin in the heart at approximately 50-fold higher levels than control WT littermates (Figure 3.3). Mean heart weights of Parkin-TG mice were not different from WT mouse heart weights (Figure 3.4). Likewise, Parkin-TG mice had the same average body weight as WT mice, and heart weight/body weight and lung weight/body weight ratios were unchanged (Figure 3.4). To determine if overexpression of Parkin affects cardiac function under baseline conditions, I performed echocardiography on Parkin-TG mice at 3 months of age. Parkin-TG hearts had modestly but significantly lower %FS and %EF than WT hearts. These hearts also had significantly thinner anterior walls during systole. However, I observed no differences in posterior wall thickness, left ventricular end diastolic, or left ventricular systolic dimensions (Table 2). Thus, Parkin-TG mice showed signs of cardiac impairment as early as 3 months of age. This finding starkly contrasts the unaffected cardiac phenotype of Parkin-/- mice.

3.3.3 Parkin Deficient Mitochondria Have Normal Respiratory Capacity

Since Parkin has been reported to play an important role in the removal of dysfunctional mitochondria via autophagy (Narendra et al., 2008), I investigated whether Parkin deficiency would result in accumulation of damaged

mitochondria. Using mitochondria isolated from 3-month old WT and Parkin-/- hearts, I assessed mitochondrial respiration by measuring the rate of oxygen consumption in a closed reaction chamber using a Clark electrode. I found that Parkin-/- mitochondria had state 3 and state 4 respiration rates that were similar to those of WT mitochondria with substrates for either respiratory complex I (Figure 3.5A) or complex II (Figure 3.5B). Furthermore, there was no difference in the respiratory control ratio (RCR) between WT and Parkin-/- mitochondria (Figure 3.5C). To ensure that I did not select for functional mitochondria in my isolation procedure, I confirmed my findings in intact cardiomyocytes. Studies measuring maximal mitochondrial respiration in myocytes isolated from 3-month old mice confirmed that there was no difference in mitochondrial function between WT and Parkin-/- cells (Figure 3.6). These data suggest that Parkin-deficient cardiac mitochondria are well coupled and capable of efficiently producing ATP. To assess oxidative stress that would be expected to result from mitochondrial dysfunction, I examined malondialdehyde content and protein carbonylation in 3-month old mice. However, neither of these indicators differed between WT and Parkin-/- mice at this age (Figures 3.7 and 3.8).

3.3.4 Parkin-Deficient Mitochondria Are Smaller Than WT Mitochondria

Mitochondrial damage caused by cardiac stress can lead to opening of the mitochondrial permeability transition pore (MPTP) and necrotic cell death (Kubli and Gustafsson, 2012). I therefore investigated whether Parkin-/- mitochondria were more susceptible to mitochondrial permeability transition (MPT).

Mitochondria isolated from 3-month old WT and Parkin-/- mice were incubated with 150 μmol/L calcium, and mitochondrial swelling was determined from the resulting decline in absorbance at 520 nm wavelength by spectrophotometry. I found no differences in the rate or amplitude of swelling between WT and Parkin-/- mitochondria (Figure 3.9 and Table 3). However, Parkin-/- mitochondria consistently had a higher baseline absorbance value than WT mitochondria (0.712 ± 0.011 for Parkin-/- vs. 0.629 ± 0.017 for WT), suggesting that Parkin-/- mitochondria might be smaller than WT mitochondria (Table 3). To confirm this finding, I examined the ultrastructure of WT and Parkin-/- mouse hearts by transmission electron microscopy (TEM). As shown in Figure 3.10A, mitochondria from WT mice at 3 months of age were of homogeneous size and shape, and organized into rows perpendicular to the myocardial Z-lines. In contrast, mitochondria in the Parkin-/- heart were more disorganized and often found in large clusters with many small, round mitochondria. Morphometric analysis showed that Parkin-deficient mitochondria were significantly smaller than WT mitochondria (Figure 3.10B). However, there was no evidence of mitochondrial degeneration at this age. I also examined hearts of 6-month old WT and Parkin-/- mice. Similarly, mitochondria from aged Parkin-/- mice were disarrayed, smaller, and clustered, but still maintained cristae density and appeared generally normal. However, at this age, I observed the appearance of some abnormal mitochondria containing electron-dense macromolecules in the matrix (Figure 3.10A).

The abnormal morphology of the mitochondria in Parkin-/- hearts prompted me to investigate the levels of proteins involved in mitochondrial fusion and fission. However, I detected no changes in the levels of the mitochondrial fusion proteins Mitofusins 1 and 2 (Mfn1 and Mfn2) or optic atrophy 1 (Opa1) (Figure 3.11A), and only a slight increase in mitochondrial fission 1 (Fis1) protein levels. The levels of the fission protein Dynamin-related protein 1 (Drp1) also remained unchanged (Figure 3.11B). Translocation of Drp1 from the cytosol to the mitochondria is a critical step in mitochondrial fission. To investigate if the smaller mitochondrial morphology observed in Parkin-/- mouse hearts was caused by aberrant Drp1 activity, I examined levels of Drp1 in the mitochondrial fractions of WT and Parkin-/- mouse hearts and found very low levels in both **(**Figure 3.12**)**. This further supports the conclusion that mitochondrial dynamics are unchanged under baseline conditions in Parkin-/- mouse hearts.

3.4 Discussion

Herein, I report several new and important findings regarding the role of Parkin in the myocardium. First, the presence of Parkin is not essential for the normal turnover of mitochondria via autophagy in the heart. Loss of Parkin resulted in smaller and more disorganized mitochondria, but did not affect mitochondrial or cardiac function. The smaller mitochondria are not due to changes in mitochondrial fission or fusion proteins, but changes to the regulation of mitochondrial dynamics have not yet been ruled out. Another key finding is that overexpression of Parkin in myocytes is sufficient to cause modest cardiac

dysfunction as early as 3 months of age. These results demonstrate that overexpressed Parkin is functional and active. However, whether the functional deficits in Parkin-TG hearts arise from changes to mitophagy remains unexplored.

Removal of mitochondria via autophagy is increasingly recognized as an important process to maintain a healthy population of mitochondria in cells. Reduced autophagy results in accumulation of dysfunctional mitochondria and has been linked to aging and development of heart failure (Gottlieb and Gustafsson, 2011; Nakai et al., 2007; Wu et al., 2009). Parkin can regulate mitophagy (Narendra et al., 2008), but my studies suggest that Parkin is not critical for the turnover of mitochondria under normal conditions. Instead, the findings presented here suggest that Parkin is maintained in a state of low or no activity under normal conditions. Turnover of mitochondria in the heart may also be compensated for by other Parkin-independent pathways of mitophagy. The Bcl-2 family protein Bnip3L/NIX is critical for removal of mitochondria during erythrocyte maturation (Schweers et al., 2007), and its homolog Bnip3 was recently shown to also promote mitophagy (Rikka et al., 2011). Both of these proteins can directly interact with LC3 and can thereby directly anchor mitochondria to the nascent autophagosome to promote clearance in a Parkin-independent manner (Hanna et al., 2012; Novak et al., 2010). In contrast, cardiac-specific Parkin overexpression results in an emergent phenotype of cardiac dysfunction. Although other studies in cell lines and *Drosophila melanogaster* have investigated the effects of Parkin overexpression, these

studies have reported protective, beneficial effects such as the rescuing of mitochondrial dysfunction caused by PINK1 knockout (Clark et al., 2006), neuroprotection against α-synuclein toxicity (Petrucelli et al., 2002), and enrichment of a healthier mitochondrial population lacking mitochondrial DNA mutations (Suen et al., 2010). To my knowledge, this is the first study to report complications caused by Parkin overexpression in any tissue or cell type. A more in-depth analysis of the effects of cardiac Parkin overexpression would help to explain the mechanisms leading to cardiac dysfunction.

Chapter 3, in part, was originally published in the *Journal of Biological Chemistry*. Kubli, D. A., Zhang, X., Lee, Y., Hanna, R. A., Quinsay, M. N., Nguyen, C. K., Jimenez, R., Petrosyan, S., Murphy, A.N., Gustafsson, A.G. Parkin Protein Deficiency Exacerbates Cardiac Injury and Reduces Survival following Myocardial Infarction. *The Journal of Biological Chemistry*. 2013; *288*(2), 915–926. © 2013 the American Society for Biochemistry and Molecular Biology. The dissertation author was the primary investigator and author of this paper.

Part of Chapter 3 was also originally published in *Communicative and Integrative Biology*. Kubli, D. A., Quinsay, M. N., & Gustafsson, A. B. Parkin Deficiency Results in Accumulation of Abnormal Mitochondria in Aging Myocytes. *Communicative & Integrative Biology*. 2013; *6*(4), e24511. doi:10.4161/cib.24511. © 2013 Landes Bioscience. The dissertation author was the primary investigator and author of this paper.

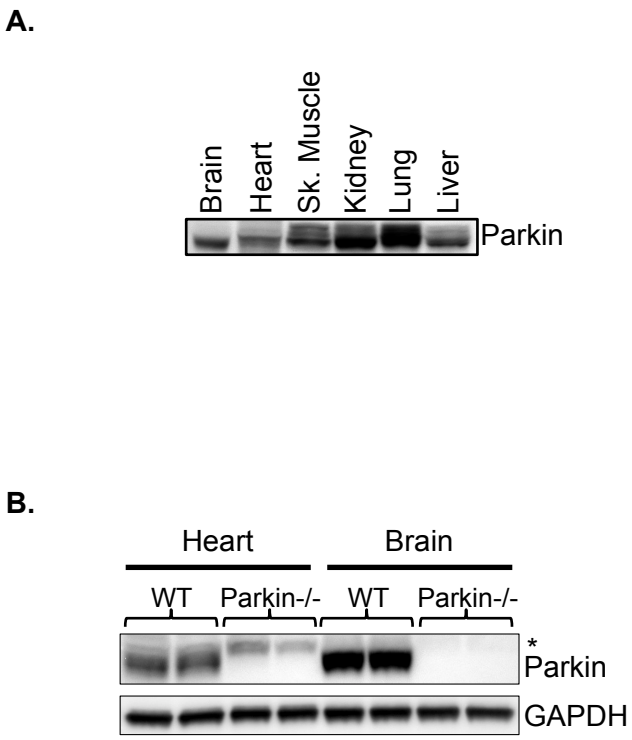

Figure 3.1. Expression of Parkin in mouse tissue. **A.** Western blot for Parkin expression in brain, heart, skeletal muscle, kidney, lung, and liver. **B.** Western blot for Parkin in heart and brain tissue of WT and Parkin-/- mice (* nonspecific band detected by the Parkin antibody).

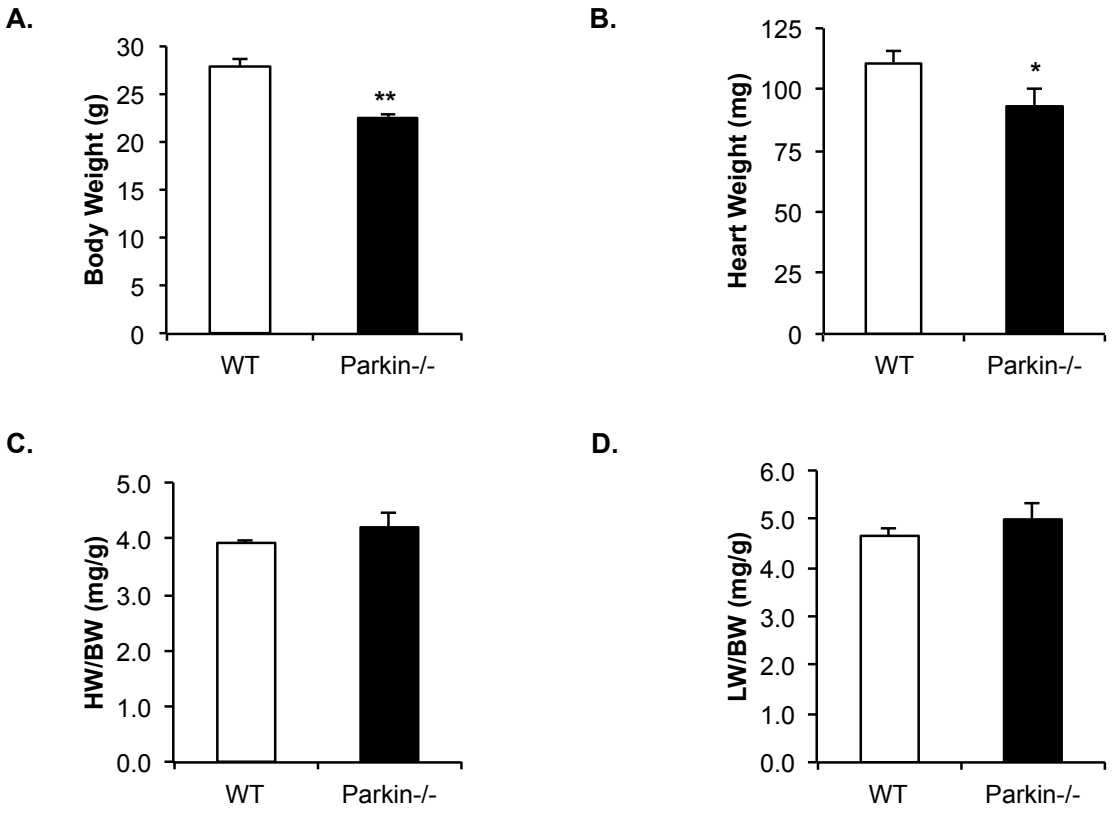

Figure 3.2. WT and Parkin-/- mouse body weight (**A**), heart weight (**B**), heart weight/body weight ratio (**C**), and lung weight/body weight ratio (**D**). Mean ± SEM (n=7-11, *p<0.05, **p<0.01 vs. WT).

Table 3.1. Echocardiographic analysis of WT and Parkin-/- mouse heart function.

Table 1: Echocardiographic analysis of WT and Parkin-/- mice

Parameter	Mean value ± SEM for:					
	3 Months Age		6 Months Age		12 Months Age	
	WT (n = 17)	Parkin-/- (n = 16)	WT (n = 8)	Parkin-/- (n = 9)	WT (n = 6)	Parkin-/- (n = 6)
HR (BPM)	582 ± 21	603 ± 25	524 ± 13	521 ± 26	567 ± 26	574 ± 10
FS (%)	49.9 ± 2.7	49.3 ± 3.6	33.6 ± 1.3	33.0 ± 2.1	48.0 ± 6.0	41.5 ± 7.0
EF (%)	80.5 ± 2.3	78.7 ± 3.6	63.0 ± 1.9	61.7 ± 3.1	77.9 ± 5.6	69.7 ± 9.1
IVSd (mm)	0.99 ± 0.06	0.96 ± 0.05	0.87 ± 0.04	0.90 ± 0.04	0.95 ± 0.06	0.87 ± 0.06
IVSs (mm)	1.49 ± 0.06	1.61 ± 0.10	1.24 ± 0.07	1.18 ± 0.04	1.64 ± 0.16	1.44 ± 0.17
LVPWd (mm)	1.06 ± 0.09	1.04 ± 0.08	0.89 ± 0.06	0.82 ± 0.06	1.12 ± 0.07	0.94 ± 0.14
LVPWs (mm)	1.61 ± 0.11	1.60 ± 0.11	1.27 ± 0.07	1.21 ± 0.07	1.63 ± 0.05	1.32 ± 0.23
LVEDD (mm)	3.33 ± 0.13	3.31 ± 0.13	3.83 ± 0.14	3.93 ± 0.17	3.47 ± 0.17	3.89 ± 0.24
LVESD (mm)	1.69 ± 0.14	1.66 ± 0.17	2.56 ± 0.13	2.66 ± 0.18	1.84 ± 0.26	2.33 ± 0.40

HR indicates heart rate; FS, fractional shortening; EF, ejection fraction; IVSd, interventricular septal thickness at diastole; IVSs, interventricular septal thickness at systole; LVEDD, left ventricular end diastolic dimension; LVESD, left ventricular end systolic dimension; LVPWd, left ventricular posterior wall thickness at diastole; LVPWs, left ventricular posterior wall thickness at systole. P>0.05 for all parameters measured.

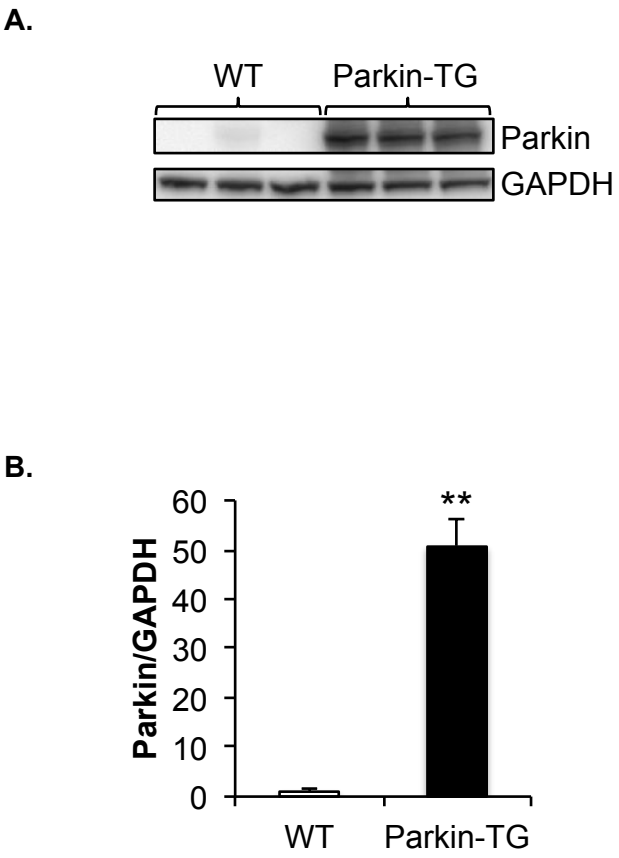

Figure 3.3. Parkin transgenic (Parkin-TG) mouse hearts have approximately 50-fold higher Parkin protein expression than WT mouse hearts. **A.** Representative western blot of WT and Parkin-TG heart tissue. **B.** Western blot quantitation of Parkin protein levels in WT and Parkin-TG hearts. Mean ± SEM (n = 4-5, **p<0.001)

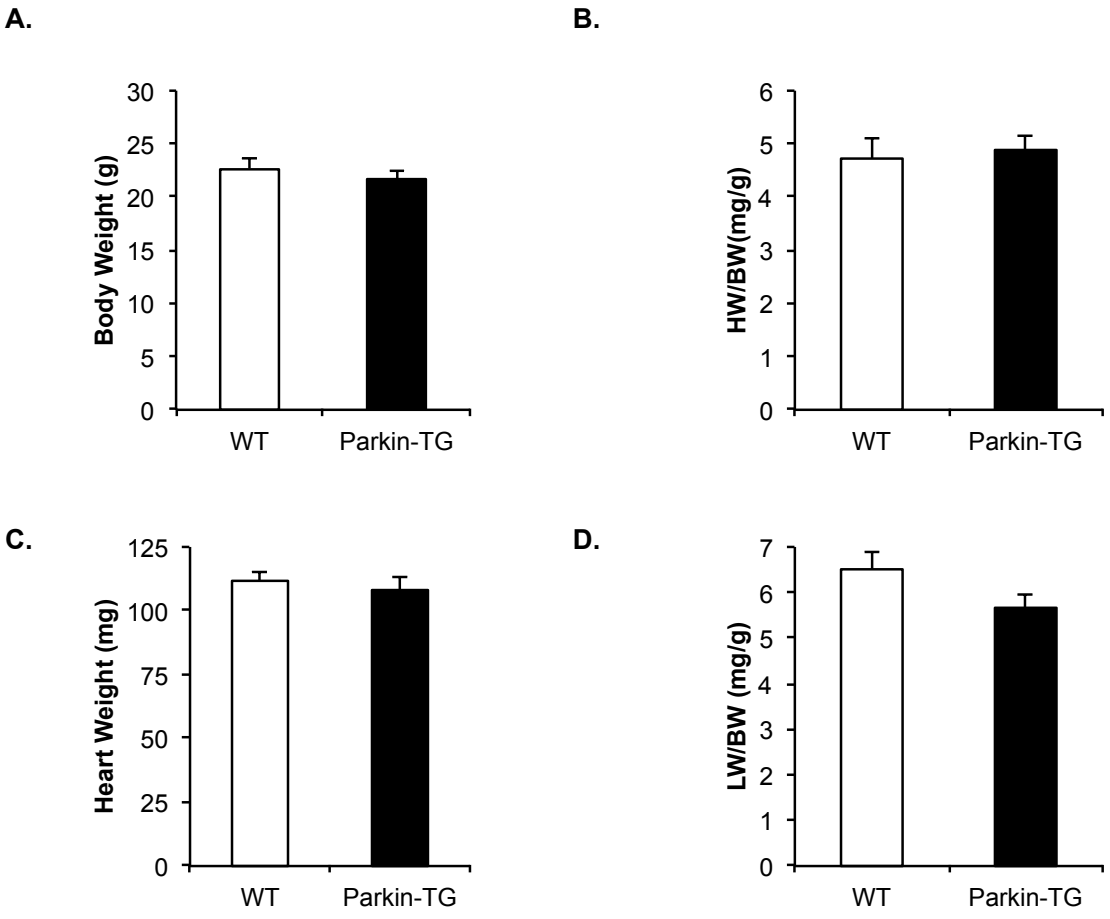

Figure 3.4. WT and Parkin-TG mouse body weight (**A**) (n=5-7), heart weight (**B**) (n=5), heart weight/body weight ratio (**C**) (n=4-5), and lung weight/body weight ratio (**D**) (n=5-6). Mean ± SEM. No significant differences were found.

Table 3.2. Echocardiographic analysis of WT and Parkin-TG mouse heart function.

Table 2: Echocardiographic analysis of WT and Parkin-TG mice

Parameter	Mean value ± SEM for: 3 Months Age	
	WT (n = 9)	Parkin-TG (n = 13)
HR (BPM)	562 ± 16	548 ± 10
FS (%)	33.9 ± 2.3	27.0 ± 0.9**
EF (%)	62.4 ± 3.35	52.7 ± 1.5**
IVSd (mm)	0.92 ± 0.07	0.77 ± 0.02*
IVSs (mm)	1.33 ± 0.07	1.12 ± 0.02**
LVPWd (mm)	0.70 ± 0.03	0.72 ± 0.04
LVPWs (mm)	1.12 ± 0.05	1.02 ± 0.03
LVEDD (mm)	4.36 ± 0.10	4.37 ± 0.06
LVESD (mm)	2.89 ± 0.14	3.19 ± 0.06*

HR indicates heart rate; FS, fractional shortening; EF, ejection fraction; IVSd, interventricular septal thickness at diastole; IVSs, interventricular septal thickness at systole; LVEDD, left ventricular end diastolic dimension; LVESD, left ventricular end systolic dimension; LVPWd, left ventricular posterior wall thickness at diastole; LVPWs, left ventricular posterior wall thickness at systole. *P<0.05 vs. WT, **P<0.01 vs. WT.

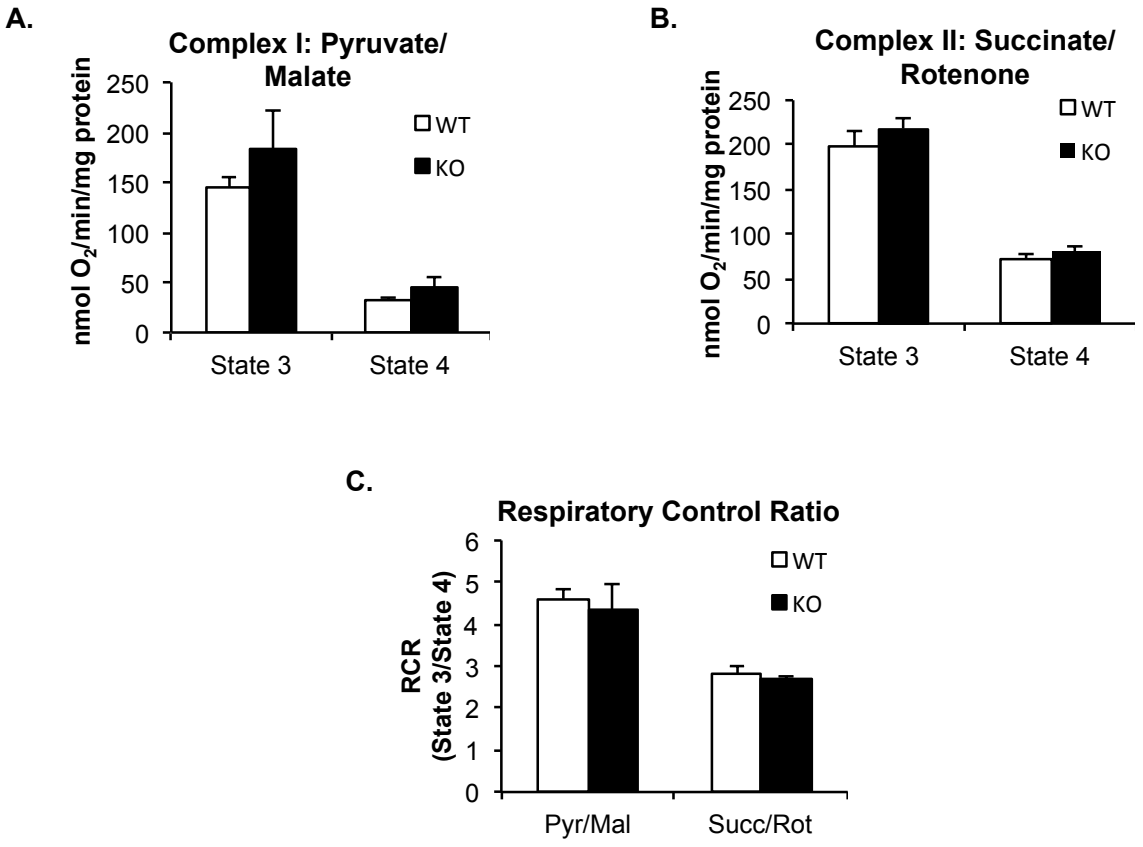

Figure 3.5. Mitochondrial respiration is normal in Parkin-/- mouse hearts at 3 months of age. State 3 and state 4 respiration rates of mitochondria isolated from WT or Parkin-/- mouse hearts with substrates for Complex I (pyruvate/malate) (**A**) or Complex II (succinate/rotenone) (**B**). **C.** Respiratory control ratios for Complex I and Complex II substrates (n=4). Mean ± SEM. No significant differences were observed.

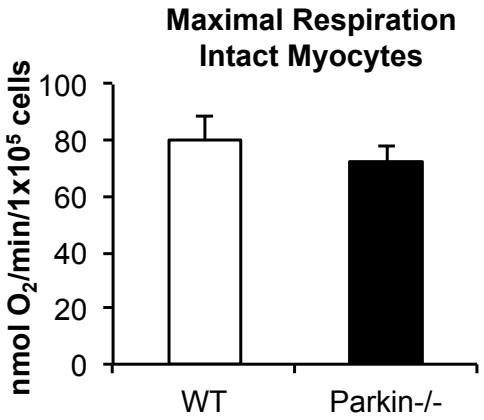

Figure 3.6. Maximal mitochondrial respiration rates in isolated intact WT and Parkin-/- adult mouse cardiomyocytes. Mean ± SEM (n=3). No significant differences were observed.

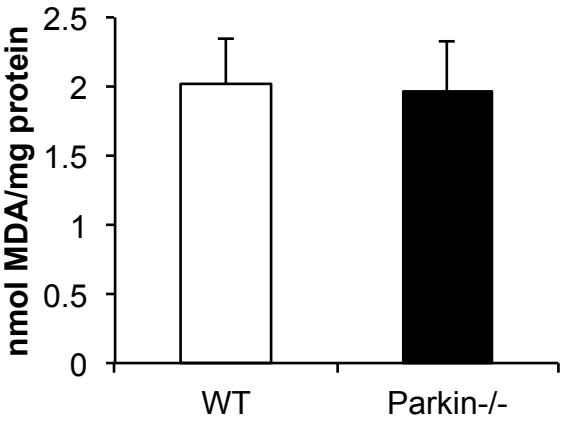

Figure 3.7. Malondialdehyde content, an indicator of oxidative stress, was unchanged in Parkin-/- mouse hearts versus WT at 3 months of age. Mean ± SEM (n =13 for each group). No significant differences were observed.

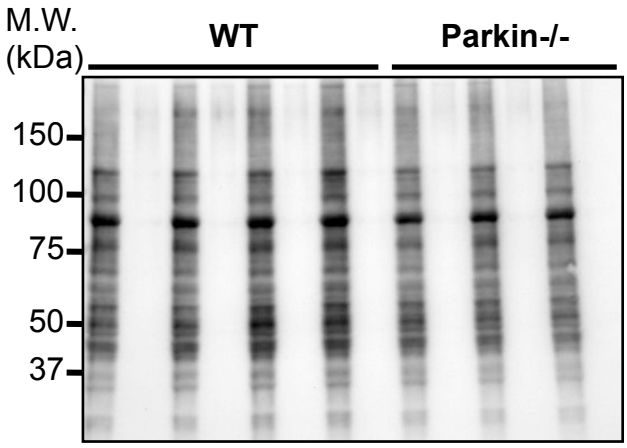

Figure 3.8. Representative blot for protein carbonylation, an indicator of oxidative stress. Protein carbonyl levels were unchanged in Parkin-/- mouse hearts versus WT at 3 months of age. Mean ± SEM (n=6 for each group). No significant differences were observed.

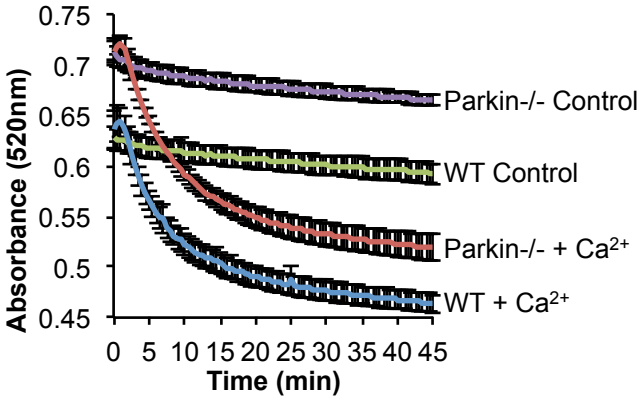

Figure 3.9. Swelling of isolated mitochondria in the presence of 150 µmol/L calcium (n=3). The degree and rate of swelling (Amplitude and V_{max}, respectively) were not significantly different between WT and Parkin-/- mitochondria. Baseline absorbance values for Parkin-/- mitochondria were significantly higher than WT.

Table 3.3. Comparison of baseline absorbance and swelling kinetics. Amplitude indicates extent of swelling, V_{max}, rate of swelling. Mean ± SEM (n=3, *p<0.05 vs. WT).

	Wildtype (n = 3)	**Parkin-/- (n = 3)**
Amplitude (A_{520})	0.191 ± 0.007	0.213 ± 0.005
V_{max} (ΔA/min)	-0.0245 ± 0.0018	-0.0233 ± 0.0023
Baseline A_{520}	0.629 ± 0.017	0.712 ± 0.011*

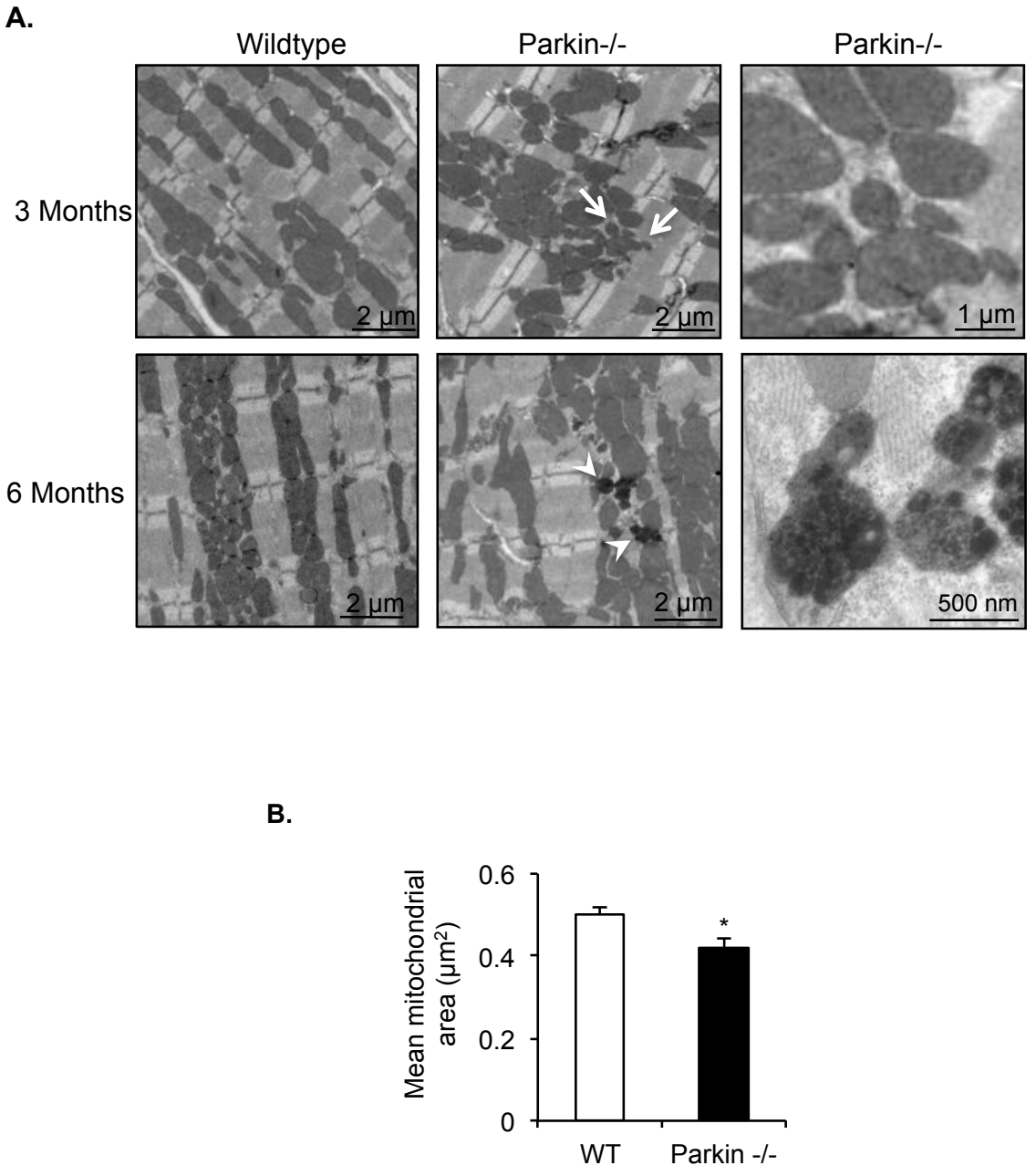

Figure 3.10. Parkin deficient hearts have disorganized and smaller mitochondria. **A.** Representative transmission electron micrographs of heart sections from 3- and 6-month old mice. Arrows signify smaller mitochondria, arrowheads signify abnormally dense mitochondria. **B.** Quantitation of mean mitochondrial area in WT and Parkin-/- hearts at 3-month of age (*$p<0.05$ vs. WT).

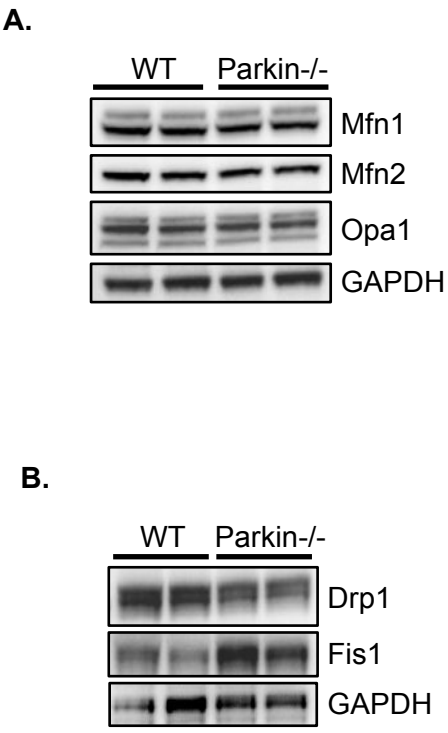

Figure 3.11. Changes to mitochondrial fission and fusion proteins do not account for smaller mitochondrial morphology in Parkin-/- mouse hearts **A.** Western blot of mitochondrial fusion proteins Mfn1, Mfn2, and Opa1. **B.** Western blot of mitochondrial fission proteins Drp1 and Fis1.

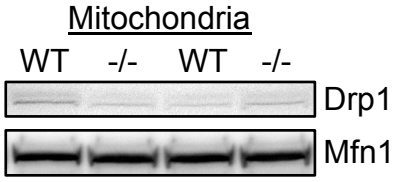

Figure 3.12. Levels of Drp1 in the mitochondrial fraction are unchanged in Parkin-/- hearts compared to WT. Representative western blot of mitochondria-associated Drp1. n=4.

CHAPTER 4: RESPONSE OF PARKIN-/- MICE TO MYOCARDIAL INFARCTION

4.1 Abstract

Parkin is highly expressed in the heart, but Parkin-/- mice do not develop any cardiac phenotypes under normal conditions. I therefore investigated how Parkin-deficient mice respond and adapt to acute cardiac stress conditions. I subjected WT and Parkin-/- mice to permanent myocardial infarction (MI) and assessed their recovery and heart function after 7 days of MI. Parkin-/- mice had increased mortality compared to WT mice as well as significantly more left ventricular remodeling than WT mice, resulting in severe dilated cardiomyopathy. Additionally, Parkin-/- myocytes had impaired clearance of mitochondria via autophagy after the infarction. This led to an accumulation of dysfunctional mitochondria in myocytes in the infarct border zone after the infarction. Parkin-deficient myocytes were also more susceptible to hypoxia-induced cell death. Thus, impaired mitophagy in Parkin-/- mouse hearts subjected to MI contributes to excessive tissue damage and an inability to adapt to stress conditions. Although Parkin is not necessary for the baseline turnover of mitochondria, it is a critical component of the cell stress response after mitochondrial damage.

4.2 Introduction

Mitochondrial damage and dysfunction occurs in the heart after both acute and chronic stress conditions (Faerber et al., 2011; Lesnefsky et al., 2001;

Tompkins et al., 2006). Mitochondrial dysfunction can produce excessive reactive oxygen species that cause cellular damage, and damaged mitochondria can release factors that promote necrotic or apoptotic cell death (Kubli and Gustafsson, 2012). Parkin is known to participate in the removal of mitochondria that have lost their $\Delta\Psi m$. Additionally, Parkin has been shown to be important in the heart during ischemic pre-conditioning, a phenomenon in which a series of short bouts of ischemia yields cardioprotection during a subsequent longer period of ischemia (Huang et al., 2011). In this chapter, I sought to determine if Parkin-/- mice are capable of adapting to severe stress conditions such as that which occurs following a myocardial infarction (MI). I assessed the response of Parkin-/- mice to MI and found that they were more sensitive than WT mice, with increased mortality, larger infarct size, and development of dilated cardiomyopathy. Parkin is therefore critical for the heart to adapt to stress.

4.3 Results:

4.3.1 Increased Sensitivity of Parkin-/- Mice to Myocardial Infarction

Since Parkin has been reported to be important in removing compromised mitochondria to prevent cell death (Narendra et al., 2008), I investigated whether Parkin-/- mice were more sensitive to cardiac stress. I subjected WT and Parkin-/- mice to MI by permanent ligation of the LAD coronary artery. I discovered that Parkin-/- mice were much more sensitive to MI, with ~65% mortality within the first week compared to ~25% for WT mice (Figure 4.1). Necropsies showed that several of these mice died due to cardiac rupture. Histological analyses

confirmed severe thinning of the left ventricular (LV) wall and enlarged LV interior dimensions in Parkin-/- mice after MI (Figure 4.2A), which indicates cardiac dilatation. I also found that a significantly larger percentage of the LV of Parkin-/- hearts had undergone remodeling compared to WT hearts (Figure 4.2B). The area at risk (AAR) was examined 24 hours after the ligation in a different cohort of mice, and was found to be comparable between WT and Parkin-/- hearts (Figure 4.3). This confirms that alterations in the vasculature in the Parkin-/- hearts did not contribute to the differences in remodeling.

I next assessed cardiac function by echocardiography on surviving mice seven days post-MI. Parkin-/- mice had significantly lower percent fractional shortening (%FS) and percent ejection fractions (%EF), as well as significantly increased LV end diastolic and systolic dimensions (LVEDD and LVESD) and LV volume compared to WT mice (Figure 4.4). These results indicate that Parkin plays an important role in the adaptive response after an MI.

I then examined the expression levels of Parkin protein in the infarct border zone in WT mouse hearts and found that Parkin was rapidly upregulated after the MI (Figure 4.5A). Parkin protein levels were significantly higher than baseline levels as early as 8 hours after the MI, and remained elevated for at least 48 hours after the infarction. In comparison, Parkin protein levels did not change in the uninfarcted remote zone (Figure 4.5B). This finding further supports the hypothesis that Parkin is particularly important after cardiac stress.

4.3.2 Autophagy is Impaired in Parkin-/- Hearts

Changes in the extra- and intracellular environments lead to rapid upregulation of autophagy in cells (Aviv et al., 2011). Numerous studies have shown that autophagy is upregulated in the heart in response to ischemia/reperfusion injury and other stress conditions (Hamacher-Brady et al., 2007; Matsui et al., 2007; Yan et al., 2005). To investigate whether autophagy was upregulated in WT and Parkin-/- hearts following the MI, I assessed the levels of LC3I and LC3II in the border zone of the infarct by western blotting. The conversion of LC3I to LC3II is indicative of autophagic activity, and the amount of LC3II correlates well with the quantity of autophagosomes (Kabeya et al., 2000). Western blot analysis of endogenous LC3 levels confirmed a significant increase in the LC3II/LC3I ratio in the border zone of the infarct in WT mice following 4 hours of MI (Figure 4.6). While autophagy was also induced in Parkin-/- border zone samples, the magnitude of induction was significantly lower than that of WT at this time point (Figure 4.6). It is currently unclear why the LC3II/I ratio in Parkin-/- mice is lower than in WT hearts after MI. Autophagy was induced to the same extent in both WT and Parkin-/- uninfarcted remote zones, suggesting that the reduced induction of autophagy in Parkin-/- mice was limited to the BZ (Figure 4.7).

Myocardial infarction leads to mitochondrial stress and damage. Therefore, Parkin would be expected to translocate to mitochondria after MI, and Parkin-mediated ubiquitination of mitochondrial proteins would subsequently be expected to increase following MI-induced stress in the infarct border zones of WT mice (Figure 4.8). I first confirmed that four hours of MI resulted in

translocation of Parkin to mitochondria in the infarct border zone of WT mouse hearts (Figure 4.9A). Next, I examined levels of ubiquitination of mitochondrial proteins after MI. Western blots of mitochondria isolated from WT border zone tissue confirmed an increase in ubiquitin levels after 4 hours of MI (Figure 4.9B). In contrast, border zone mitochondria from Parkin-/- mice showed a failure to increase ubiquitination after 4 hours of MI (Figure 4.9B). Unexpectedly, ubiquitination of cytosolic proteins in WT mice was also increased after 4 hours of MI, while Parkin-/- cytosol samples had no signs of increased ubiquitination (Figure 4.9B). This suggests that in addition to ubiquitinating mitochondrial substrates, Parkin also ubiquitinates cytosolic proteins after cardiac stress. In comparison, samples from the uninfarcted remote zones of WT mice showed no translocation of Parkin to mitochondria and also had no increase in mitochondrial ubiquitination, confirming that Parkin-mediated ubiquitination of mitochondrial proteins was specific to the infarct border zone (Figure 4.10).

It has been proposed that the nascent autophagosome can be anchored to its target mitochondrion by the scaffolding protein p62, which binds to LC3II on the autophagosome and ubiquitinated proteins on mitochondria (Kubli and Gustafsson, 2012) (Figure 4.8). As an indicator of mitophagy, I assessed levels of LC3II associated with mitochondria in the border zones of WT and Parkin-/- mouse hearts after 4 hours of MI. In WT border zone samples, I observed an increase in LC3II binding to mitochondria that occurred concomitantly with Parkin translocation (Figure 4.11). I also found reduced levels of LC3II in mitochondria

from Parkin-/- border zone (Figure 4.11), which is suggestive of impaired mitophagy.

4.3.3 Dysfunctional Mitochondria Accumulate in Parkin-/- Hearts After MI

An ultrastructural examination using TEM confirmed the induction of autophagy and mitophagy in WT myocytes in the border zone at 4-hours post-MI (Figure 4.12A). In contrast, I did not detect any autophagosomes containing mitochondria in Parkin-/- myocytes. Instead, mitochondria in Parkin-/- myocytes in the border zone were swollen and displayed severe cristae remodeling. The accumulation of swollen mitochondria also appeared to contribute to disruption of the contractile elements in the Parkin-/- myocytes (Figure 4.12A, white arrows). To confirm that the mitochondria in Parkin-/- border zone tissue were dysfunctional, I assessed respiration of mitochondria isolated from WT and Parkin-/- mice 4 hours after ligation of the LAD. Parkin-/- border zone mitochondria had significantly lower oxygen consumption rates (OCR) compared to mitochondria in the remote zone (Figures 4.12B and 4.12C). Although mitochondria from WT border zones had reduced oxygen consumption rates, the decrease was not significant (Figures 4.12B and 4.12C).

To further confirm that Parkin-/- myocytes have impaired mitophagy in response to mitochondrial damage, I treated isolated WT and Parkin-/- myocytes with rotenone. Rotenone is a mitochondrial Complex I inhibitor and induces translocation of Parkin to mitochondria (Tang et al., 2011). In WT cells, rotenone treatment caused an increase in mitophagy, as determined by increased co-

localization between mitochondria and LC3-GFP-positive autophagosomes (Figures 4.13A and 4.13B). In contrast, rotenone did not increase mitophagy in Parkin-deficient myocytes. Consistent with the *in vivo* data, I found that induction of autophagy was also reduced in Parkin-deficient myocytes, as rotenone treatment induced fewer LC3-GFP-positive autophagosomes in Parkin-/- cells than in WT myocytes (Figure 4.13C). These data further confirm that Parkin deficiency confers mitophagy impairment in cardiac myocytes with mitochondrial damage.

To confirm that Parkin deficiency and impaired mitophagy contribute to increased susceptibility to cell death, I next subjected isolated WT and Parkin-/- myocytes to hypoxia and quantified cell death by YoPro1 staining and fluorescence microscopy. Hypoxia is known to cause mitochondrial damage and induce mitophagy in cardiac myocytes (Band et al., 2009; Regula et al., 2002; Zhang et al., 2008). Parkin-/- myocytes had significantly more cell death than WT mouse myocytes after 4 hours of hypoxia (Figure 4.14). This increased sensitivity of Parkin-/- cardiac myocytes to hypoxia was abrogated when Parkin expression was restored in the knockout cells by adenoviral overexpression (Figure 4.14). I then tested the potential for Parkin overexpression to confer increased resistance to cell death by infecting adult rat cardiac myocytes with adenoviruses encoding Parkin or the disease-associated Parkin mutants Parkin-R42P and Parkin-G430D. Parkin-R42P fails to translocate to mitochondria (Lee et al., 2010), whereas Parkin-G430D is deficient in its ubiquitin ligase activity (Matsuda et al., 2010). Overexpression of wild-type Parkin significantly reduced myocyte death

after hypoxia treatment, while overexpression of either of the mutants had no effect (Figure 4.15). This suggests that the protective effect of Parkin is dependent both on Parkin's ubiquitin ligase activity and its mitochondrial localization. These data cumulatively suggest that Parkin deficiency results in defective mitochondrial clearance and subsequent increased susceptibility to cell death after stress.

4.4 Discussion

Although Parkin-/- mice are seemingly unaffected by the disruption of the *PARK2* gene under normal conditions, cardiac stress by MI evokes disproportionate ventricular remodeling and increased mortality. Thus, my data indicate that in the myocardium, Parkin is important in the adaptation to stress by promoting mitophagy. In response to MI, Parkin-/- mice had a much greater percentage of remodeling of the LV, and developed severe thinning of the LV walls, increased LV interior dimensions, and impaired cardiac function. These are hallmarks of dilated cardiomyopathy. In contrast to WT mice, which retained much of their LV function and wall thickness after the MI, Parkin-/- mice adapted very poorly to the stress. Although it is possible that the loss of Parkin in other cell types such as fibroblasts or macrophages could contribute to the expansion of tissue damage, the accumulation of swollen and dysfunctional mitochondria in the border zone coupled with the absence of autophagosomes strongly suggests that a failure of mitophagy is largely responsible for the observed effects.

Studies in *Drosophila melanogaster* initially suggested that Parkin participates in mitochondrial turnover because Parkin gene mutations cause striking changes in both mitochondrial structure and performance (Greene et al., 2003). However, it is now clear that Parkin has a different role in mammalian cells. Parkin null mice do not suffer from major neurological phenotypes or motor impairments, and do not lose dopaminergic neurons of the substantia nigra until they are exposed to stress conditions such as chronic systemic inflammation induced by lipopolysaccharide administration (Frank-Cannon et al., 2008). Similarly, my most striking finding in this chapter was the increased sensitivity of Parkin-/- mice to MI compared to WT mice. Thus, in mammalian cells, Parkin does not play a critical role in maintaining normal mitochondrial function. Rather, Parkin appears to play an important role in the adaptation to stress. Another prominent finding was the ubiquitous deterioration of mitochondria in Parkin-/- myocytes in the border zone after the infarction. In WT myocytes, I detected some dysfunctional mitochondria after the MI, whereas nearly all mitochondria in Parkin-/- myocytes were swollen and displayed cristae remodeling. Parkin-deficient cardiac mitochondria were normal under baseline conditions, but dysfunctional mitochondria accumulated rapidly after the MI, indicating that Parkin is also involved in maintaining mitochondrial function in response to stress by selectively removing mitochondria of compromised integrity.

It was recently reported that Parkin-mediated removal of mitochondria plays an important role in cardiac ischemic preconditioning (IPC) (Huang et al., 2011). This study found that IPC induces translocation of Parkin to mitochondria,

and that Parkin-deficient mice are resistant to IPC-induced cardioprotection due to impaired Parkin-mediated mitophagy. My data show that autophagy is rapidly increased in the border zone of the infarct after permanent ligation of the LAD and in isolated myocytes treated with rotenone. Unexpectedly, the Parkin-/- myocytes showed reduced formation of autophagosomes in response to MI or rotenone treatment. My lab recently reported that Bnip3-mediated mitochondrial autophagy in cardiac myocytes involves translocation of Parkin to mitochondria (Lee et al., 2011). Similar to the findings in this chapter, it was discovered that induction of autophagy by Bnip3 is reduced in Parkin-/- myocytes. Thus, my data here suggest that Parkin is not only responsible for targeting dysfunctional mitochondria for autophagy, but may also participate in initiating the autophagy response. My data also demonstrate that initiation of autophagy is only impaired in the border zone, where the most mitochondrial damage is occurring. Induction of autophagy in the remote zone was not affected in Parkin-/- mice. Thus, an in-depth investigation into the mechanisms of Parkin function in the heart is warranted. Further studies will help to dissociate the role of Parkin in response to stress from its purpose under baseline conditions.

Chapter 4, in part, was originally published in the Journal of Biological Chemistry. Kubli, D. A., Zhang, X., Lee, Y., Hanna, R. A., Quinsay, M. N., Nguyen, C. K., Jimenez, R., Petrosyan, S., Murphy, A.N., Gustafsson, A.G. Parkin Protein Deficiency Exacerbates Cardiac Injury and Reduces Survival following Myocardial Infarction. *The Journal of Biological Chemistry*. 2013;

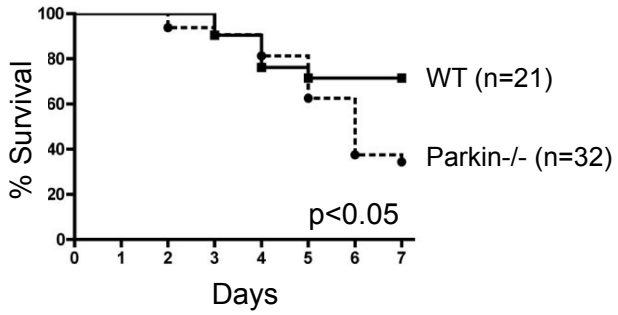

Figure 4.1. Kaplan-Meyer survival curve. Parkin-/- mice have increased susceptibility to myocardial infarction (MI). $p<0.05$ vs. WT by logrank test.

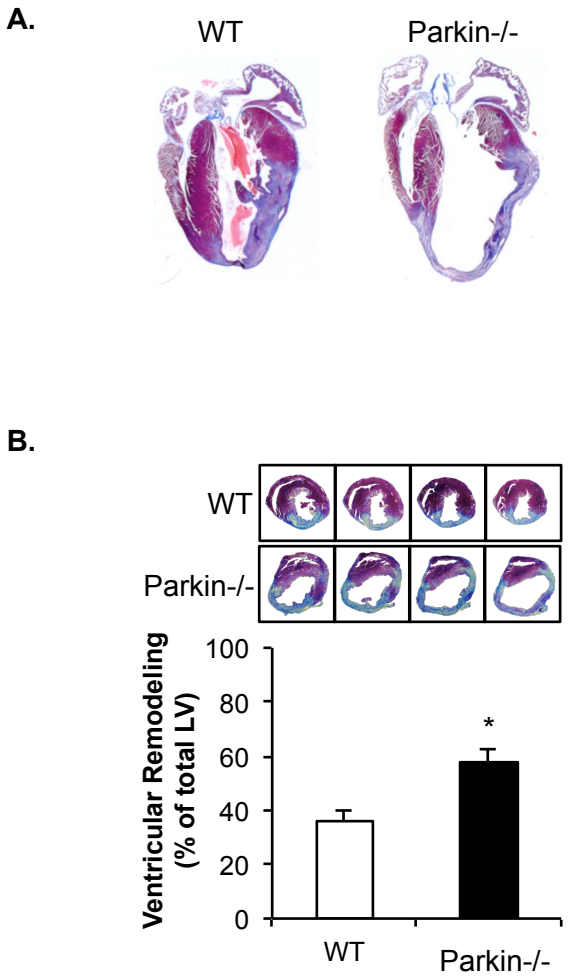

Figure 4.2. A. Representative Masson's trichrome staining of WT and Parkin-/- hearts seven days post-MI. **B.** Ventricular remodeling was determined by Masson's trichrome staining of cross sections taken at 300 μm intervals. (n=8, *p<0.01 vs. WT).

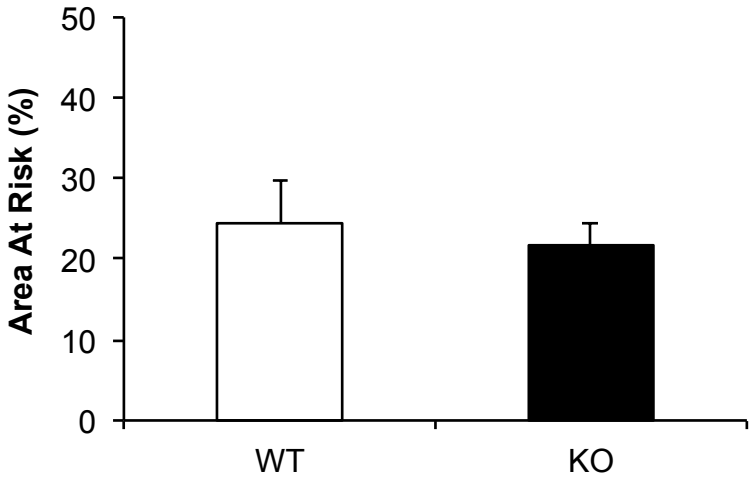

Figure 4.3. The area at risk 24 hours after MI was not significantly different in 3-month old Parkin-/- hearts compared to WT. The LAD coronary artery was ligated for 24 hours before hearts were perfused with Evans Blue dye to delineate the area at risk. Mean ± SEM (n=5).

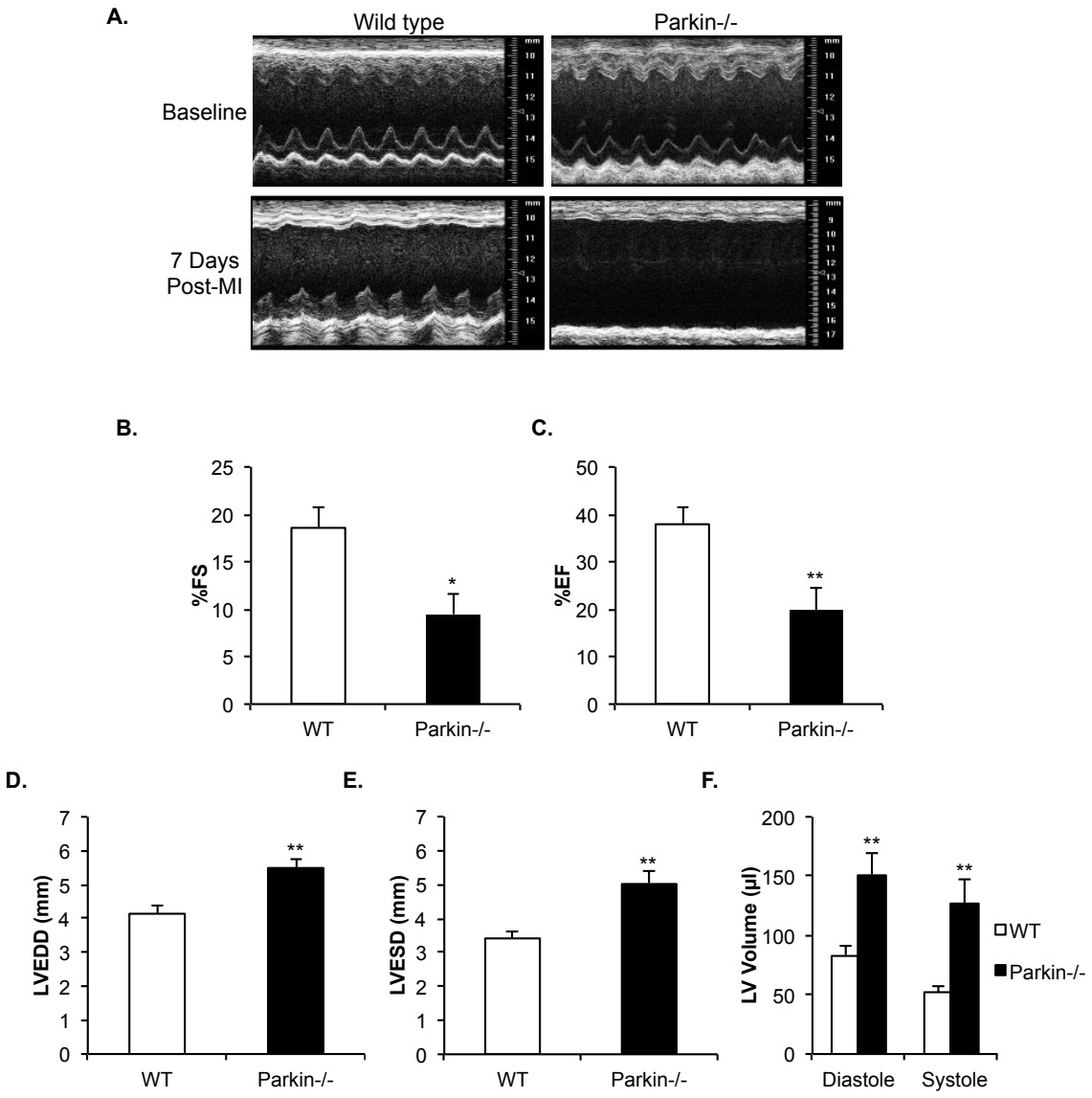

Figure 4.4. Echocardiography of WT and Parkin-/- mice 7 days post-MI. **A.** Representative M-mode echocardiograms of WT and Parkin-/- hearts prior to MI and 7 days post-MI. Echocardiographic analysis revealed reduced fractional shortening (%FS) (**B**) and ejection fraction (%EF) (**C**), as well as enlarged left ventricular end diastolic dimension (LVEDD) (**D**), end systolic dimension (LVESD) (**E**), and LV volume (**F**) in Parkin-/- hearts. Mean ± SEM (WT n=13, Parkin-/- n=10, *p<0.05, **p<0.01 vs. WT)

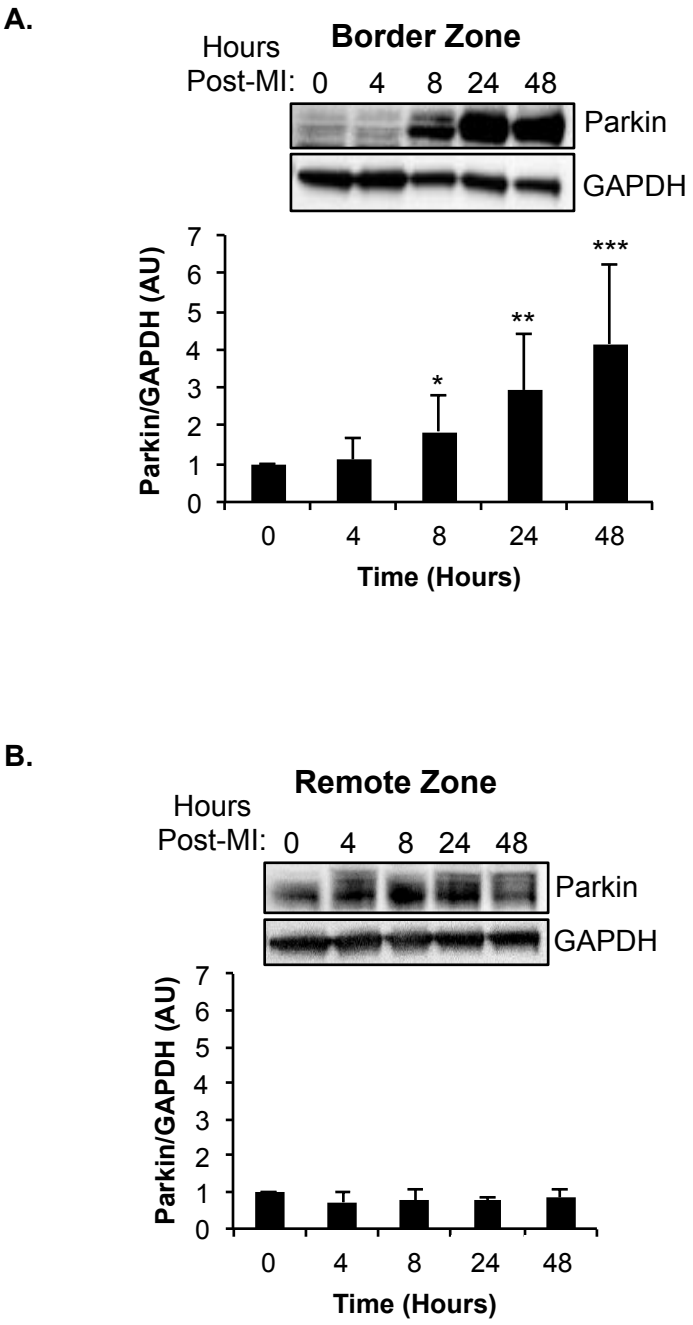

Figure 4.5. Representative western blots and densitometry demonstrating rapid upregulation of Parkin in the border zone of WT mice after MI (**A**), and no change in Parkin in the remote zone of WT mice (**B**). Parkin/GAPDH ratios are Means ± SEM (*, **,*** $p<0.05$ vs. 0 hour, n=5).

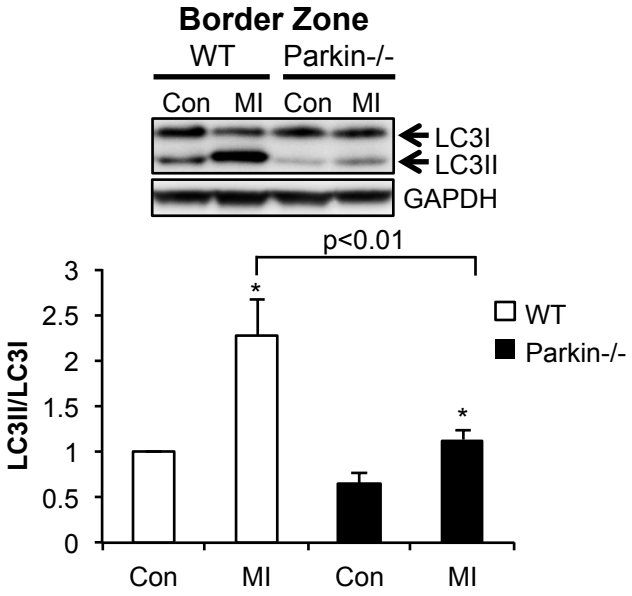

Figure 4.6. Induction of autophagy is reduced in the infarct border zone in Parkin-/- mouse hearts**.** Western blot and quantitation analyses for LC3I and II protein levels in the border zone at baseline (Con) and in the border zone four hours post-MI. Mean ± SEM (*p<0.05, **p<0.01 vs. Con, n=8).

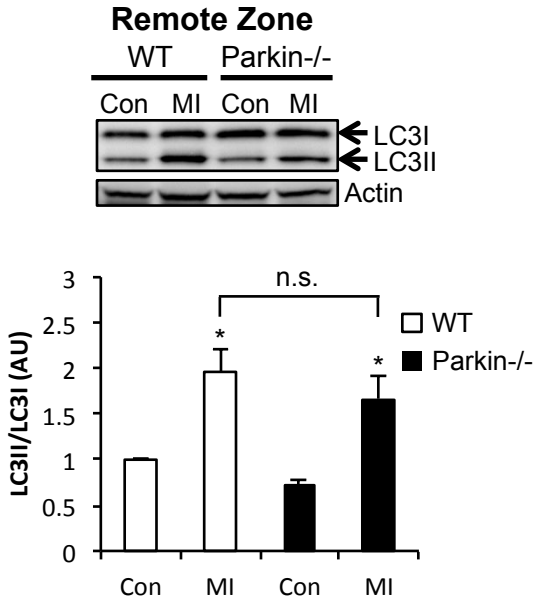

Figure 4.7. Western blot and quantitation analyses for LC3I and II protein levels in the remote zone at baseline (Con) and four hours post-MI. Mean ± SEM (*p<0.05, **p<0.01 vs. Con, n=8)

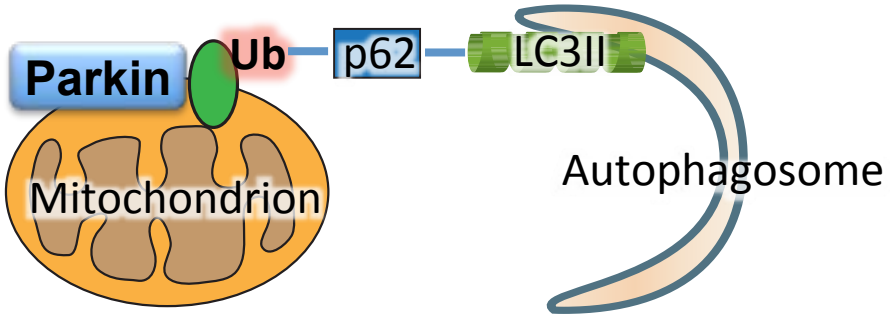

Figure 4.8. Schematic of Parkin-mediated ubiquitination (Ub) of mitochondrial proteins and subsequent LC3II binding to ubiquitinated mitochondria via the scaffolding protein p62.

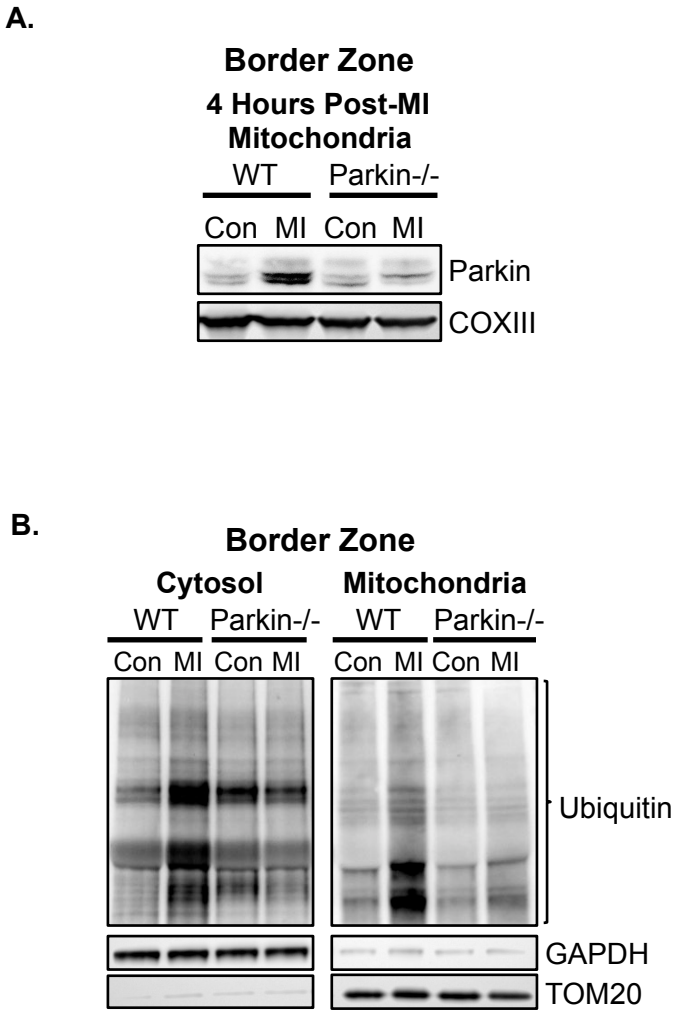

Figure 4.9. Parkin translocates to mitochondria and ubiquitinates mitochondrial proteins after myocardial infarction. **A.** Representative western blot of mitochondrial Parkin in wild type (WT) and Parkin-knockout (Parkin-/-) mouse border zone samples at baseline (Con) and 4 hours post-myocardial infarction (MI). **B.** Representative western blot of cytosolic and mitochondrial protein ubiquitination at baseline and 4 hours post-MI. n=4 for each group.

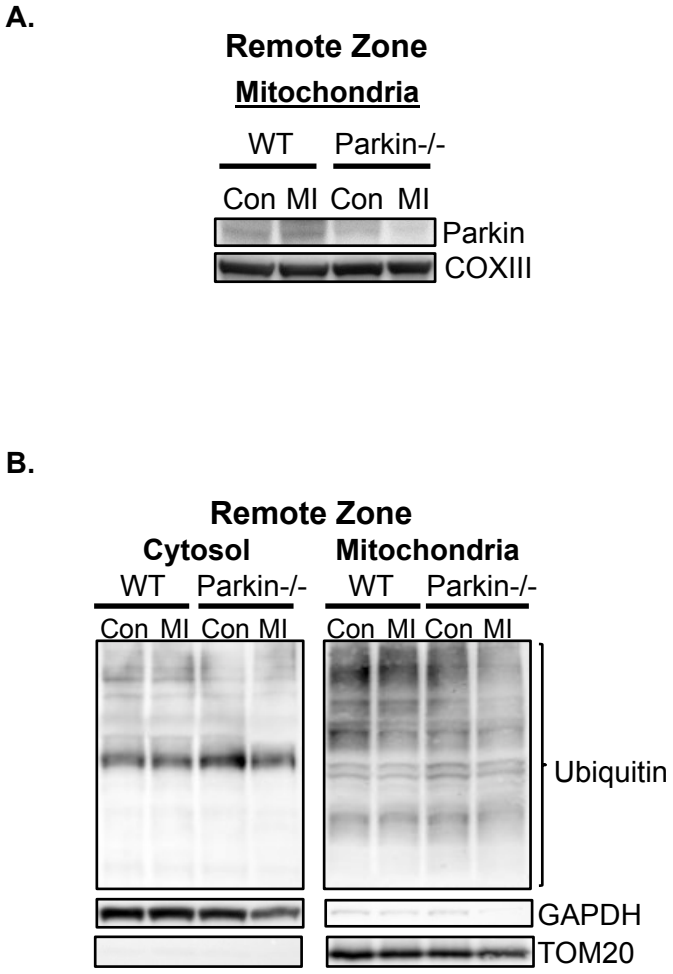

Figure 4.10. Representative western blot images of remote zone samples of WT and Parkin-/- mouse hearts at baseline (Con) and 4 hours post-MI. **A.** Parkin does not translocate to mitochondria in WT remote zone after MI. **B.** Ubiquitination is not increased in WT cytosol or mitochondria fractions after 4 hours of MI. n=4 for all.

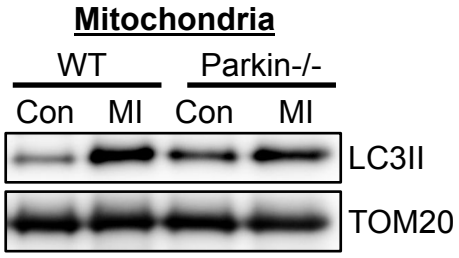

Figure 4.11. Mitochondria-associated LC3II is an indicator of mitophagy. Representative western blot of mitochondria-associated LC3II in border zone mitochondria after 4 hours of MI. n=4 for each group.

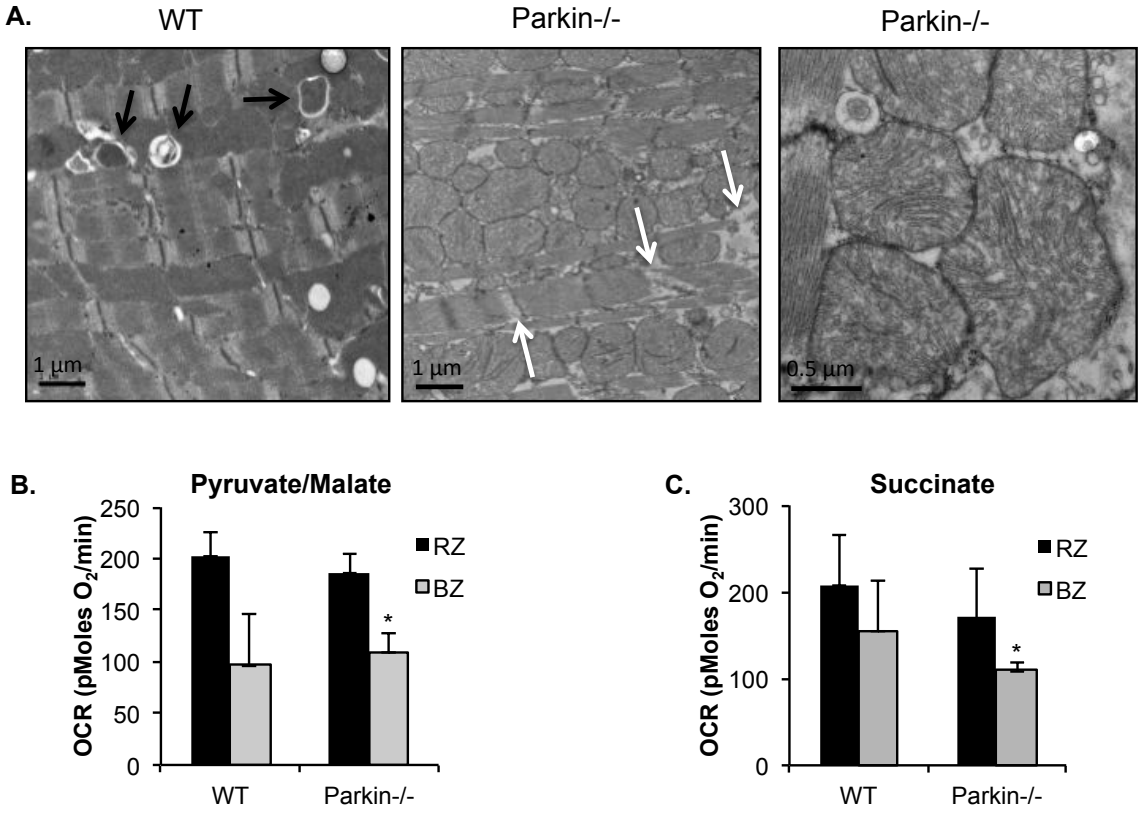

Figure 4.12. Accumulation of damaged mitochondria in Parkin-deficient hearts after MI. **A.** Ultrastructural analysis by transmission electron microscopy of WT and Parkin-/- myocytes in the border zone of the infarct 4 h post-MI. Black arrows indicate autophagosomes and white arrows indicate disrupted contractile elements. Oxygen consumption rates (OCR) of mitochondria in the remote zone (RZ) and border zone (BZ) 4 h post-MI with pyruvate/malate **(B)** or succinate/rotenone **(C)** as substrates. Mean ± SEM (n=5 for WT, n=6 for Parkin-/-).

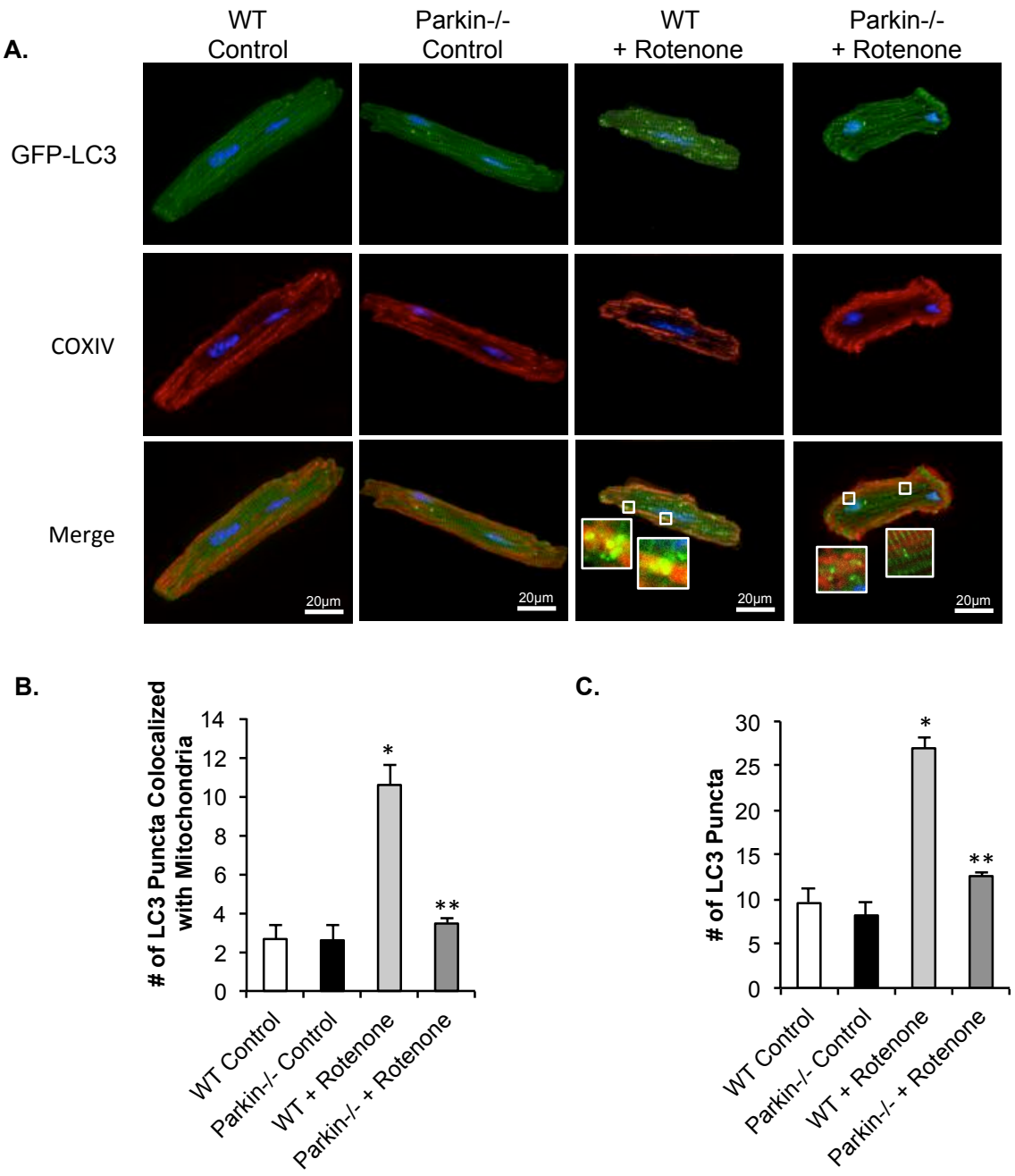

Figure 4.13. Rotenone treatment fails to induce mitophagy in Parkin-/- myocytes. **A.** Representative images of WT and Parkin-/- myocytes. Cells infected with LC3-GFP were treated with DMSO or 40μM rotenone for 1 h. After fixation, mitochondria were stained with anti-COXIV. **B.** Quantitation of autophagosomes colocalizing with mitochondria. Mean ± SEM (n=3;*p<0.05 vs. WT Con, **p>0.05 vs. Parkin-/- Control)**. C.** Quantitation of the mean number of LC3-GFP positive autophagosomes per cell in WT and Parkin-/- myocytes. Mean ± SEM (n=3;*p<0.05 vs. WT Con, **p>0.05 vs. Parkin-/- Control).

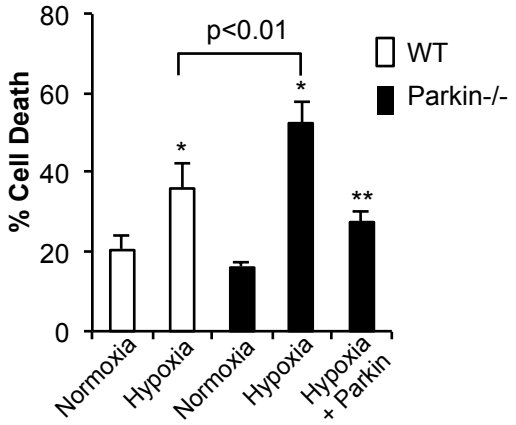

Figure 4.14. Adult myocytes from WT or Parkin-/- mice were infected with Ad-β-Gal or Ad-Parkin for 24 h prior to 4 h of hypoxia and quantitation of cell death. Mean ± SEM (n=3, *p<0.05 vs. Normoxia, **p<0.05 vs. Hypoxia). The increased susceptibility to hypoxia-induced cell death in Parkin-/- myocytes was rescued by Parkin overexpression.

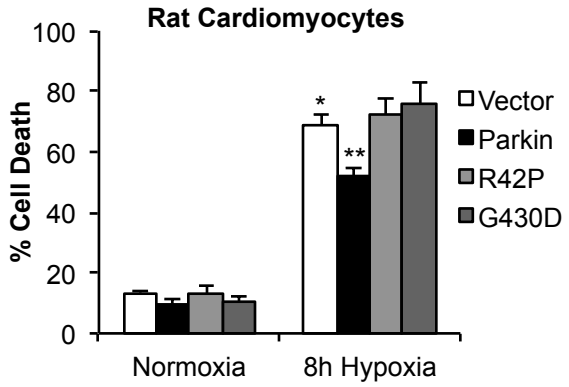

Figure 4.15. Overexpression of Parkin protects cardiac myocytes against hypoxia-mediated cell death. Adult rat cardiomyocytes were infected with adenoviruses encoding empty vector, Parkin, ParkinR42P (R42P) or ParkinG430D (G430D) for 24 h prior to 8 hours of hypoxia and quantitation of cell death. Mean ± SEM (n=3-5, *$p<0.05$ vs. Normoxia + Vector, **$p<0.05$ vs. Hypoxia + Vector).

CHAPTER 5: MECHANISMS OF PARKIN FUNCTION IN THE HEART

5.1 Abstract

The mechanisms by which Parkin and PINK1 promote mitophagy have been studied in neuronal cell culture systems, but are still incompletely understood in the mammalian heart. It is also unclear how mitochondrial fission influences Parkin-mediated mitophagy. In this chapter, I investigated the interplay between Parkin, PINK1, and mitochondrial fission during cardiac stress. I found that the mitochondrial fission protein Dynamin-related protein 1 (Drp1) translocated to uncoupled mitochondria in Parkin-/- hearts perfused with FCCP. Moreover, overexpression of a dominant negative mutant of Drp1 (Drp1K38E) blocked Parkin translocation. I also found that Parkin was able to translocate to dysfunctional mitochondria in hearts from PINK1-/- mice following FCCP perfusion or MI. These data indicate that Drp1 translocation precedes Parkin translocation to dysfunctional mitochondria, and that Parkin translocation is dependent upon Drp1 function. Because Parkin was able to translocate to uncoupled mitochondria in the absence of PINK1, Parkin translocation is not dependent on PINK1 function and it is likely that alternative pathways for Parkin recruitment exist.

5.2 Introduction

Most studies on the mechanism of Parkin activity in mammalian cells have been performed in neuronal or immortalized cell lines. I have found that Parkin-

deficient mice develop cardiac dysfunction after stress (Chapters 4), and that Parkin translocates to border zone mitochondria soon after a myocardial infarction (MI), where it ubiquitinates proteins and promotes mitophagy (Chapter 4). Prior studies have shown that Parkin translocation from the cytosol to dysfunctional mitochondria is preceded by accumulation of the serine/threonine kinase PINK1 on those mitochondria. Parkin translocation is thought to depend upon PINK1 first accumulating on mitochondria that have lost their membrane potential ($\Delta\Psi m$) (Chen and Dorn, 2013; Matsuda et al., 2010; Narendra et al., 2010a). However, overexpressed Parkin may be able to function in the absence of PINK1 in *Drosophila* and neuronal cell cultures (Clark et al., 2006; Dagda et al., 2009; Park et al., 2006). Parkin's dependence on PINK1 has not yet been explored in the myocardium.

Studies have also shown that mitochondrial fission and fusion can influence mitophagy. Dynamin-related protein 1 (Drp1) is a cytosolic GTPase that oligomerizes on mitochondria as part of the fission process (Smirnova et al., 2001). Deficiency of the mitochondrial fission protein Drp1 in MEFs impairs Parkin-mediated mitochondrial clearance (Tanaka et al., 2010), and fission has been found to be a prerequisite for mitophagy in cardiac myocytes (Lee et al., 2011). However, the dynamic between Parkin, PINK1, and mitochondrial fission mediated by Drp1 has not been explored in the myocardium *in vivo*. In this chapter, I examined the molecular mechanisms for Parkin function in the mammalian heart, particularly in response to stress conditions. I investigated Drp1 translocation in response to MI in wild type (WT) and Parkin-deficient

(Parkin-/-) mice. Although Drp1 translocation was determined to not depend on Parkin, translocation of Parkin was dependent on activity of Drp1. Fission is therefore a prerequisite for Parkin translocation. I then investigated Parkin and Drp1 activity in the hearts of PINK1-knockout (PINK1-/-) mice following mitochondrial stress. I determined that Parkin translocation could occur independently of PINK1 in the heart, a finding that has not previously been reported. These results demonstrate novel properties of Parkin function that have previously not been found in the mammalian heart.

5.3 Results

5.3.1 Drp1 Activity Is Not Dependent on Parkin, But is Required for Parkin Function

Mitochondrial fission has been reported to precede mitophagy, and impairment of mitochondrial fission is also known prevent mitophagy (Lee et al., 2011; Twig et al., 2008). For these reasons, I examined the activity of the mitochondrial fission protein Drp1 following MI. I assessed the levels of Drp1 that were associated with mitochondria after 2 hours of MI in the border zones from WT and Parkin-/- mice and found elevated Drp1 levels on border zone mitochondria from WT mice, but not on Parkin-/- mitochondria after 2 hours of MI. This suggested a possible impairment in the fission process in mice lacking Parkin (Figure 5.1A). Alternatively, Drp1 translocation in Parkin-/- mice could either have been delayed, or could have occurred earlier and had already terminated at the 2-hour time point. To test whether Drp1 was translocating to

Parkin-/- mitochondria in a delayed fashion, I assessed mitochondrial Drp1 levels in the border zone after 4 hours of MI. However, mitochondrial Drp1 levels were not found to be above baseline in either WT or Parkin-/- border zone samples, suggesting that Drp1 translocation was not delayed in Parkin-/- mice (Figure 5.1B). Therefore, I tested whether Drp1 retained its capability of translocating to mitochondria in Parkin-/- mice by perfusing hearts *ex vivo* with the mitochondrial uncoupler FCCP. FCCP is a strong protonophore and a potent uncoupler of oxidative phosphorylation. By extinguishing the intermembrane proton gradient, FCCP causes rapid loss of mitochondrial membrane potential. Perfusion of WT hearts with FCCP resulted in Parkin translocation within 5 minutes, with mitochondrial Parkin levels remaining elevated for at least 15 minutes (Figure 5.2B). Concomitantly, Drp1 began accumulating on WT mitochondria after 5 minutes of perfusion and reached maximal levels by 15 minutes of perfusion time. I also observed a similar pattern of Drp1 translocation in Parkin-/- mitochondria from hearts perfused with FCCP despite the absence of Parkin (Figure 5.2B). These results confirm that Drp1 is able to translocate to uncoupled mitochondria in Parkin-/- mouse hearts and is therefore not dependent on the presence of Parkin. This also suggests that Drp1 translocation in Parkin-/- mouse hearts was either impaired after MI *in vivo* or occurred at a time point earlier than 2 hours after LAD ligation.

To further clarify the role of Drp1 in Parkin recruitment, I infected isolated adult rat cardiac myocytes with an adenovirus expressing mCherry-Parkin and subjected them to hypoxia. Translocation of Parkin to mitochondria was

confirmed after 4 hours of hypoxia by pseudo-linescan analyses of mCherry-Parkin colocalization with COXIV-labeled mitochondria (Figure 5.3A and 5.3C). However, co-overexpression of a dominant-negative mutant of Drp1 (Drp1K38E) abrogated Parkin translocation during hypoxia (Figure 5.3A – 5.3C). This suggests that Drp1-mediated mitochondrial fission is a prerequisite for Parkin translocation.

5.3.2 Parkin Translocation is Independent of PINK1

PINK1 is a mitochondrial kinase that is upstream of Parkin and accumulates on mitochondria in response to uncoupling by the protonophore CCCP (Matsuda et al., 2010; Narendra et al., 2010a). To further explore the relation between the Parkin/PINK1 pathway and Drp1 function, I utilized PINK1-deficient (PINK1-/-) mice (Gispert et al., 2009) for *ex vivo* protonophore (FCCP) perfusion experiments. Although FCCP treatment of cell lines causes mitochondrial accumulation of PINK1 (Matsuda et al., 2010; Narendra et al., 2010a), 15 min of FCCP perfusion did not result in the accumulation of PINK1 on mitochondria in WT mouse hearts (Figure 5.4). Thus, Parkin was found to translocate to the mitochondria in FCCP-perfused WT hearts despite the absence of PINK1 accumulation on mitochondria. Notably, FCCP perfusion of PINK1-/- hearts resulted in rapid translocation of Drp1 to mitochondria, indicating that PINK1 does not participate in recruitment of Drp1 (Figure 5.5B). Surprisingly, Parkin was also found to translocate to the mitochondria in FCCP-perfused

PINK1-/- hearts within 5 minutes (Figure 5.5B), suggesting that PINK1 is not required for initiating Parkin translocation in the myocardium.

To further investigate whether or not PINK1 is a required component for Parkin translocation *in vivo*, I subjected WT and PINK1-/- mice to MI. Four hours of MI resulted in Parkin accumulation in the mitochondrial fraction of border zone tissue from both WT and PINK1-/- mice (Figure 5.6). Interestingly, I also found that PINK1-/- hearts had significantly higher total Parkin protein levels than WT mice under baseline conditions (Figure 5.7). Since PINK1 deficiency has been reported to lead to mitochondrial dysfunction and development of cardiac hypertrophy (Billia et al., 2011), this finding further supports the conclusion that Parkin is involved in adapting to mitochondrial stress in the myocardium. I observed a similar upregulation of Parkin in isolated adult rat cardiac myocytes overexpressing Bnip3 (Figure 5.8), a mitochondrial BH3-only protein that is known to cause mitochondrial dysfunction in cells (Regula et al., 2002; Rikka et al., 2011). Taken together, these data suggest that Parkin protein levels are elevated during times of myocyte stress, and that activation of Parkin occurs rapidly in response to mitochondrial damage.

5.4 Discussion

Most studies on Parkin have focused on its role in mitophagy and its potential mitochondrial substrates. In this chapter, I investigated the relationship between the PINK1/Parkin pathway and mitochondrial fission in the heart. Mitochondrial fission has been proposed to precede mitophagy (Lee et al., 2011;

Twig et al., 2008). In agreement with this, I found that translocation of the fission protein Drp1 precedes Parkin translocation. Moreover, Drp1 function is a prerequisite for Parkin translocation to mitochondria. Further, although Drp1 has been identified as a substrate of Parkin (Wang et al., 2011a), I found that Parkin is not necessary for Drp1 recruitment following mitochondrial damage. Therefore, Parkin-mediated ubiquitination may help to stabilize Drp1 on mitochondria. In support of this, Drp1 accumulation on mitochondria was not observed in Parkin-/- border zones at either 2 or 4 hours after MI. Alternatively, this could suggest that the mitochondria in Parkin-/- hearts are pre-sensitized to stress, such that MI causes translocation of Drp1 at a time point earlier than in WT hearts. Drp1 accumulation on mitochondria was confirmed in Parkin-/- hearts perfused with FCCP, indicating that Drp1 is functional and capable of translocation in the absence of Parkin and supporting the notion that Drp1 translocation might occur earlier in Parkin-/- hearts than in WT hearts after MI. These studies help clarify the interplay between mitochondrial dynamics and Parkin-mediated mitophagy.

The most notable finding reported here is that Parkin is able to translocate to mitochondria in the heart in the absence of PINK1. Accumulation of PINK1 on mitochondria that have lost $\Delta\Psi m$ and subsequent phosphorylation of Mfn2 by PINK1 are events that have been reported to precede and promote Parkin translocation (Chen and Dorn, 2013). In contrast to prior studies, I found that Parkin was able to accumulate mitochondria in PINK1-/- hearts both in an *ex vivo* model of FCCP perfusion as well as *in vivo* after MI. In *Drosophila*, loss of PINK1 can be compensated for by transgenic overexpression of Parkin (Clark et al.,

2006; Park et al., 2006). Likewise, the increase in Parkin protein levels that I found in the hearts of PINK1-/- mice may be sufficient to compensate for loss of PINK1. These mice have been reported to develop cardiac and mitochondrial dysfunction (Billia et al., 2011). The elevated levels of mitochondria-associated Parkin in PINK1-/- mice at baseline may therefore be indicative of mitochondrial damage. The upregulation of total Parkin levels in PINK1-/- mice may be in response to accumulating myocyte damage, a hypothesis that is congruent with the upregulation of Parkin observed in the border zone following MI (Chapter 4) and in cardiomyocytes overexpressing the pro-apoptotic and pro-mitophagy protein Bnip3.

Although it was previously assumed that PINK1 stabilization on mitochondria was necessary for Parkin recruitment and subsequent activation of mitophagy in mammalian cells, the data presented here indicate that other pathways independent of PINK1 may also activate Parkin. Parkin may respond to both mitochondrial and cytosolic signals to initiate mitophagy, and although we now understand some of the events that lead to Parkin activation, the mechanisms for Parkin transport and anchoring to mitochondria are still unclear. My data demonstrate that Parkin translocation is not dependent on PINK1, but whether these mitochondria can still be removed by autophagosomes has not yet been investigated. Lastly, while Parkin is clearly important in acute cardiac stress that results in rapid mitochondrial damage, the involvement of Parkin in the response to more chronic cardiac disease states remains unexplored.

Chapter 5, in part, was originally published in the Journal of Biological Chemistry. Kubli, D. A., Zhang, X., Lee, Y., Hanna, R. A., Quinsay, M. N., Nguyen, C. K., Jimenez, R., Petrosyan, S., Murphy, A.N., Gustafsson, A.G. Parkin Protein Deficiency Exacerbates Cardiac Injury and Reduces Survival following Myocardial Infarction. *The Journal of Biological Chemistry*. 2013; *288*(2), 915–926.

A.

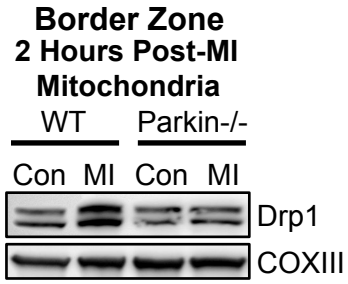

B.

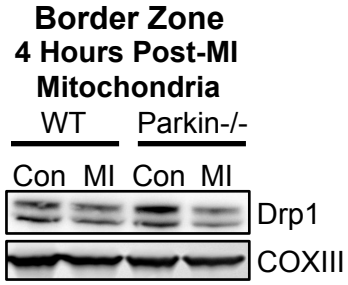

Figure 5.1. Representative western blots of mitochondrial Drp1 in WT and Parkin-/- mouse border zones at baseline (Con) and at 2 hours **(A)** or 4 hours **(B)** post-MI. n=4 for each group.

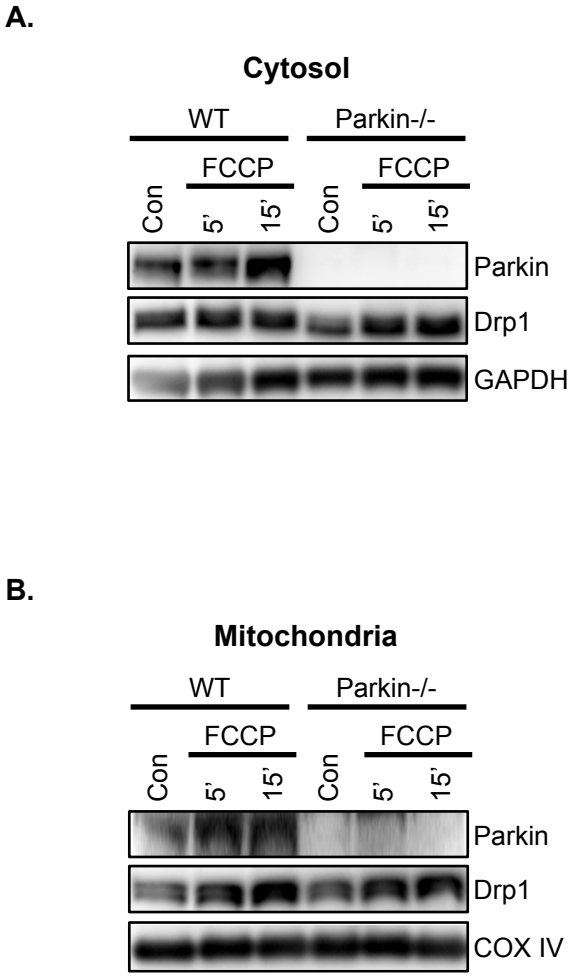

Figure 5.2. Drp1 translocation to mitochondria occurs before Parkin translocation and is not dependent on the presence of Parkin. Western blot of cytosolic **(A)** and mitochondrial **(B)** fractions of WT and Parkin-/- hearts perfused with either control buffer (Con) for 15 minutes or 100 nM FCCP for 5 or 15 minutes (n=4).

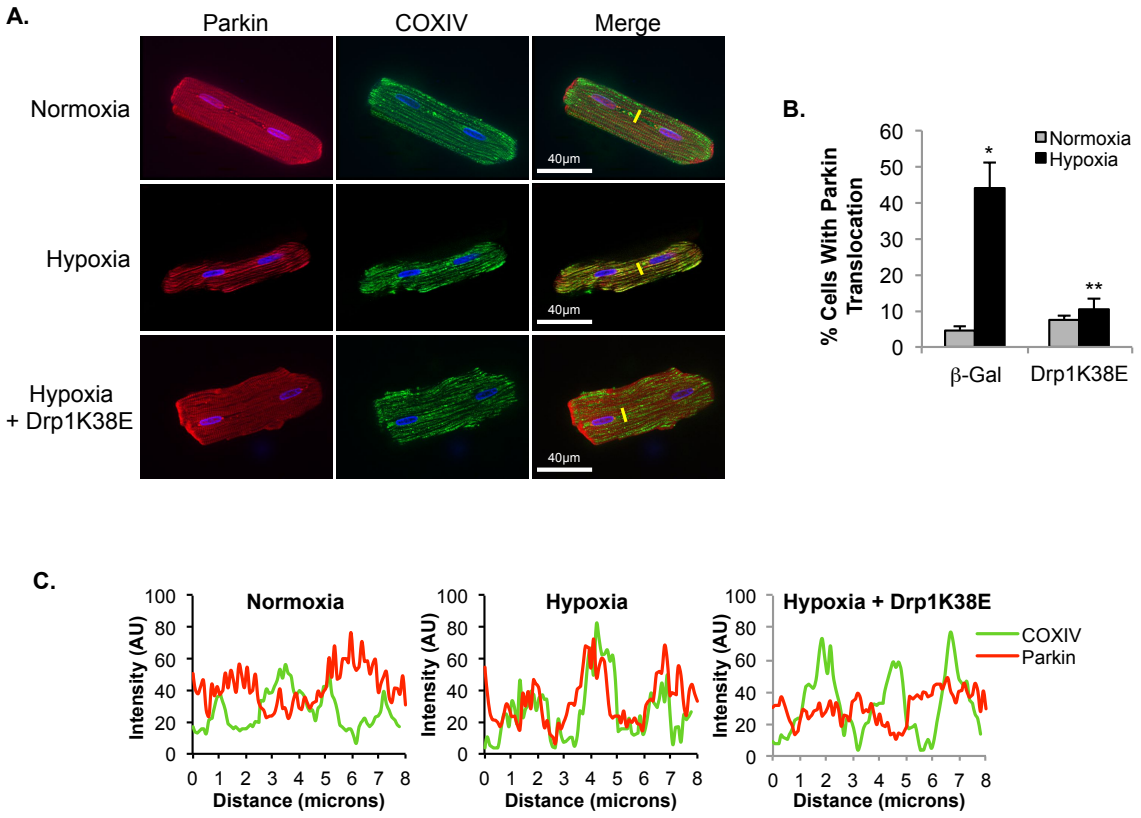

Figure 5.3. Four hours of hypoxia induced Parkin translocation to mitochondria that is abrogated by dominant-negative Drp1K38E. **A.** Representative images of adult rat cardiac myocytes infected with mCherry-Parkin adenovirus ± Drp1K38E and stained for mitochondrial COXIV. Yellow lines represent line scans. **B.** Quantitation of myocytes with mCherry-Parkin translocation. Data are Mean ± SEM (n=3-5, *p<0.01 vs. Normoxia, **p<0.01 vs. b-Gal). **C.** Representative line-scan analyses of adult rat cardiac myocytes demonstrating colocalization of Parkin (red line) with mitochondrial COXIV (green line).

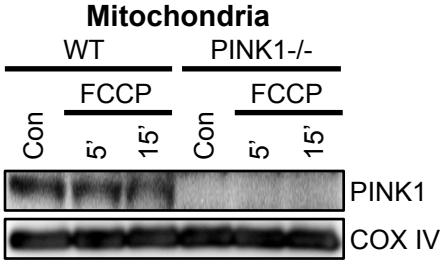

Figure 5.4. Western blot of mitochondrial fractions of WT and PINK1-/- hearts perfused with either control buffer for 15 minutes, or 100 nM FCCP for 5 or 15 minutes (n=3). Mitochondrial levels of PINK1 do not increase in WT hearts following *ex vivo* perfusion with FCCP.

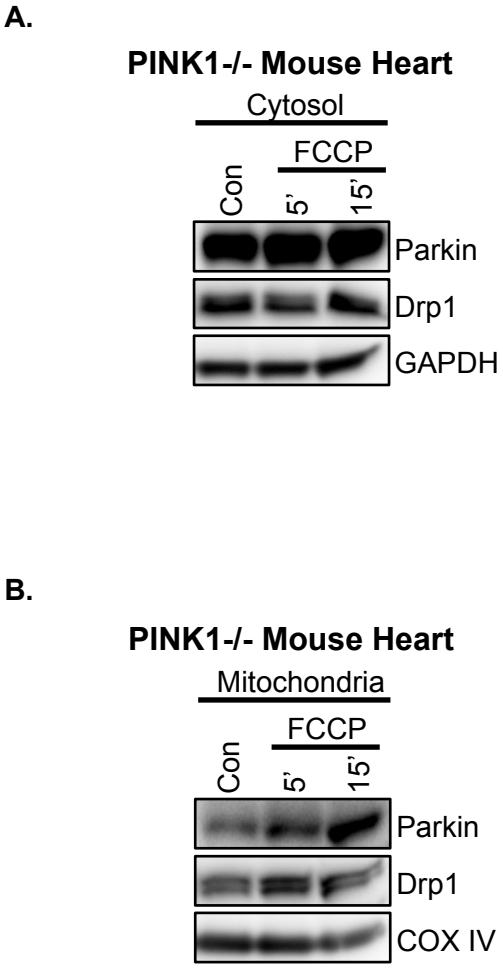

Figure 5.5. Parkin and Drp1 translocate to uncoupled mitochondria in the absence of PINK1. Western blot of cytosolic **(A)** and mitochondrial **(B)** fractions of PINK1-/- hearts perfused with either control buffer for 15 minutes or 100 nM FCCP for 5 or 15 minutes (n=3).

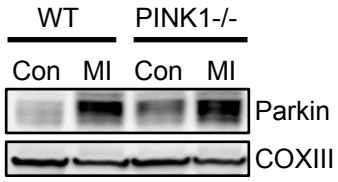

Figure 5.6. Parkin translocation to mitochondria is not dependent on PINK1. Western blot of the mitochondrial fractions of WT and PINK1-/- hearts at baseline (Con) or four hours post-MI (n=3).

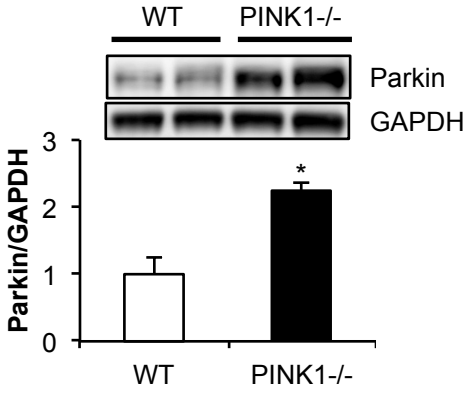

Figure 5.7. PINK1-/- hearts from 10 – 12-week old mice have significantly higher total Parkin protein levels than WT hearts under baseline conditions. Western blots and quantitation of Parkin protein levels in PINK1-/- hearts. Mean ± SEM (*$p<0.01$ vs. WT, n=4-5).

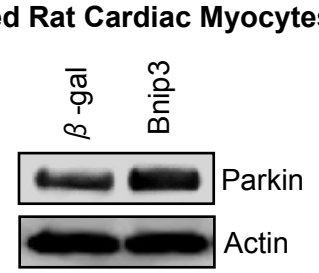

Figure 5.8. Overexpression of the mitochondrial stressor and mitophagy promoting-protein Bnip3 for 24 hours results in elevated Parkin protein levels in isolated adult rat cardiac myocytes (n = 4).

CHAPTER 6: PARKIN IS ESSENTIAL FOR DEVELOPMENT OF CARDIAC HYPERTROPHY

6.1 Abstract

I have found that Parkin is critical for the adaptation response to acute cardiac stress. Parkin ubiquitinates mitochondrial and cytosolic components following myocardial infarction, and promotes removal of dysfunctional mitochondria in the infarct border zone. Here, I investigate the involvement of Parkin in the response to chronic stress conditions. I subjected wild type (WT) and Parkin knockout (Parkin-/-) mice to swimming exercise for two weeks before evaluating cardiac hypertrophy. Parkin-/- mice showed impaired cardiac hypertrophy in response to the physiological stress. Similarly, when subjected to 2 weeks of cardiac pressure overload by transverse aortic constriction (TAC), Parkin-/- mice had an impaired pathological hypertrophy response. For comparison, I also subjected cardiac-specific Parkin-transgenic (Parkin-TG) mice to 2 weeks of TAC. Although cardiac hypertrophy was found to be equivalent between WT and Parkin-TG mice, Parkin-TG mice had hallmarks of early heart failure and showed significant declines in heart function. Thus, Parkin plays an important role in the cardiac hypertrophy response. However, excessive levels of Parkin can be detrimental and may prime the heart for accelerated heart failure in response to some stressors.

6.2 Introduction

In previous chapters, I have shown that Parkin-/- mice respond poorly to acute cardiac stress as is experienced during MI. The poor adaptation to cardiac stress in Parkin-/- mice appears to be primarily due to impaired mitophagy and autophagy, particularly in the border zone of the infarct. Autophagy is also involved in the cardiac hypertrophy that occurs in response to physiological or pathological stress (He et al., 2012; Zhu et al., 2007). In response to physiological stress such as regular exercise or pregnancy, the myocardium expands via enlargement of the cardiomyocytes. This expansion is accompanied by increased cardiac performance, but is reversible when the stimulus is removed (Maillet et al., 2013). In comparison, pathological stimuli such as hypertension or aortic stenosis also lead to expansion of the myocardium, but eventually decompensation results in the development of dilated cardiomyopathy (Maillet et al., 2013). The resulting functional decline is irreversible and can lead to heart failure. Although the etiology and progression of these two hypertrophy responses differ greatly, several signaling pathways are common to both. For instance, *Akt1*-null mice show deficits in exercise-induced physiological hypertrophy, but pressure overload induces exacerbated pathological hypertrophy and heart failure, which demonstrates the distinct role of the AKT signaling pathway in each context (DeBosch et al., 2006).

In this chapter, I investigated the role of Parkin in the response to pathophysiological stress conditions that are known to elicit a cardiac hypertrophy response. To investigate the role of Parkin in physiological

hypertrophy, I subjected Parkin-/- mice to long-term swimming exercise. I found that mice lacking Parkin have an impaired physiological hypertrophy response in comparison with WT mice. Additionally, Parkin-/- mice have impaired pathological hypertrophy in response to cardiac pressure overload. In contrast, mice overexpressing Parkin in cardiac myocytes (Parkin-TG) have a pathological hypertrophy response that is similar to WT mice, but rapidly develop heart failure in response to pressure overload. Thus, Parkin plays an important role in promoting hypertrophy, but excessive Parkin levels can also be detrimental during cardiac stress.

6.3 Results

6.3.1 Physiological Hypertrophy is Impaired in Parkin-/- Mice

I previously found that Parkin-/- mice are more sensitive to myocardial infarction (MI) as a result of impaired clearance of dysfunctional mitochondria that accumulate after the MI (Chapter 4). To test if the mitophagy deficits observed in Parkin-/- mice during cardiac stress would affect physiological cardiac hypertrophy or heart function in response to exercise, I subjected WT and Parkin-/- mice to swimming exercise. Mice were first acclimated to swimming for a period of 9 days, with twice-daily swimming sessions beginning with 10 minutes and increasing in length by 10 minutes daily. Thus, by the 9^{th} day, mice were swimming for 90 minutes twice daily, and this regimen was maintained for 2 weeks. At the end of the study, the cohort of Parkin-/- mice that had exercised had significantly lower mean body weight than both the non-swimming (resting)

Parkin-/- mouse cohort and the swimming WT cohort (Figure 6.1). When normalized to tibia length, Parkin-/- swimming mice had significantly lower heart weight/tibia length ratios than WT swimming mice (Figure 6.2), which is indicative of impaired hypertrophy in response to the exercise stimulus.

To determine if the smaller heart sizes observed in Parkin-/- mice after swimming had an effect on heart function, I performed echocardiography 24-hours after the final swimming session. Remarkably, despite having smaller hearts, Parkin-/- mice had normal cardiac function, with fractional shortening (%FS) and ejection fraction (%EF) values that were equivalent to WT (Figure 6.3). However, hearts from swimming Parkin-/- mice showed significantly lower endocardial stroke volume than hearts from swimming WT mice (Figure 6.4), which reflects the finding that Parkin-/- mice failed to increase heart size in response to exercise. Taken together, these data indicate that Parkin-/- mice had impaired physiological hypertrophy in response to swimming exercise, although cardiac function was not affected in Parkin-/- mice.

To investigate if changes in autophagy were contributing to the failure of Parkin-/- mice to undergo cardiac hypertrophy after exercise, I assessed autophagy levels WT and Parkin-/- mouse hearts. At the end of the two-week swimming period, WT mice showed no increase in LC3II/LC3I ratio, indicating that autophagy was occurring at the same rate as in resting WT mice (Figure 6.5). In contrast, Parkin-/- mice showed a significant decrease in LC3II/LC3I ratio, suggesting a reduction or possibly an impairment in autophagy following chronic exercise (Figure 6.5). To determine if this signified an inability of Parkin-/- mice to

upregulate autophagy following exercise, I assessed changes in autophagy in WT and Parkin-/- hearts after mice were subjected to acute swimming. After two days of training, I subjected mice to a single 90-minute session of swimming and collected hearts immediately afterwards. Western blots of LC3I and LC3II protein levels demonstrated that Parkin-/- mice upregulate autophagy in response to exercise to the same extent as WT mice (Figure 6.6). This suggests that the impairment in physiological hypertrophy observed in Parkin-/- mice is not due to an inability to upregulate autophagy in response to exercise, but may be the result of chronically suppressed autophagy instead.

6.3.2 Parkin-/- Mice Have Impaired Pathological Hypertrophy

To further investigate the cardiac hypertrophy response of Parkin-/- mice, I subjected WT and Parkin-/- mice to cardiac pressure overload by transverse aortic constriction (TAC). After 2 weeks of TAC, WT mice showed a 30% increase in heart weight to tibia length (HW/TL) ratios compared to sham WT mice (Figure 6.7). In contrast, Parkin-/- HW/TL ratio did not increase after 2 weeks of TAC, and was significantly lower than the WT HW/TL ratio (Figure 6.7). These data suggest that Parkin-/- mice have impaired pathological hypertrophy in addition to blunted physiological hypertrophy. I evaluated the contractile function of Parkin-/- mice by echocardiography after TAC to determine if a failure to increase heart size correlated with augmented cardiac dysfunction. However, both WT and Parkin-/- mice displayed similar declines in function compared to sham animals (Figure 6.8). Thus, although the hearts of Parkin-/- mice do not

increase in size after TAC, the cardiac functional decline is equivalent to that of WT mice.

To further assess hypertrophy after 2 weeks of TAC, I evaluated mRNA transcript levels of the hypertrophy markers skeletal muscle actin (SMA), β-myosin heavy chain (β-MHC), and atrial natriuretic factor (ANF) by real time quantitative PCR (qPCR). All three hypertrophy markers were elevated in WT mice after 2 weeks of TAC. However, Parkin-/- mice showed no increase in any of these three markers, suggesting an impaired pathological hypertrophy response (Figure 6.9). To confirm the hypertrophy deficiency, I calculated the mean myocyte area from cross-sections of heart tissue that had been stained with Alexa Fluor 488-conjugated wheat germ agglutinin to stain cell surfaces. After 2 weeks of TAC, the mean myocyte area in WT mice increased significantly compared to sham animals (Figure 6.10). Mean myocyte area in Parkin-/- TAC mice did not significantly increase compared to sham mice after 2 weeks (Figure 6.10). These data confirm that Parkin-/- mice have an impaired pathological hypertrophy response in addition to physiological hypertrophy deficits.

6.3.3 Parkin Transgenic Heart Function Rapidly Declines After TAC

Because Parkin deficiency conferred a defect in both pathological and physiological hypertrophy, I next sought to determine if Parkin overexpression would exacerbate hypertrophy. To further investigate the role of Parkin in hypertrophy in response to chronic stress, I subjected cardiac-specific Parkin transgenic mice (Parkin-TG, described in Chapter 3) to 2 weeks of TAC.

Compared to WT mice, Parkin-TG mice showed equivalent increases in HW/TL ratios after 2 weeks of TAC, suggesting that pathological hypertrophy is not disproportionately high in Parkin-TG mice (Figure 6.11). In addition, I found that mean cardiac myocyte area was significantly increased in Parkin-TG mice in response to TAC, but this increase was not different when compared to WT mice that had received the TAC (Figure 6.11). To confirm that pathological hypertrophy in Parkin-TG mice is on par with that of WT mice, I assessed transcript levels of hypertrophy marker genes by qPCR. Parkin-TG mice subjected to TAC were found to have transcript levels of SMA and ANF that were similar to WT levels, while transcript levels of β-MHC were highly variable but tended to be higher than in WT TAC mice (Figure 6.12).

Interestingly, Parkin-TG mouse lung weight to tibia length (LW/TL) ratio was markedly increased compared to WT values after TAC (Figure 6.13). Increased lung weight is an indicator of pulmonary edema resulting from cardiac insufficiency. I also assessed contractile function in Parkin-TG mice subjected to TAC by echocardiography. Parkin-TG mice had significantly impaired %FS and %EF after 2 weeks of TAC compared to WT mice (Figure 6.14). This supports the conclusion that Parkin overexpression in cardiac myocytes leads to accelerated development of heart failure in response to cardiac pressure overload.

To determine if the rapid progression to heart failure observed in Parkin-TG animals after TAC was due to excessive Parkin-mediated mitophagy, I assessed levels of autophagy and mitochondria in WT and Parkin-TG hearts

after 2 weeks of TAC. At the endpoint, autophagy levels were not increased in either WT or Parkin-TG hearts based on LC3II/LC3I western blots (Figure 6.15). Additionally, mitochondria levels were slightly elevated in both WT and Parkin-TG hearts after 2 weeks of TAC, as determined from densitometry of immunoblots for the mitochondrial outer membrane protein TOM20 and the inner membrane protein TIM23 (Figure 6.15). The early heart failure phenotype observed in Parkin-TG mice subjected to TAC is therefore unlikely to be the result of excessive mitochondrial clearance.

6.4 Discussion

Here, I demonstrated that Parkin plays an important role in promoting cardiac hypertrophy. Mice deficient in Parkin have a failure in physiological hypertrophy in response to exercise, as well as in pathological hypertrophy in response to chronic cardiac pressure overload. However, no differences in cardiac function were noted between WT and Parkin-/- mice. A later endpoint may help to determine whether a failure to hypertrophy eventually becomes detrimental, or whether the eventual progression to decompensation and heart failure are delayed. Of note, the lack of transcriptional upregulation of hypertrophy markers in Parkin-/- mice subjected to TAC suggests that Parkin may directly influence the function of transcription factors. Additional studies are necessary to discern how Parkin deficiency confers an impairment in the hypertrophy response.

The most noteworthy finding presented here is that Parkin-TG mice rapidly progress to heart failure in response to cardiac pressure overload. This strongly suggests that excessive Parkin is harmful to the heart. The cardiomyopathy observed does not appear to be related to excessive hypertrophy, based on the comparable levels of hypertrophy marker gene transcripts and myocyte area between Parkin-TG and WT mice after TAC. Moreover, this detriment is apparently not due to excessive mitochondrial clearance. The possibility of mitochondrial dysfunction, however, has not yet been ruled out. Additionally, it is possible that changes in mitophagy may occur at a time point earlier than 2 weeks. A third possibility is that Parkin is affecting hypertrophy or cell survival pathways in previously uncharacterized ways. Parkin is known to have several cytosolic ubiquitination substrates (Sandebring and Mínguez, 2012), and I have previously noted increased Parkin-dependent ubiquitination of cytosolic proteins in response to myocardial infarction (Chapter 4). Therefore, future studies should focus on discerning between changes in mitophagy caused by Parkin deficiency or overexpression, and potential novel roles for Parkin in regulating cell survival, hypertrophy, and mitochondrial biogenesis pathways.

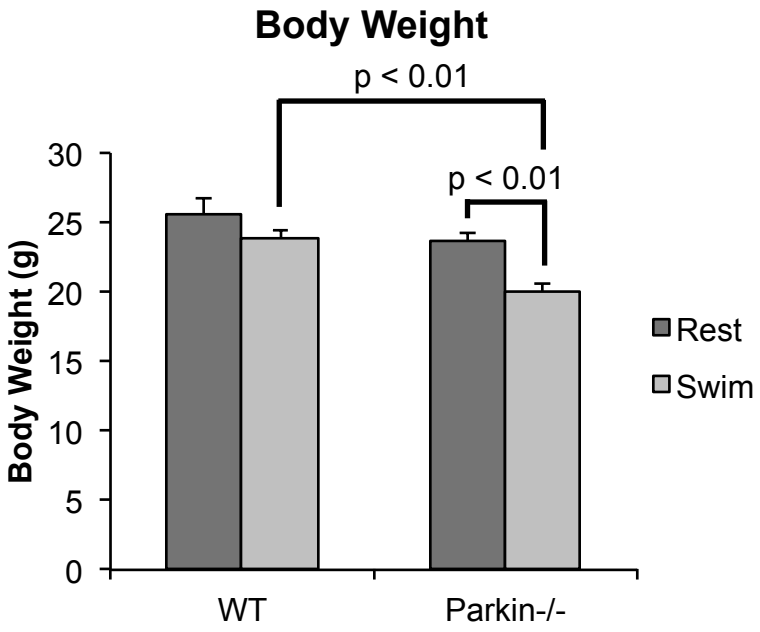

Figure 6.1. Two weeks of twice-daily exercise by swimming induced weight loss in 3-month old Parkin-/- mice. Mean ± SEM (n=3-6).

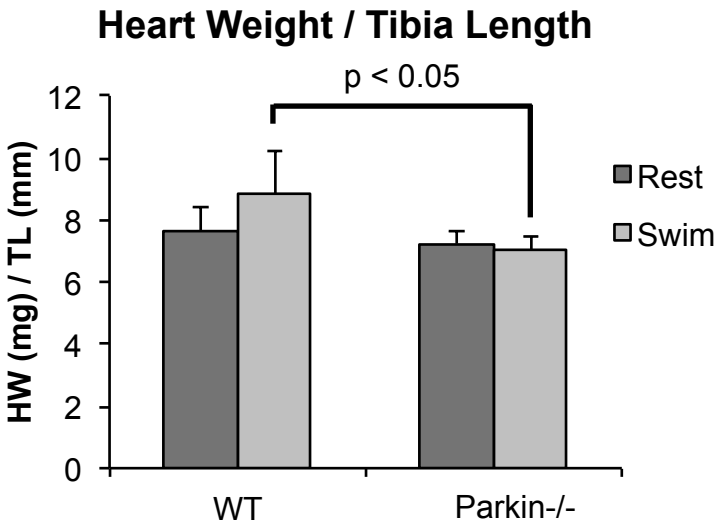

Figure 6.2. Parkin-/- mice failed to increase their heart weight (HW)/tibia length (TL) ratio after two weeks of twice-daily exercise by swimming. Mean ± SEM (n=4-6).

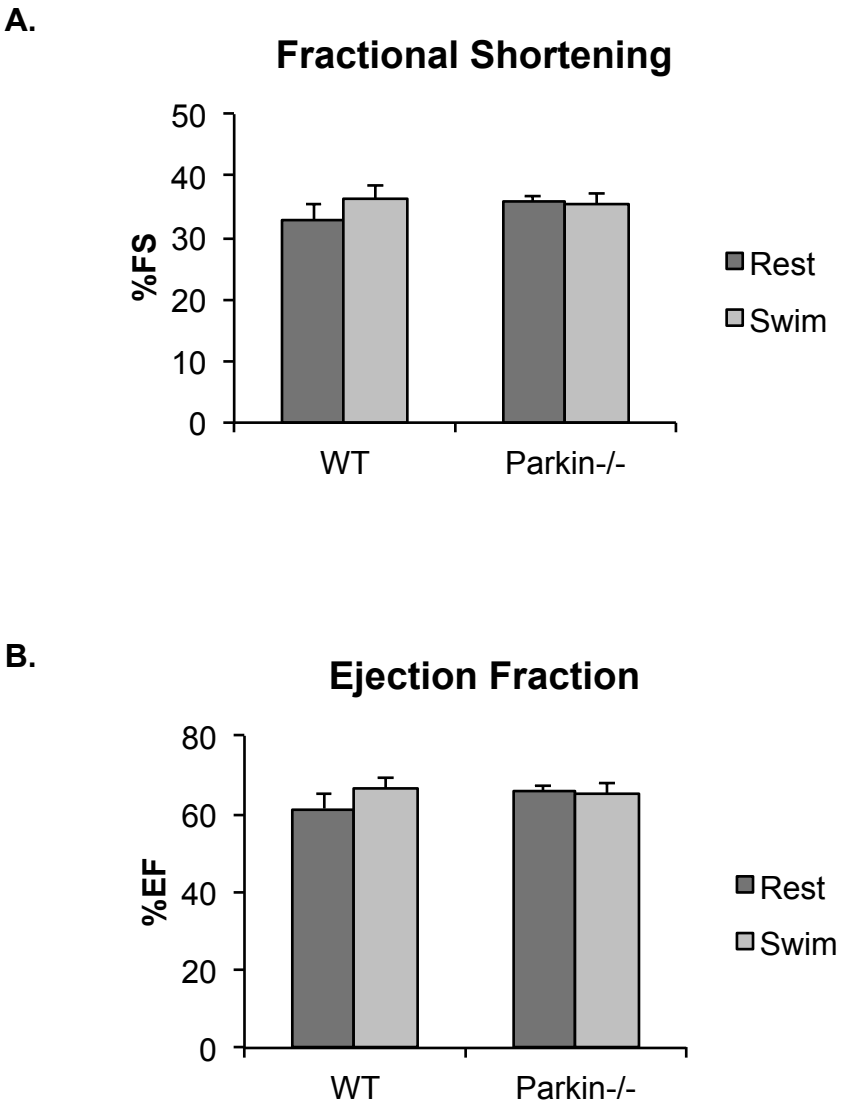

Figure 6.3. Neither WT nor Parkin-/- mice experienced changes in contractile function after two weeks of twice-daily swimming. No significant differences were observed in fractional shortening (%FS) **(A)** or ejection fraction (%EF) **(B)**. Mean ± SEM (n=4-6).

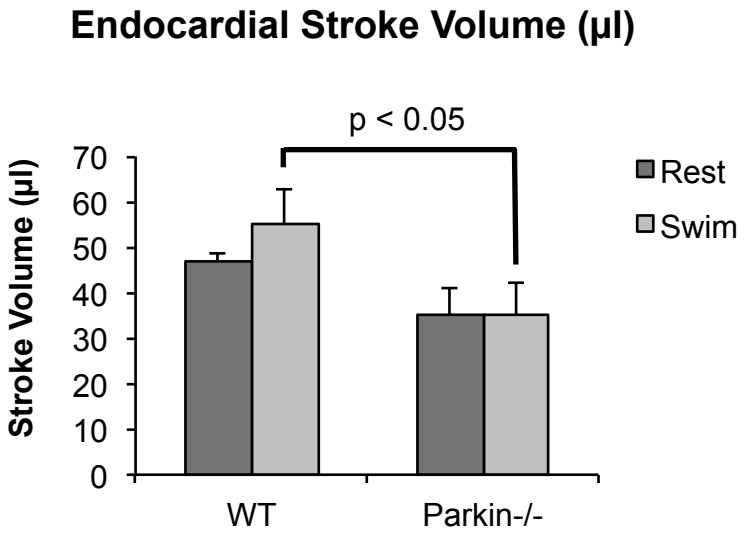

Figure 6.4. Parkin-/- mice did not increase their endocardial stroke volume after 2 weeks of swimming. Mean ± SEM (n=4-6).

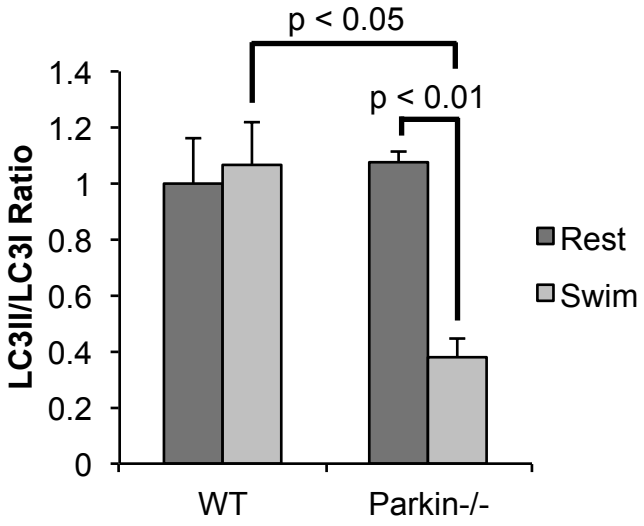

Figure 6.5. Autophagy was reduced in Parkin-/- mice after chronic exercise. Western blot densitometry revealed decreased LC3II/LC3I ratio in Parkin-/- swimming mice. Mean ± SEM (n=3-4).

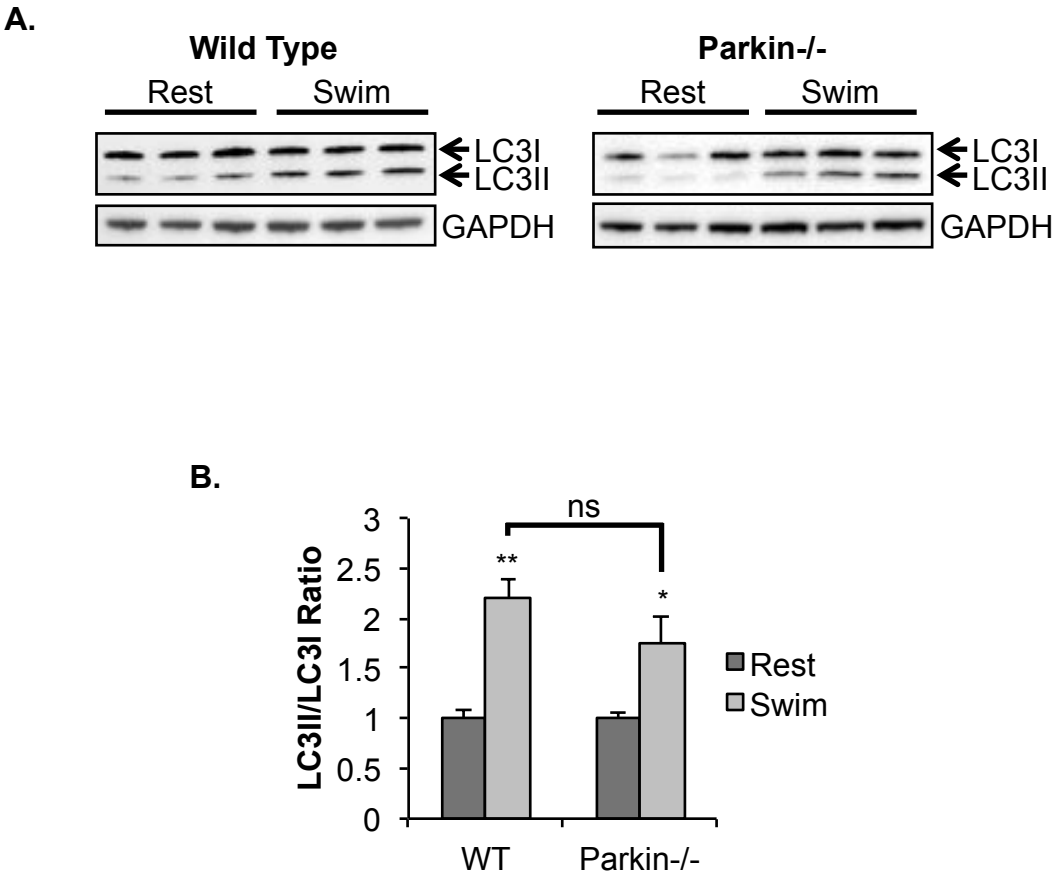

Figure 6.6. Acute exercise by swimming induces autophagy in 3-month old WT and Parkin-/- mouse hearts. **A.** Representative western blots of LC3I and LC3II in resting and swimming WT and Parkin-/- mice. **B.** Quantitation of LC3II/LC3I in WT and Parkin-/- at baseline and after acute swimming exercise. Mean ± SEM (n=5-6, *p<0.05, **p<0.01 vs. Rest)

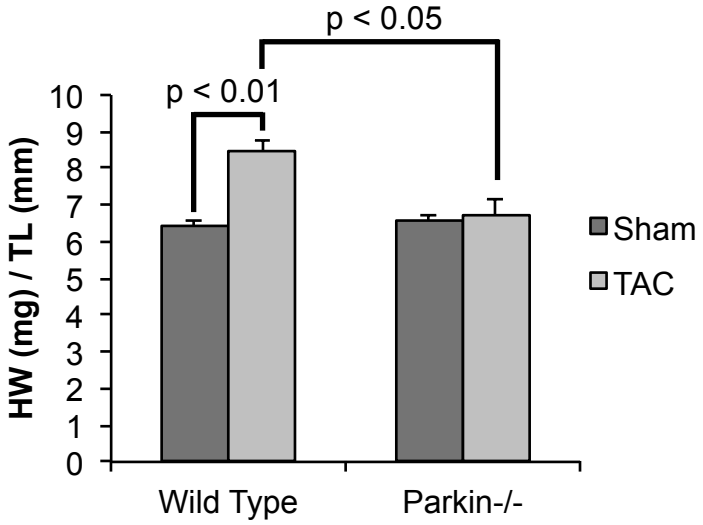

Figure 6.7. Two weeks of transverse aortic constriction (TAC)-induced pressure overload resulted in significantly elevated heart weight (HW)/tibia length (TL) ratio in WT mice compared to sham. Parkin-/- mice failed in increase HW/TL in response to TAC. Mean ± SEM (n=3-5).

A.

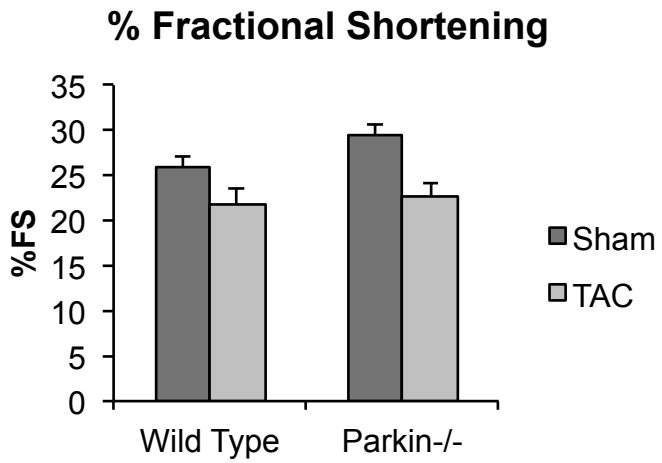

B.

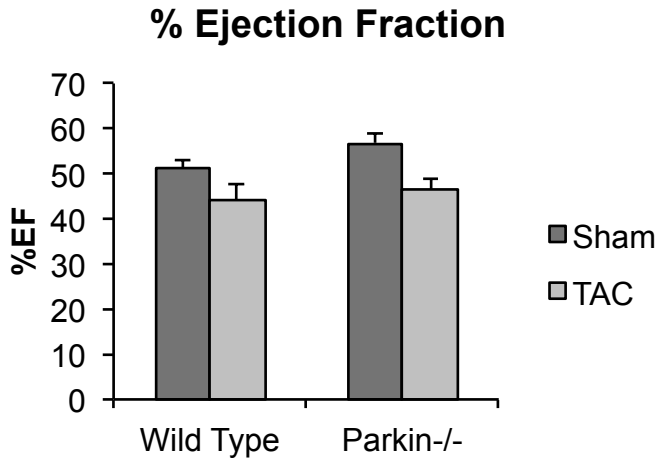

Figure 6.8. Echocardiography of WT and Parkin-/- mice after two weeks of TAC or Sham revealed no significant changes in fractional shortening (%FS) **(A)** or ejection fraction (%EF) **(B)**. Mean ± SEM (n=5-7)

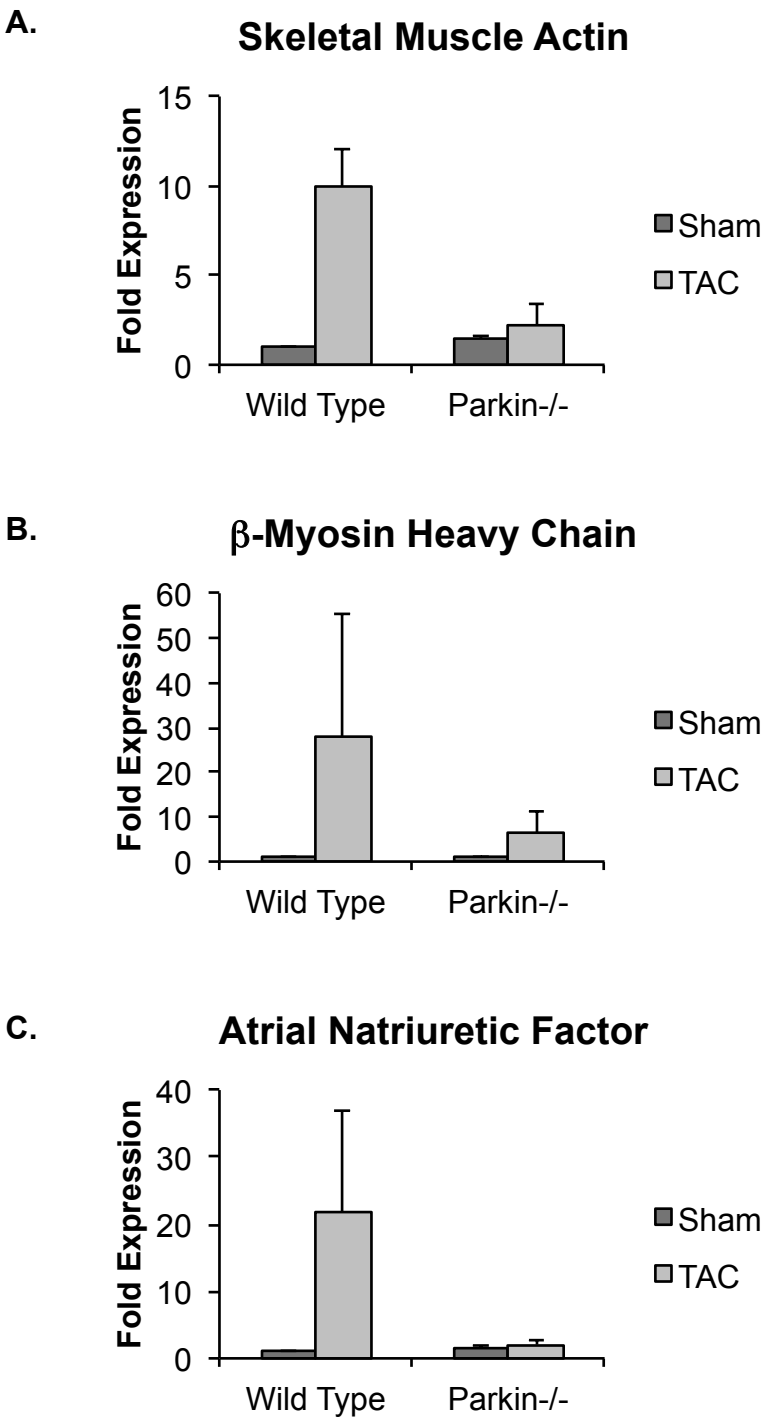

Figure 6.9. Transcript levels of the hypertrophy marker genes for skeletal muscle actin **(A)**, β-myosin heavy chain **(B)**, and atrial natriuretic factor **(C)** showed trends towards upregulation in WT mouse hearts after TAC, but not in Parkin-/- mouse hearts. Mean ± SEM (n=3-4)

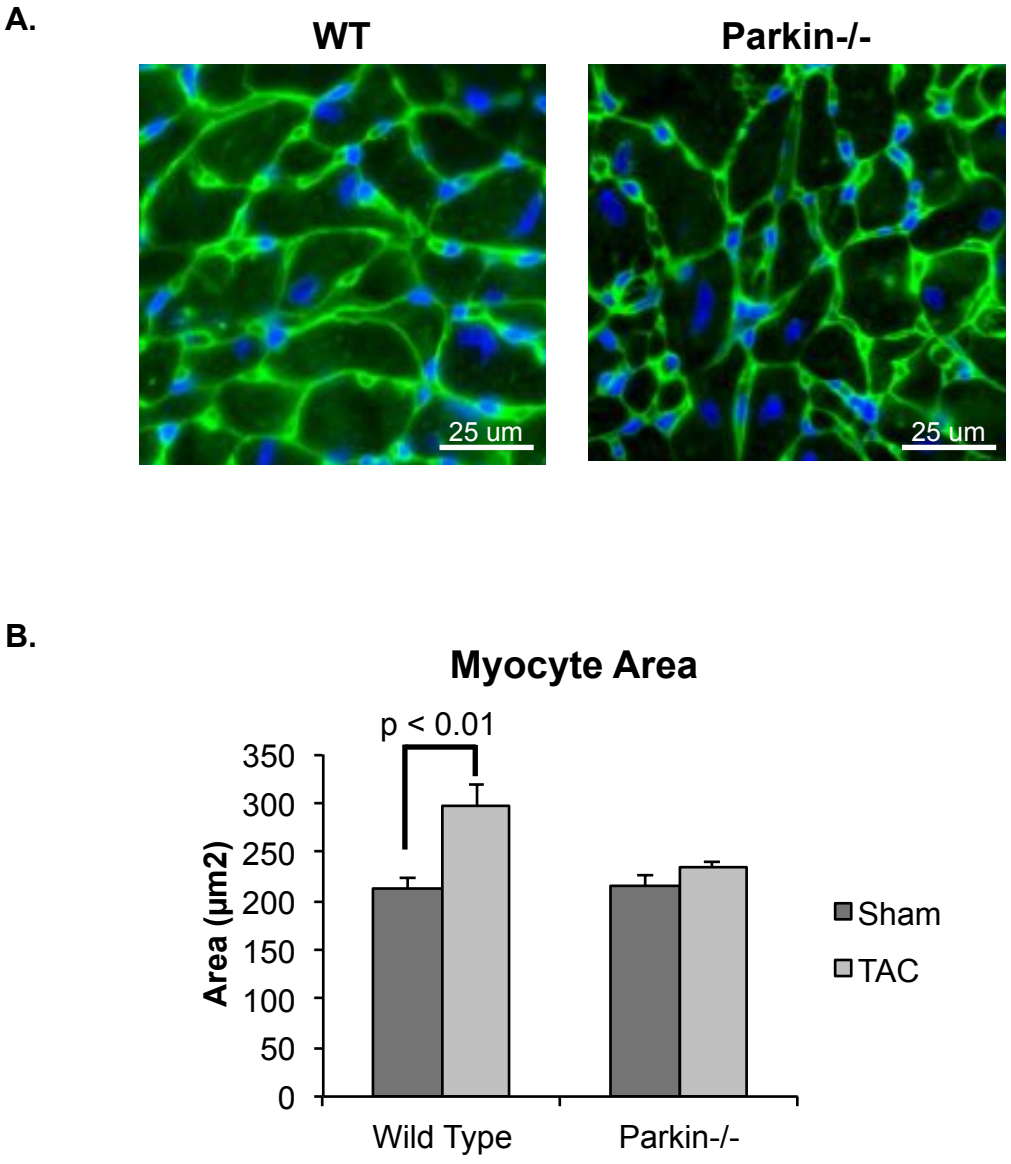

Figure 6.10. A. Representative fluorescence micrograph of heart cross sections from WT and Parkin-/- mice stained with Alexa Fluor 488-WGA after 2 weeks of TAC for myocyte area quantitation. **B.** Parkin-/- mouse cardiac myocytes did not increase in size after 2 weeks of TAC. Mean ± SEM (n=3-5).

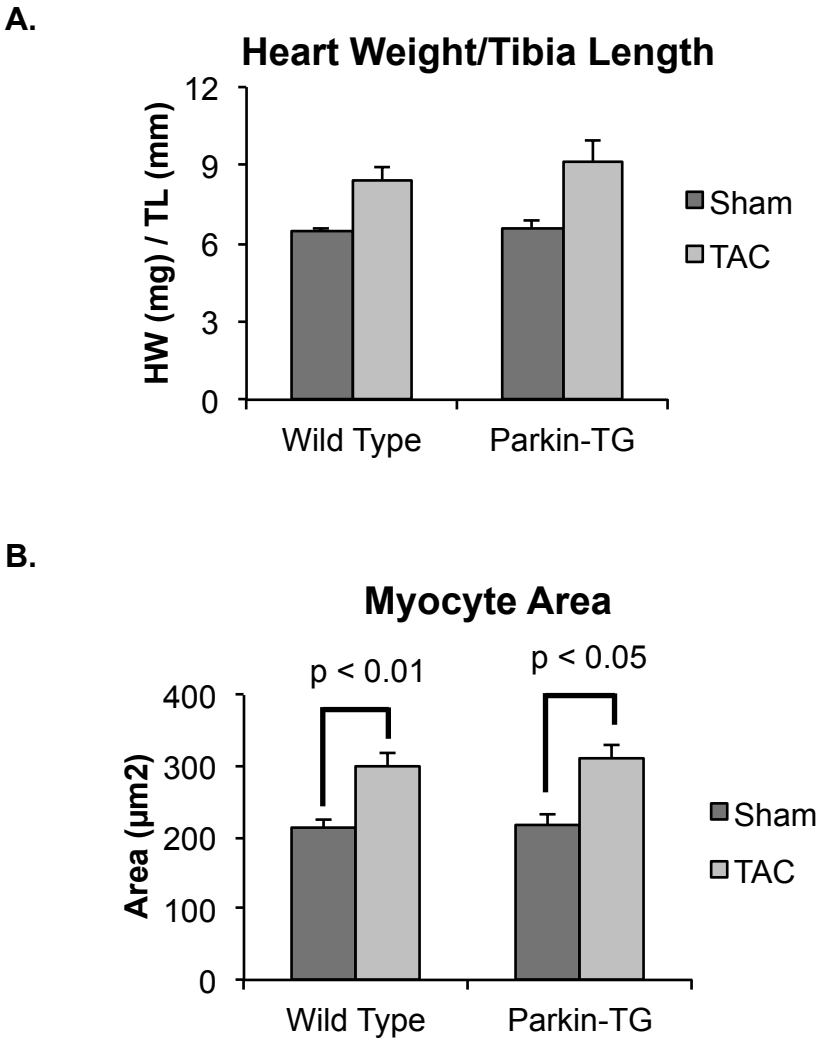

Figure 6.11. A. Heart weight (HW)/tibia length (TL) ratios increased equivalently in WT and Parkin-TG mice after 2 weeks of TAC. Mean ± SEM (n=3-6). **B.** Quantitation of myocyte area in WT and Parkin-TG mice revealed myocyte hypertrophy in both WT and Parkin-TG mice after TAC. Mean ± SEM (n=3-6).

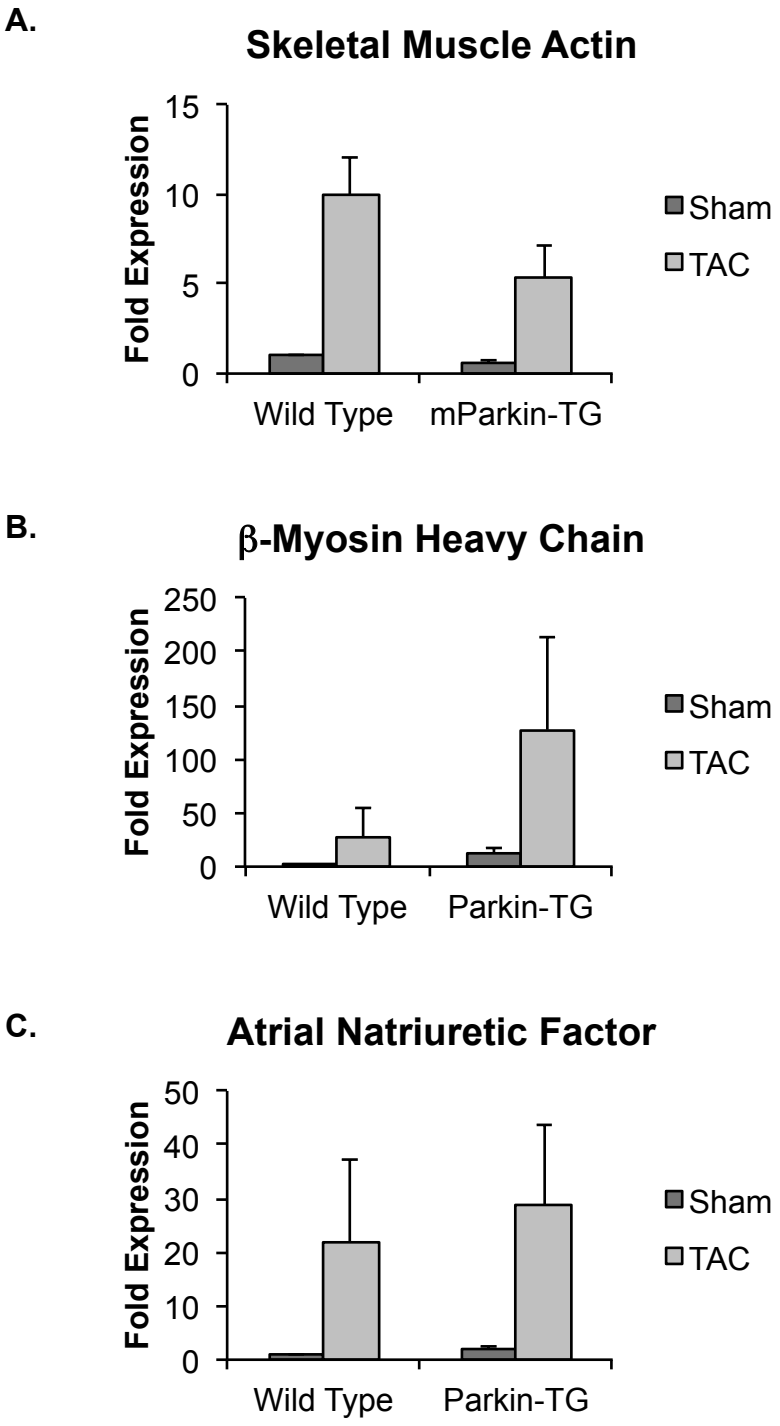

Figure 6.12. Upregulation of transcripts of the hypertrophy marker genes for skeletal muscle actin **(A)**, b-myosin heavy chain **(B)**, and atrial natriuretic factor **(C)** were not different between WT and Parkin-TG mice. Mean ± SEM (n=3-6).

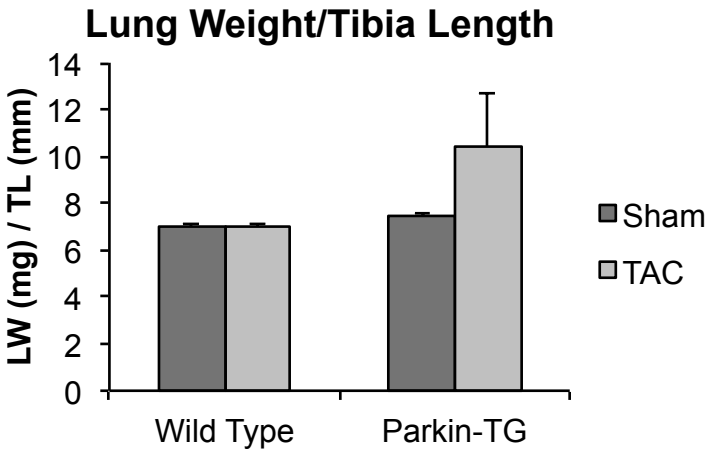

Figure 6.13. Lung weight (LW)/tibia length (TL) ratios in WT and Parkin-TG mice after 2 weeks of TAC or sham. Elevated LW/TL ratios were found in Parkin-TG mice. Mean ± SEM (n=3-5).

A.

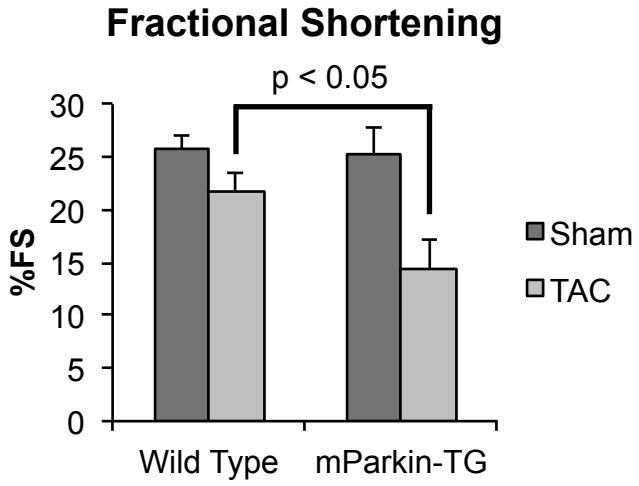

B.

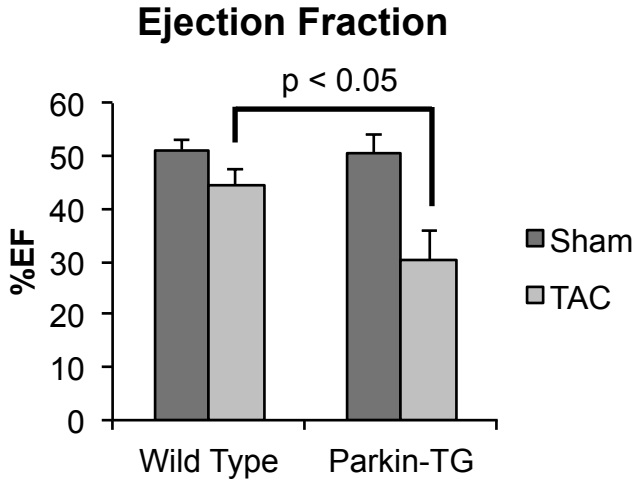

Figure 6.14. Echocardiography of WT and Parkin-TG mice after 2 weeks of TAC or sham. Parkin-TG mice showed significantly declined fractional shortening (%FS) **(A)** and ejection fraction (%EF) **(B)** compared to WT mice that had received the TAC. Mean ± SEM (n=3-7).

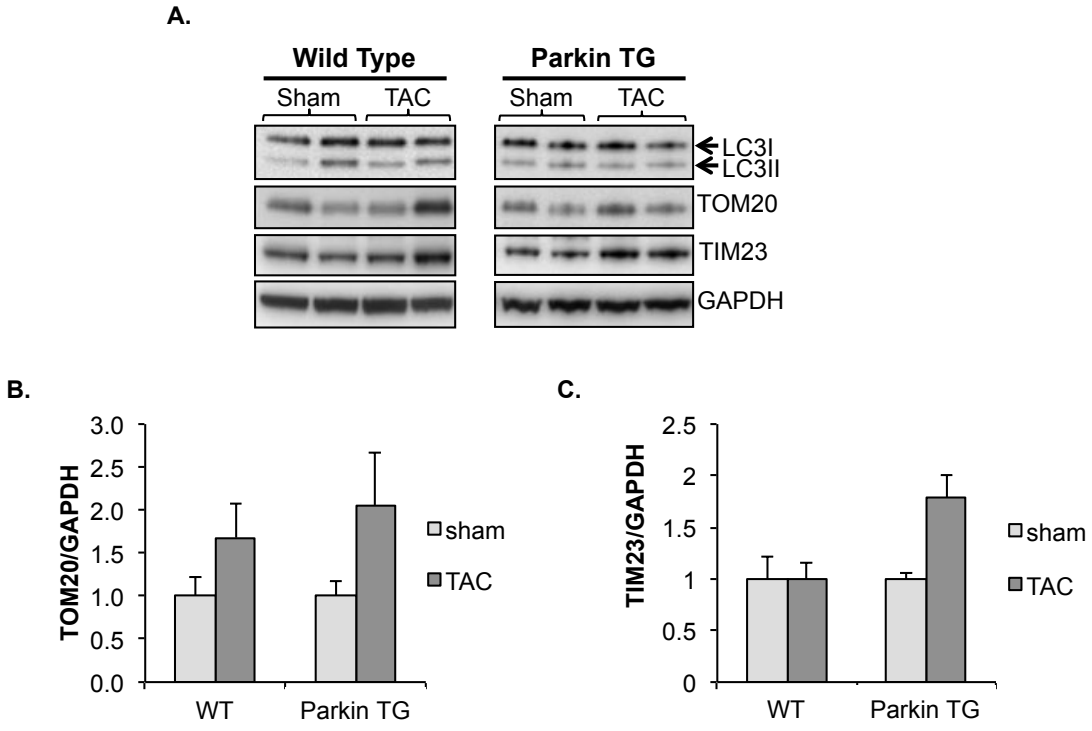

Figure 6.15. A. Representative western blots of WT and Parkin-TG mouse hearts after 2 weeks of TAC or sham. Western blot densitometry of the outer mitochondrial membrane protein TOM20 **(B)** and the inner mitochondrial membrane protein TIM23 **(C)** revealed no significant changes in mitochondria levels after 2 weeks of TAC in either WT or Parkin-TG mice. Mean ± SEM (n=5).

CHAPTER 7: DISCUSSION

7.1 Introduction

While substantial progress in recent years for the treatment and prevention of coronary artery disease has improved outcomes for many patients, the development of novel treatment strategies that work synergistically with available therapies becomes all the more important. Many treatments are available to control the risk of heart disease, but there is currently no treatment that effectively repairs tissue damage after an acute myocardial infarction (MI). Interventions directed towards pathways that are not currently being targeted, such as autophagy modulation, would allow for the development of new treatment strategies and multifaceted therapies for the growing number of cardiovascular disease patients in an aging population.

The administration of statins or metformin to reduce cholesterol and control diabetes is now commonplace and can be efficacious for the prevention of heart disease. Recent evidence indicates that these standard treatments also work to upregulate autophagy (Andres et al., 2013; Xie et al., 2011). Therefore, although modulation of autophagy may have been an off target effect, autophagy upregulation has become part of standard pharmacotherapy. My research adds to the understanding of the events that occur after MI, including the autophagic clearance of dysfunctional mitochondria by Parkin and the importance of mitochondrial fission. Autophagy-enhancing treatments may improve outcomes by increasing removal of misfolded protein aggregates and dysfunctional

organelles that accumulate after MI. Thus, the ability to enhance targeted mitophagy may prove to be a benefit for remedial treatments following acute myocardial infarction or cardiomyopathies caused by chronic conditions. The pathway currently most recognized for establishing specificity in mitophagy involves Parkin and PINK1. Advancements in the understanding of the mechanisms and functions of Parkin in the myocardium provide intriguing alternative approaches for pharmacologically modulating mitophagy.

The studies presented herein revealed some key findings regarding the role of Parkin in the myocardium. First, I found that Parkin is not necessary for the basal turnover of mitochondria but is instead critical for the heart to adapt to acute stress. Next, I demonstrated that mitophagy driven by Parkin in cardiac myocytes is dependent on Drp1-mediated mitochondrial fission, but does not require the presence of PINK1. Lastly, I found that although Parkin is required for cardiac hypertrophy in response to exercise or pressure overload, excessive Parkin is detrimental to the stress adaptation process. These discoveries add greatly to the existing knowledge concerning the function of Parkin in not only the myocardium, but also potentially other tissue types. Although many of the implications of these findings are immediately obvious, it will take additional research to more thoroughly explore the significance of these discoveries. In this discussion, I will provide additional context to the data presented in this dissertation in an effort to explain the relevance of my findings.

7.2 Parkin Is Dispensable for Normal Mitochondrial Turnover in the Heart

The data presented in Chapter 3 provide the first thorough investigation of the baseline cardiac phenotype of Parkin-deficient mice. Prior to this, only one study had investigated the role of Parkin in the mammalian heart. Huang et al. demonstrated that Parkin participates in the cardioprotective ischemic preconditioning response via a mechanism that involves the scaffolding protein p62 and enhancement of mitophagy (Huang et al., 2011). Although the authors did investigate mitophagy in Parkin-/- mice following ischemic preconditioning, they did not characterize contractile or mitochondrial function in Parkin-/- mice. Except for the work presented in this dissertation, Chen and Dorn published the only other study to investigate the role of cardiac Parkin. Their results showed that the heart tubes from *Drosophila melanogaster* lacking Parkin had contractile dysfunction, with enlarged cardiac mitochondria that had impaired respiration (Chen and Dorn, 2013). These data are clearly in contrast to the results described herein, where I demonstrated the absence of cardiac mitochondria respiration deficits and contractile dysfunction in unstimulated Parkin-/- mice (Chapter 3). I also observed that cardiac mitochondria in Parkin-/- mice were smaller, rather than enlarged as seen in Parkin-deficient *Drosophila* (Chapter 3). Although the study by Chen and Dorn followed the publication of the results presented in this dissertation (Kubli et al., 2013), there remains to be a rationalization for the differences between mammalian and insect Parkin-/- cardiac phenotypes. It is plausible that *Drosophila* lack alternative mitophagy pathways that provide redundancy in mammals to ensure proper mitochondrial

fission and mitophagy. For instance Bnip3L/NIX and Bnip3 have been shown to participate in Parkin/PINK1-independent mitophagy in erythrocytes and HeLa cells, respectively, by acting as direct linkers between mitochondria and autophagosomes (Hanna et al., 2012; Novak et al., 2010; Sandoval et al., 2008; Schweers et al., 2007). To my knowledge, such a mechanism has not yet been described in *Drosophila melanogaster*. This may account for the discrepancies between their findings and mine. The study by Chen and Dorn is not the first to report distinctions between *Parkin-/-* fly and mouse models. Early studies on Parkin reported that Parkin-deficient flies spontaneously develop muscle defects and dysfunctional mitochondria (Greene et al., 2003; Whitworth et al., 2005), which again contrasts my findings that Parkin-/- mice are devoid of abnormalities in cardiac and mitochondrial function for at least 1 year of age.

The involvement of Parkin in the day-to-day turnover of mitochondria under normal conditions was unexpectedly minimal. Loss of Parkin had no apparent bearing on cardiac function in untreated mice up to at least one year of age (Chapter 3). This again might be due to other Parkin-independent pathways for mitochondrial clearance, including those involving Bnip3 and Bnip3L/NIX as alternative mechanisms for regular turnover. Other studies have also found that Parkin is always involved in mitochondrial clearance. Sterky et al. reported that Parkin is not recruited to mitochondria of dopaminergic (DA) neurons in a Parkinson's disease mouse model of DA-neuron specific mitochondrial respiratory chain deficiency (Sterky et al., 2011). This would suggest that an external stressor is required, and that a threshold of mitochondrial damage must

be surpassed before Parkin is recruited to aid in mitochondrial clearance. In accord with this hypothesis, Frank-Cannon et al. showed that while Parkin-/- mice do not normally develop motor dysfunction or loss of DA neurons, systemic inflammation caused by low-dose lipopolysaccharide administration is sufficient to cause DA neuron loss that does not occur in WT mice (Frank-Cannon et al., 2008). Thus, loss of Parkin precludes the neuronal and cardiac stress response and results in an inability to curb damage. By extension, the high baseline level of Parkin in the heart and in neurons is therefore not for the purpose of standard mitochondrial turnover, but is instead for maintaining a high degree of preparedness to rapidly clear dysfunctional mitochondria in response to severe acute stress. Further, because of the high volume density of mitochondria in cardiac myocytes, it is particularly critical to remove dysfunctional mitochondria as quickly as possible after stress before they can release pro-apoptotic factors or initiate necrotic cell death. High basal Parkin expression may thereby prime the myocyte for rapid stress response.

7.3 Parkin is Critical for Limiting Tissue Damage After Acute Cardiac Stress

One of the most striking findings in my studies was the increased sensitivity of Parkin-/- mice to MI, suggesting that Parkin plays a critical role in adapting the myocardium to acute pathological stress. Parkin was previously known to have an important role in cardioprotection by ischemic preconditioning via recruitment of p62 to uncoupled cardiac mitochondria. Parkin-deficient mice are resistant to ischemic preconditioning-induced cardioprotection (Huang et al.,

2011). However, the participation of Parkin in mitigating cardiac tissue damage after acute stress went uncharacterized until now. Other evidence also suggests that Parkin may be important during and after cardiac stress. For instance, my lab recently reported that mitophagy induced by the BH3-only protein Bnip3 in cardiac myocytes involved translocation of Parkin to mitochondria (Lee et al., 2011). Bnip3 is a pro-apoptotic Bcl-2 family protein that has been implicated in cardiac myocyte apoptosis following ischemia/reperfusion (Graham et al., 2007; Regula et al., 2002), but Bnip3 is also a potent inducer of autophagy/mitophagy and may contribute to the removal of damaged mitochondria after I/R injury in the heart (Hamacher-Brady et al., 2007; Rikka et al., 2011). Previous studies have also shown that Bnip3 can become activated by oxidative stress (Kubli et al., 2008). Bnip3 may therefore be a putative upstream activator of Parkin that responds to I/R-induced cell stress to initiate Parkin recruitment and mitophagy in a preventative manner before substantial dysfunction occurs. Although there is crosstalk between PINK1/Parkin-mediated and NIX/Bnip3-mediated Parkin-independent mitophagy, perturbation of the system via Parkin knockout must result in an inability to compensate during severe stress such as an MI.

7.4 New Insights into the Mechanisms of Parkin Function in the Heart

Studies have linked Drp1-mediated mitochondrial fission with mitophagy (Lee et al., 2011; Tanaka et al., 2010). In the present study, I confirmed that Drp1 is required for translocation of Parkin to mitochondria in myocytes, but Drp1 translocation is independent of Parkin and the upstream serine/threonine kinase

PINK1. Another important finding is that PINK1 is not required for the translocation of Parkin to mitochondria in the myocardium. PINK1 has been reported to play a central role in recruiting Parkin to mitochondria with collapsed $\Delta\Psi m$ (Matsuda et al., 2010; Narendra et al., 2010a). However, my findings clearly show that Parkin translocation to mitochondria still occurs in PINK1-deficient hearts. Other studies have also reported that Parkin does not require PINK1. Parkin overexpression rescues the mitochondrial abnormalities observed in PINK1 knockout flies, suggesting that Parkin is downstream of PINK1 and does not require the presence of PINK1 for its function (Clark et al., 2006; Park et al., 2006). Similarly, Dagda et al. discovered that Parkin is still effective in clearing mitochondria in SH-SY5Y neuroblastoma cells with silenced PINK1 (Dagda et al., 2009). They conclude that PINK1 and Parkin function complementarily in mammalian cells as parts of distinct pathways; PINK1 may help to stabilize mitochondrial function, while Parkin acts as a safeguard to remove mitochondria that are beyond repair (Dagda et al., 2009).

Both PINK1 and Parkin knockout *Drosophila* have similar phenotypes with accumulation of dysfunctional mitochondria and degeneration of muscle fibers (Clark et al., 2006; Park et al., 2006). Interestingly, PINK1- and Parkin-deficient mice have very different cardiac phenotypes. PINK1 deficiency results in increased oxidative stress and mitochondrial dysfunction in the myocardium, and these mice develop cardiac dysfunction and hypertrophy by two months of age (Billia et al., 2011). In contrast, Parkin-deficient mice have normal mitochondria and cardiac function. Thus, although PINK1 and Parkin function might overlap in

cells, they clearly have additional and separate functions in the myocardium. PINK1 appears to be important in maintaining normal mitochondrial function in the heart under baseline conditions, whereas Parkin plays an important role in the adaptation to stress.

7.5 Parkin Mediates Physiological and Pathological Hypertrophy

Another surprising finding came by way of exposing mice to stress that would less acutely disrupt mitochondrial function and more chronically affect the heart. The finding that Parkin participates in cardiac hypertrophy in response to both physiological exercise and pathological cardiac pressure overload is completely novel. Even more intriguing is the finding that Parkin-TG mice develop heart failure at an accelerated rate (Chapter 6). Although it is known that Parkin can drive complete removal of mitochondria in cells treated with uncouplers or simulated I/R (Geisler et al., 2010; Huang et al., 2010a; Narendra et al., 2008), the accelerated heart failure phenotype found in Parkin-TG mice after TAC was not due to excessive mitochondrial clearance. These two findings collectively indicate that Parkin plays a critical role in moderating the hypertrophy response and maintaining contractility by promoting adaptation to cardiac stress. Together with my findings that Parkin ubiquitinates cytosolic substrates following MI (Chapter 4), mounting evidence suggests that Parkin participates in signaling pathways beyond its canonical role in mitophagy. Indeed, the identification of more than 20 cytosolic substrates further supports this conclusion (Sandebring and Mínguez, 2012). Parkin may therefore support cell survival by both

promoting the clearance of dysfunctional mitochondria and simultaneously initiating pro-survival signaling pathways (Fallon et al., 2006; Henn et al., 2007; Yang et al., 2005). The identification of this unique Parkin function provokes the need for additional experiments to characterize these pathways. It will be vital to thoroughly characterize Parkin's ubiquitination substrates and identify the circumstances surrounding their ubiquitination to determine their relevance.

Recent studies support the notion of a much broader functional role for Parkin beyond mitophagy. Parkin can facilitate fatty acid uptake by increasing the stability of the CD36 fatty acid translocase in the liver via monoubiquitination (Kim et al., 2011). CD36 plays an important role in supplying the heart with long-chain fatty acids (FA), its major energy substrate, and CD36-deficient mouse hearts are more vulnerable to ischemic injury than WT mice (Irie et al., 2003). Thus, disturbances in cellular energy production associated with reduced *CD36*-mediated long-chain FA uptake in Parkin-deficient hearts could reduce tolerance to myocardial ischemia. In addition, Parkin was recently reported to regulate degradation of Paris/Znf746, a repressor of PGC-1α gene expression (Shin et al., 2011). Since PGC-1α is a central regulator of mitochondrial biogenesis, Parkin may also play a role in regulating synthesis of new mitochondria.

My finding of reduced ubiquitination in the cytosolic fraction of Parkin-/- mouse after MI hearts suggests that Parkin has cytosolic substrates that may also be important in post-stress damage control. Parkin has been shown to assist the ubiquitin-proteasome system (UPS) in removing misfolded and aggregated proteins during stress by ubiquitinating cytosolic proteins (Tsai et al., 2003).

Thus, it is possible that Parkin deficiency could result in impairment of the UPS and accumulation of cytotoxic protein aggregates. Determining whether defects in these processes contribute to increased susceptibility to MI in Parkin-/- hearts requires further investigation.

7.6 Future Experiments – Exploring Putative Roles of Parkin in Cardiac Homeostasis

The research presented here adds greatly to the body of knowledge on the function of Parkin in the heart and possibly in other cell types as well. During the course of these studies, several new unanswered questions have arisen that should be addressed in future work. First, it is important to more thoroughly investigate potential changes to mitophagy in Parkin-TG mice both under basal conditions and in response to stress such as MI or cardiac pressure overload. Mice with cardiac-specific overexpression of Parkin showed impaired contractile function as early as 3 months of age (Chapter 3). Hence, Parkin overexpression may result in detrimental levels of mitophagy under baseline conditions. However, in light of the findings that Parkin does not appear to participate in mitophagy unless there is severe mitochondrial damage, an alternative hypothesis would be that Parkin overexpression results in aberrant ubiquitination of cytosolic components that are important for cardiac myocyte homeostasis. Thus, an investigation of the ubiquitination of known cytosolic Parkin substrates should follow. Some notable candidate substrates include TRAF2 and IKKγ, both upstream components of NF-κB signaling (Henn et al., 2007). A search for novel

Parkin substrates may uncover additional putative signaling pathways and stress response mechanisms, thereby clarifying our understanding of Parkin's effects and possibly allowing for the tailoring of treatments with fewer unintended consequences. It would also be informative to titrate the levels of Parkin overexpression in cells or additional Parkin-TG mouse lines to determine if elevating Parkin only partially could confer a resistance to stress without negatively affecting cardiac function. This would help to determine if regulation of Parkin expression is a viable therapeutic target, or whether undesirable effects of Parkin overexpression negate any possible cardioprotection.

A more complete investigation of the pathological hypertrophy response in both Parkin-/- and Parkin-TG mice must next be initiated. The current study focused only on a 2-week endpoint, at which time hypertrophy could be expected without a substantial functional decline in WT mice. Future studies should be extended to a later time point that would allow for a comparison of the progression to heart failure between Parkin-/- and WT mice to determine if impaired hypertrophy delays the onset of decompensation, or whether Parkin-/- mice progress directly to heart failure without hypertrophy.

To more thoroughly characterize the changes observed in Parkin-/- and Parkin-TG mice in response to cardiac pressure overload, the activity of overlapping hypertrophy signaling pathways must be assessed. For instance, p38 MAPK, ERK1/2, and JNK are all known to be activated in response to cardiac stress signals including stretch caused by pressure overload (Heineke and Molkentin, 2006). Further, the AKT pathway is involved in both physiological

and pathological hypertrophy, and mice deficient in AKT-null mice have phenotypes that resemble those of the Parkin-TG mice described here. AKT-/- mice develop minor but significant systolic dysfunction spontaneously and have exacerbated pathological hypertrophy with early heart failure (DeBosch et al., 2006). These mice also have impaired physiological hypertrophy (DeBosch et al., 2006), which indicates a need to test the physiological hypertrophy response in Parkin-TG mice. Parkin deficiency has been shown to upregulate AKT signaling by disrupting binding of Eps15 to the epidermal growth factor receptor (EGFR). However, no pathways have yet been characterized that could account for inhibition of AKT signaling by Parkin overexpression. Assessing the activity of these factors in Parkin-/- and Parkin-TG mice in response to physiological hypertrophy from exercise as well as pathological hypertrophy in response to TAC could provide clues to determining the aberrant pathways responsible for the respective blunted hypertrophy and accelerated heart failure observed in these mice. Findings in these studies could also help identify Parkin ubiquitination substrates that are upstream of these core signaling molecules that would explain how Parkin modulates hypertrophy and how overexpression sensitizes the heart to chronic stress. This may aid in identifying potential Parkin-mediated cell survival functions that could be pharmacologically regulated.

7.7 Proposed Model/Paradigm

In light of the new findings regarding the mechanism by which Parkin improves the cell stress response, I propose a modified model of Parkin function

in the heart that fits congruently with the current paradigm of Parkin-mediated mitophagy (Figure 7.1). In this model, Parkin normally participates in cellular maintenance that may involve ubiquitination of Drp1 to limit mitochondrial fission and regulation of NF-κB (IKKγ, TRAF2 (Henn et al., 2007)), and AKT (Eps15 (Fallon et al., 2006)) signaling pathways. In this manner, Parkin supports cellular homeostasis. However, acute stress that causes widespread loss of $\Delta\Psi$m would lead to PINK1 stabilization on mitochondria to bolster mitochondrial function, as well as concomitant Parkin recruitment to mitochondria that are beyond recovery. Under these conditions, Parkin ubiquitinates proteins that regulate mitochondrial fusion (Mfn1/2 (Tanaka et al., 2010; Wang et al., 2011a)) and mitochondria motility (Miro (Wang et al., 2011b)) to facilitate mitophagy. Thus, Parkin-mediated mitophagy is only called upon during times of extensive mitochondrial damage, such as occurs following ischemia/reperfusion injury or myocardial infarction. Results from future studies will help to further refine or disprove this model of Parkin function in the heart.

7.8 Therapeutic Relevance

The prospect of utilizing Parkin as a therapeutic target is very intriguing. Upregulation of Parkin following MI appears to be a beneficial event that confers resistance to cell death by enhancing mitochondrial autophagy (Chapter 4). It may be possible to determine how Parkin is upregulated in the infarct border zone within 4 hours of MI with the goal of developing pharmacotherapies to drive Parkin upregulation and enhance cardioprotection. However, as other studies

have discovered, excessive or prolonged activation of autophagy may be detrimental and lead to loss of myocytes (Matsui et al., 2007). It is not surprising that removal of too many mitochondria via autophagy in a contracting myocyte is detrimental since it results in an energy deficiency. Similarly, Parkin-TG mice had worse prognoses after pressure overload than both WT and Parkin-/- mice, which shows that overexpression of Parkin may not be as protective as one would hope. Determining the level of expression at which Parkin becomes detrimental versus beneficial would be informative of the practicality of Parkin-upregulation as an intervention. Whether cardioprotection by Parkin depends on the stress stimulus also remains to be determined. Still, Parkin upregulation to enhance targeted mitophagy may be a feasible therapy for minimizing tissue damage post-MI. Although Parkin represents a great potential therapeutic target to promote clearance of damaged mitochondria and reduce cell death, further studies are clearly necessary to enhance our understanding of mitochondrial autophagy in the myocardium.

My findings are consistent with existing patient data insofar as there are currently no reports that Parkinson's disease (PD) patients with loss-of-function mutations in the *PARK2* gene have abnormal heart function. Instead, my findings suggest that these patients might be at increased risk of developing heart failure in response to stress such as myocardial ischemia. Based on my data, PD patients with *PARK2* mutations would not be expected to have abnormally high incidences of heart failure caused by hypertensive heart disease, although this may mean that underlying risk factors may go unnoticed. Of note, studies that

were conducted over a decade ago found an increase in mortality of PD patients with ischemic heart disease (Ben-Shlomo and Marmot, 1995; Bennett et al., 1996). However, it is not known what percentage of the patients included in these studies had mutations in the *PARK2* gene. An epidemiological study with additional genetic data, or an investigation of the correlated risk factors associated with *PARK2* gene mutations would aid in answering these questions. Additional studies are therefore needed to determine if PD patients with cardiovascular disease are at elevated risk for recurrent or more severe myocardial infarctions, particularly those with mutations in the *PARK2* gene.

7.9 Concluding Remarks

In the decade between 1999 and 2009, the death rate for cardiovascular disease in the U.S. dropped by nearly 33% (Go et al., 2013). Much of this progress was the result of improvements in treatments following myocardial infarctions. For the next decade between 2010 and 2020, the American Heart Association has set new goals of lowering improving cardiovascular health of all Americans by 20%, and reducing deaths related to cardiovascular disease and stroke by 20% (Go et al., 2013). Accomplishing these goals will require faster response times between onset of symptoms and treatment administration, and even greater improvements in treatment options. But whether or not mitophagy modulation proves to be a viable therapeutic in the future, each new discovery opens a wealth of novel avenues for research and the development of new treatments.

Parts of Chapter 7 were originally published in Circulation Research. Kubli, D. A., & Gustafsson, A. B. Mitochondria and Mitophagy: The Yin and Yang of Cell Death Control. *Circulation Research*, *111*(9), 1208–1221. doi:10.1161/CIRCRESAHA.112.265819 The dissertation author was the primary author of this paper.

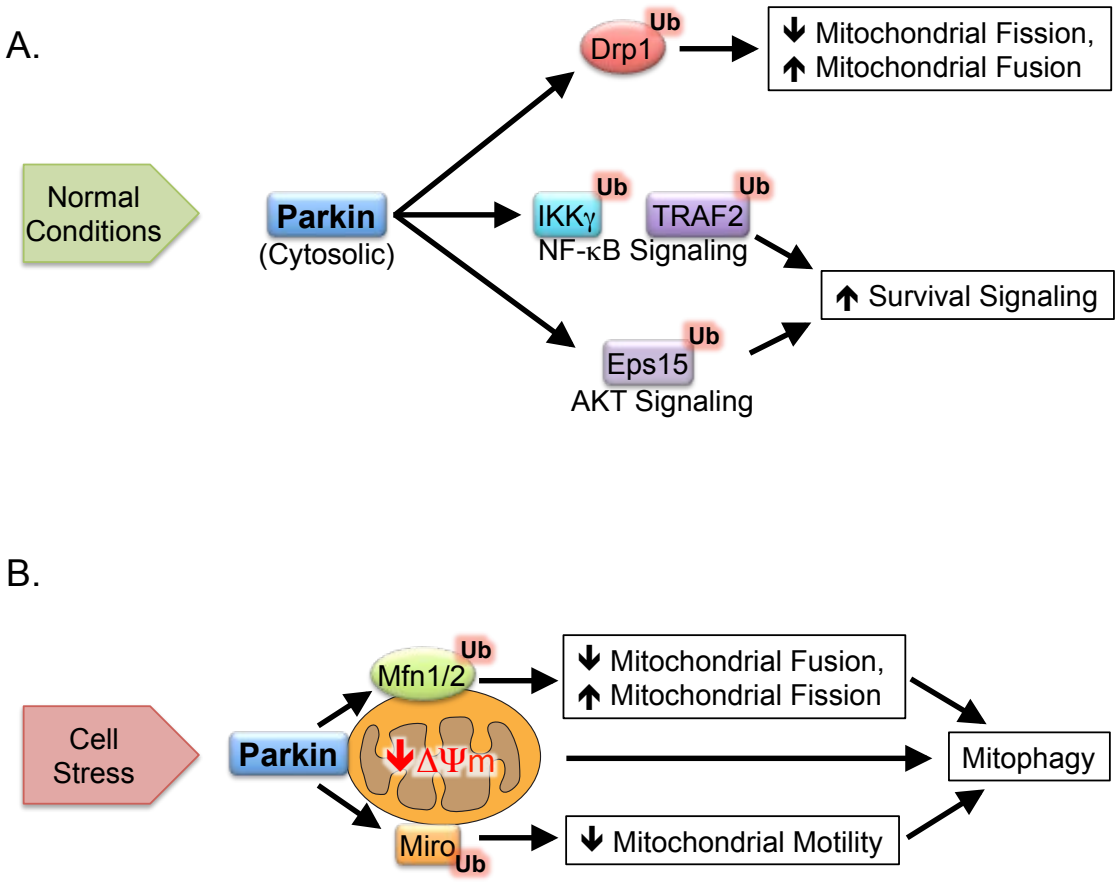

Figure 7.1. Proposed model of Parkin function in the heart. A. Under normal cellular conditions, cytosolic Parkin participates in regulation of cell survival pathways mediated by NF-κB and AKT. Parkin also promotes mitochondrial fusion through ubiquitination of Drp1. **B.** During times of cellular stress, Parkin translocates to mitochondria where it promotes mitophagy via ubiquitination of Mitofusin (Mfn) proteins to halt mitochondrial fusion and ubiquitination of Miro to stop mitochondrial movement and permit engulfment by autophagosomes.

REFERENCES

Andres, A.M., Hernandez, G., Lee, P., Huang, C., Ratliff, E.P., Sin, J., Thornton, C.A., Damasco, M.V., and Gottlieb, R.A. (2013). Mitophagy is required for acute cardioprotection by simvastatin. Antioxid Redox Signal.

Ashrafian, H., Docherty, L., Leo, V., Towlson, C., Neilan, M., Steeples, V., Lygate, C.A., Hough, T., Townsend, S., Williams, D., et al. (2010). A mutation in the mitochondrial fission gene Dnm1l leads to cardiomyopathy. PLoS Genet *6*, e1001000.

Aviv, Y., Shaw, J., Gang, H., and Kirshenbaum, L.A. (2011). Regulation of autophagy in the heart: "you only live twice". Antioxid Redox Signal *14*, 2245–2250.

Band, M., Joel, A., Hernandez, A., and Avivi, A. (2009). Hypoxia-induced BNIP3 expression and mitophagy: in vivo comparison of the rat and the hypoxia-tolerant mole rat, Spalax ehrenbergi. Faseb J. *23*, 2327–2335.

Becker, L.B. (2004). New concepts in reactive oxygen species and cardiovascular reperfusion physiology. Cardiovascular Research *61*, 461–470.

Ben-Shlomo, Y., and Marmot, M.G. (1995). Survival and cause of death in a cohort of patients with parkinsonism: possible clues to aetiology? J. Neurol. Neurosurg. Psychiatr. *58*, 293–299.

Bennett, D.A., Beckett, L.A., Murray, A.M., Shannon, K.M., Goetz, C.G., Pilgrim, D.M., and Evans, D.A. (1996). Prevalence of parkinsonian signs and associated mortality in a community population of older people. *334*, 71–76.

Billia, F., Hauck, L., Konecny, F., Rao, V., Shen, J., and Mak, T.W. (2011). PTEN-inducible kinase 1 (PINK1)/Park6 is indispensable for normal heart function. Proceedings of the National Academy of Sciences *108*, 9572–9577.

Braunwald, E., and Kloner, R.A. (1985). Myocardial reperfusion: a double-edged sword? J. Clin. Invest. *76*, 1713–1719.

Capano, M., and Crompton, M. (2006). Bax translocates to mitochondria of heart cells during simulated ischaemia: involvement of AMP-activated and p38 mitogen-activated protein kinases. Biochem. J. *395*, 57–64.

Carreira, R.S., Lee, Y., Ghochani, M., Gustafsson, A.B., and Gottlieb, R.A. (2010). Cyclophilin D is required for mitochondrial removal by autophagy in cardiac cells. Autophagy *6*.

Cereghetti, G.M., and Scorrano, L. (2006). The many shapes of mitochondrial

death. Oncogene *25*, 4717–4724.

Chen, H., Detmer, S.A., Ewald, A.J., Griffin, E.E., Fraser, S.E., and Chan, D.C. (2003). Mitofusins Mfn1 and Mfn2 coordinately regulate mitochondrial fusion and are essential for embryonic development. The Journal of Cell Biology *160*, 189–200.

Chen, Y., and Dorn, G.W. (2013). PINK1-phosphorylated mitofusin 2 is a Parkin receptor for culling damaged mitochondria. Science *340*, 471–475.

Cipolat, S., Martins de Brito, O., Dal Zilio, B., and Scorrano, L. (2004). OPA1 requires mitofusin 1 to promote mitochondrial fusion. Proc. Natl. Acad. Sci. U.S.a. *101*, 15927–15932.

Clark, I.E., Dodson, M.W., Jiang, C., Cao, J.H., Huh, J.R., Seol, J.H., Yoo, S.J., Hay, B.A., and Guo, M. (2006). Drosophila pink1 is required for mitochondrial function and interacts genetically with parkin. Nature *441*, 1162–1166.

Clarke, S.J., McStay, G.P., and Halestrap, A.P. (2002). Sanglifehrin A acts as a potent inhibitor of the mitochondrial permeability transition and reperfusion injury of the heart by binding to cyclophilin-D at a different site from cyclosporin A. J Biol Chem *277*, 34793–34799.

Dagda, R.K., Cherra, S.J., Kulich, S.M., Tandon, A., Park, D., and Chu, C.T. (2009). Loss of PINK1 function promotes mitophagy through effects on oxidative stress and mitochondrial fission. J Biol Chem *284*, 13843–13855.

DeBosch, B., Treskov, I., Lupu, T.S., Weinheimer, C., Kovacs, A., Courtois, M., and Muslin, A.J. (2006). Akt1 is required for physiological cardiac growth. Circulation *113*, 2097–2104.

Delettre, C., Lenaers, G., Griffoin, J.M., Gigarel, N., Lorenzo, C., Belenguer, P., Pelloquin, L., Grosgeorge, J., Turc-Carel, C., Perret, E., et al. (2000). Nuclear gene OPA1, encoding a mitochondrial dynamin-related protein, is mutated in dominant optic atrophy. Nat. Genet. *26*, 207–210.

Ding, W.-X., Ni, H.-M., Li, M., Liao, Y., Chen, X., Stolz, D.B., Dorn, G.W., and Yin, X.-M. (2010). Nix is critical to two distinct phases of mitophagy, reactive oxygen species-mediated autophagy induction and Parkin-ubiquitin-p62-mediated mitochondrial priming. J Biol Chem *285*, 27879–27890.

Dorn, G.W., Clark, C.F., Eschenbacher, W.H., Kang, M.-Y., Engelhard, J.T., Warner, S.J., Matkovich, S.J., and Jowdy, C.C. (2011). MARF and Opa1 control mitochondrial and cardiac function in Drosophila. Circulation Research *108*, 12–17.

Faerber, G., Barreto-Perreia, F., Schoepe, M., Gilsbach, R., Schrepper, A.,

Schwarzer, M., Mohr, F.W., Hein, L., and Doenst, T. (2011). Induction of heart failure by minimally invasive aortic constriction in mice: reduced peroxisome proliferator-activated receptor γ coactivator levels and mitochondrial dysfunction. J. Thorac. Cardiovasc. Surg. *141*, 492–500–500.e1.

Fallon, L., Bélanger, C.M.L., Corera, A.T., Kontogiannea, M., Regan-Klapisz, E., Moreau, F., Voortman, J., Haber, M., Rouleau, G., Thorarinsdottir, T., et al. (2006). A regulated interaction with the UIM protein Eps15 implicates parkin in EGF receptor trafficking and PI(3)K-Akt signalling. Nat. Cell Biol. *8*, 834–842.

Frank-Cannon, T.C., Tran, T., Ruhn, K.A., Martinez, T.N., Hong, J., Marvin, M., Hartley, M., Treviño, I., O'Brien, D.E., Casey, B., et al. (2008). Parkin deficiency increases vulnerability to inflammation-related nigral degeneration. Journal of Neuroscience *28*, 10825–10834.

Gegg, M.E., Cooper, J.M., Chau, K.Y., Rojo, M., Schapira, A.H.V., and Taanman, J.W. (2010). Mitofusin 1 and mitofusin 2 are ubiquitinated in a PINK1/parkin-dependent manner upon induction of mitophagy. Human Molecular Genetics *19*, 4861–4870.

Geisler, S., Holmström, K.M., Skujat, D., Fiesel, F.C., Rothfuss, O.C., Kahle, P.J., and Springer, W. (2010). PINK1/Parkin-mediated mitophagy is dependent on VDAC1 and p62/SQSTM1. Nat. Cell Biol. *12*, 119–131.

Gispert, S., Ricciardi, F., Kurz, A., Azizov, M., Hoepken, H.-H., Becker, D., Voos, W., Leuner, K., Müller, W.E., Kudin, A.P., et al. (2009). Parkinson phenotype in aged PINK1-deficient mice is accompanied by progressive mitochondrial dysfunction in absence of neurodegeneration. PLoS ONE *4*, e5777.

Go, A.S., Mozaffarian, D., Roger, V.L., Benjamin, E.J., Berry, J.D., Borden, W.B., Bravata, D.M., Dai, S., Ford, E.S., Fox, C.S., et al. (2013). The “Heart Disease and Stroke Statistics--2013 Update” and the Need for a National Cardiovascular Surveillance System. Circulation *127*, 21–23.

Goldberg, M.S., Fleming, S.M., Palacino, J.J., Cepeda, C., Lam, H.A., Bhatnagar, A., Meloni, E.G., Wu, N., Ackerson, L.C., Klapstein, G.J., et al. (2003). Parkin-deficient mice exhibit nigrostriatal deficits but not loss of dopaminergic neurons. J Biol Chem *278*, 43628–43635.

Gomes, L.C., Benedetto, G.D., and Scorrano, L. (2011). During autophagy mitochondria elongate, are spared from degradation and sustain cell viability. Nat. Cell Biol. *13*, 589–598.

Gottlieb, R.A., Burleson, K.O., Kloner, R.A., Babior, B.M., and Engler, R.L. (1994). Reperfusion injury induces apoptosis in rabbit cardiomyocytes. J. Clin. Invest. *94*, 1621–1628.

Gottlieb, R.A., and Gustafsson, A.B. (2011). Mitochondrial turnover in the heart. Biochimica Et Biophysica Acta *1813*, 1295–1301.

Graham, R.M., Thompson, J.W., Wei, J., Bishopric, N.H., and Webster, K.A. (2007). Regulation of Bnip3 death pathways by calcium, phosphorylation, and hypoxia-reoxygenation. Antioxid Redox Signal *9*, 1309–1315.

Greene, A.W., Grenier, K., Aguileta, M.A., Muise, S., Farazifard, R., Haque, M.E., McBride, H.M., Park, D.S., and Fon, E.A. (2012). Mitochondrial processing peptidase regulates PINK1 processing, import and Parkin recruitment. EMBO Rep. *13*, 378–385.

Greene, J.C., Whitworth, A.J., Kuo, I., Andrews, L.A., Feany, M.B., and Pallanck, L.J. (2003). Mitochondrial pathology and apoptotic muscle degeneration in Drosophila parkin mutants. Proc. Natl. Acad. Sci. U.S.a. *100*, 4078–4083.

Griffiths, E.J., and Halestrap, A.P. (1993). Protection by Cyclosporin A of ischemia/reperfusion-induced damage in isolated rat hearts. Journal of Molecular and Cellular Cardiology *25*, 1461–1469.

Gustafsson, A.B., and Gottlieb, R.A. (2003). Mechanisms of apoptosis in the heart. J. Clin. Immunol. *23*, 447–459.

Gustafsson, A.B., Tsai, J.G., Logue, S.E., Crow, M.T., and Gottlieb, R.A. (2004). Apoptosis repressor with caspase recruitment domain protects against cell death by interfering with Bax activation. J Biol Chem *279*, 21233–21238.

Hamacher-Brady, A., Brady, N.R., Logue, S.E., Sayen, M.R., Jinno, M., Kirshenbaum, L.A., Gottlieb, R.A., and Gustafsson, A.B. (2007). Response to myocardial ischemia/reperfusion injury involves Bnip3 and autophagy. Cell Death Differ *14*, 146–157.

Hamacher-Brady, A., Brady, N.R., and Gottlieb, R.A. (2006). Enhancing macroautophagy protects against ischemia/reperfusion injury in cardiac myocytes. J Biol Chem *281*, 29776–29787.

Hanna, R.A., Quinsay, M.N., Orogo, A.M., Giang, K., Rikka, S., and Gustafsson, A.B. (2012). Microtubule-associated protein 1 light chain 3 (LC3) interacts with Bnip3 protein to selectively remove endoplasmic reticulum and mitochondria via autophagy. J Biol Chem *287*, 19094–19104.

He, C., Bassik, M.C., Moresi, V., Sun, K., Wei, Y., Zou, Z., An, Z., Loh, J., Fisher, J., Sun, Q., et al. (2012). Exercise-induced BCL2-regulated autophagy is required for muscle glucose homeostasis. Nature *481*, 511–515.

Heineke, J., and Molkentin, J.D. (2006). Regulation of cardiac hypertrophy by intracellular signalling pathways. Nat. Rev. Mol. Cell Biol. *7*, 589–600.

Henn, I.H., Bouman, L., Schlehe, J.S., Schlierf, A., Schramm, J.E., Wegener, E., Nakaso, K., Culmsee, C., Berninger, B., Krappmann, D., et al. (2007). Parkin mediates neuroprotection through activation of IkappaB kinase/nuclear factor-kappaB signaling. Journal of Neuroscience *27*, 1868–1878.

Hilal-Dandan, R., Kanter, J.R., and Brunton, L.L. (2000). Characterization of G-protein signaling in ventricular myocytes from the adult mouse heart: differences from the rat. Journal of Molecular and Cellular Cardiology *32*, 1211–1221.

Hochhauser, E., Kivity, S., Offen, D., Maulik, N., Otani, H., Barhum, Y., Pannet, H., Shneyvays, V., Shainberg, A., Goldshtaub, V., et al. (2003). Bax ablation protects against myocardial ischemia-reperfusion injury in transgenic mice. Am J Physiol Heart Circ Physiol *284*, H2351–H2359.

Hoyert, D.L., and Xu, J. (2012). Deaths: preliminary data for 2011. Natl Vital Stat Rep *61*, 1–65.

Huang, C., Andres, A.M., Ratliff, E.P., Hernandez, G., Lee, P., and Gottlieb, R.A. (2011). Preconditioning involves selective mitophagy mediated by Parkin and p62/SQSTM1. PLoS ONE *6*, e20975.

Huang, C., Yitzhaki, S., Perry, C.N., Liu, W., Giricz, Z., Mentzer, R.M., and Gottlieb, R.A. (2010a). Autophagy induced by ischemic preconditioning is essential for cardioprotection. J. of Cardiovasc. Trans. Res. *3*, 365–373.

Huang, C., Zhang, X., Ramil, J.M., Rikka, S., Kim, L., Lee, Y., Gude, N.A., Thistlethwaite, P.A., Sussman, M.A., Gottlieb, R.A., et al. (2010b). Juvenile exposure to anthracyclines impairs cardiac progenitor cell function and vascularization resulting in greater susceptibility to stress-induced myocardial injury in adult mice. Circulation *121*, 675–683.

Huynh, K.K., Eskelinen, E.-L., Scott, C.C., Malevanets, A., Saftig, P., and Grinstein, S. (2007). LAMP proteins are required for fusion of lysosomes with phagosomes. Embo J. *26*, 313–324.

Irie, H., Krukenkamp, I.B., Brinkmann, J.F.F., Gaudette, G.R., Saltman, A.E., Jou, W., Glatz, J.F.C., Abumrad, N.A., and Ibrahimi, A. (2003). Myocardial recovery from ischemia is impaired in CD36-null mice and restored by myocyte CD36 expression or medium-chain fatty acids. Proc. Natl. Acad. Sci. U.S.a. *100*, 6819–6824.

Jin, S.M., Lazarou, M., Wang, C., Kane, L.A., Narendra, D.P., and Youle, R.J. (2010). Mitochondrial membrane potential regulates PINK1 import and proteolytic destabilization by PARL. The Journal of Cell Biology *191*, 933–942.

Kabeya, Y., Mizushima, N., Ueno, T., Yamamoto, A., Kirisako, T., Noda, T.,

Kominami, E., Ohsumi, Y., and Yoshimori, T. (2000). LC3, a mammalian homologue of yeast Apg8p, is localized in autophagosome membranes after processing. Embo J. *19*, 5720–5728.

Kabeya, Y., Mizushima, N., Yamamoto, A., Oshitani-Okamoto, S., Ohsumi, Y., and Yoshimori, T. (2004). LC3, GABARAP and GATE16 localize to autophagosomal membrane depending on form-II formation. J Cell Sci *117*, 2805–2812.

Kanamori, H., Takemura, G., Goto, K., Maruyama, R., Ono, K., Nagao, K., Tsujimoto, A., Ogino, A., Takeyama, T., Kawaguchi, T., et al. (2011). Autophagy limits acute myocardial infarction induced by permanent coronary artery occlusion. Am J Physiol Heart Circ Physiol *300*, H2261–H2271.

Kang, R., Zeh, H.J., Lotze, M.T., and Tang, D. (2011). The Beclin 1 network regulates autophagy and apoptosis. Cell Death Differ *18*, 571–580.

Kim, I., Rodriguez-Enriquez, S., and Lemasters, J.J. (2007). Selective degradation of mitochondria by mitophagy. Arch Biochem Biophys *462*, 245–253.

Kim, K.-Y., Stevens, M.V., Akter, M.H., Rusk, S.E., Huang, R.J., Cohen, A., Noguchi, A., Springer, D., Bocharov, A.V., Eggerman, T.L., et al. (2011). Parkin is a lipid-responsive regulator of fat uptake in mice and mutant human cells. J. Clin. Invest. *121*, 3701–3712.

Kim, Y., Park, J., Kim, S., Song, S., Kwon, S.-K., Lee, S.-H., Kitada, T., Kim, J.-M., and Chung, J. (2008). PINK1 controls mitochondrial localization of Parkin through direct phosphorylation. Biochem Biophys Res Commun *377*, 975–980.

Kirkin, V., Lamark, T., Sou, Y.-S., Bjørkøy, G., Nunn, J.L., Bruun, J.-A., Shvets, E., McEwan, D.G., Clausen, T.H., Wild, P., et al. (2009). A role for NBR1 in autophagosomal degradation of ubiquitinated substrates. Mol Cell *33*, 505–516.

Kitada, T., Asakawa, S., Hattori, N., Matsumine, H., Yamamura, Y., Minoshima, S., Yokochi, M., Mizuno, Y., and Shimizu, N. (1998). Mutations in the parkin gene cause autosomal recessive juvenile parkinsonism. Nature *392*, 605–608.

Knodler, L.A., and Celli, J. (2011). Eating the strangers within: host control of intracellular bacteria via xenophagy. Cell. Microbiol. *13*, 1319–1327.

Komatsu, M., and Ichimura, Y. (2010). Selective autophagy regulates various cellular functions. Genes Cells *15*, 923–933.

Kubli, D.A., and Gustafsson, A.B. (2012). Mitochondria and mitophagy: the yin and yang of cell death control. Circulation Research *111*, 1208–1221.

Kubli, D.A., Quinsay, M.N., Huang, C., Lee, Y., and Gustafsson, A.B. (2008).

Bnip3 functions as a mitochondrial sensor of oxidative stress during myocardial ischemia and reperfusion. Am J Physiol Heart Circ Physiol *295*, H2025–H2031.

Kubli, D.A., Zhang, X., Lee, Y., Hanna, R.A., Quinsay, M.N., Nguyen, C.K., Jimenez, R., Petrosyan, S., Murphy, A.N., and Gustafsson, A.B. (2013). Parkin Protein Deficiency Exacerbates Cardiac Injury and Reduces Survival following Myocardial Infarction. J Biol Chem *288*, 915–926.

Kuwana, T., Mackey, M.R., Perkins, G., Ellisman, M.H., Latterich, M., Schneiter, R., Green, D.R., and Newmeyer, D.D. (2002). Bid, Bax, and lipids cooperate to form supramolecular openings in the outer mitochondrial membrane. Cell *111*, 331–342.

Lee, J.-Y., Nagano, Y., Taylor, J.P., Lim, K.L., and Yao, T.-P. (2010). Disease-causing mutations in parkin impair mitochondrial ubiquitination, aggregation, and HDAC6-dependent mitophagy. The Journal of Cell Biology *189*, 671–679.

Lee, Y., Lee, H.-Y., Hanna, R.A., and Gustafsson, A.B. (2011). Mitochondrial autophagy by Bnip3 involves Drp1-mediated mitochondrial fission and recruitment of Parkin in cardiac myocytes. Am J Physiol Heart Circ Physiol *301*, H1924–H1931.

Lesnefsky, E.J., Moghaddas, S., Tandler, B., Kerner, J., and Hoppel, C.L. (2001). Mitochondrial dysfunction in cardiac disease: ischemia--reperfusion, aging, and heart failure. Journal of Molecular and Cellular Cardiology *33*, 1065–1089.

Liu, Y., Fiskum, G., and Schubert, D. (2002). Generation of reactive oxygen species by the mitochondrial electron transport chain. J Neurochem *80*, 780–787.

Maillet, M., van Berlo, J.H., and Molkentin, J.D. (2013). Molecular basis of physiological heart growth: fundamental concepts and new players. Nat. Rev. Mol. Cell Biol. *14*, 38–48.

Matsuda, N., Sato, S., Shiba, K., Okatsu, K., Saisho, K., Gautier, C.A., Sou, Y.-S., Saiki, S., Kawajiri, S., Sato, F., et al. (2010). PINK1 stabilized by mitochondrial depolarization recruits Parkin to damaged mitochondria and activates latent Parkin for mitophagy. The Journal of Cell Biology *189*, 211–221.

Matsui, Y., Takagi, H., Qu, X., Abdellatif, M., Sakoda, H., Asano, T., Levine, B., and Sadoshima, J. (2007). Distinct roles of autophagy in the heart during ischemia and reperfusion: roles of AMP-activated protein kinase and Beclin 1 in mediating autophagy. Circulation Research *100*, 914–922.

Mizushima, N., Noda, T., and Ohsumi, Y. (1999). Apg16p is required for the function of the Apg12p-Apg5p conjugate in the yeast autophagy pathway. Embo J. *18*, 3888–3896.

Mizushima, N., Levine, B., Cuervo, A.M., and Klionsky, D.J. (2008). Autophagy fights disease through cellular self-digestion. Nature *451*, 1069–1075.

Nakai, A., Yamaguchi, O., Takeda, T., Higuchi, Y., Hikoso, S., Taniike, M., Omiya, S., Mizote, I., Matsumura, Y., Asahi, M., et al. (2007). The role of autophagy in cardiomyocytes in the basal state and in response to hemodynamic stress. Nat Med *13*, 619–624.

Narendra, D.P., Jin, S.M., Tanaka, A., Suen, D.-F., Gautier, C.A., Shen, J., Cookson, M.R., and Youle, R.J. (2010a). PINK1 is selectively stabilized on impaired mitochondria to activate Parkin. PLoS Biol. *8*, e1000298.

Narendra, D., Kane, L.A., Hauser, D.N., Fearnley, I.M., and Youle, R.J. (2010b). p62/SQSTM1 is required for Parkin-induced mitochondrial clustering but not mitophagy; VDAC1 is dispensable for both. Autophagy *6*, 1090–1106.

Narendra, D., Tanaka, A., Suen, D.-F., and Youle, R.J. (2008). Parkin is recruited selectively to impaired mitochondria and promotes their autophagy. The Journal of Cell Biology *183*, 795–803.

Novak, I., Kirkin, V., McEwan, D.G., Zhang, J., Wild, P., Rozenknop, A., Rogov, V., Löhr, F., Popovic, D., Occhipinti, A., et al. (2010). Nix is a selective autophagy receptor for mitochondrial clearance. EMBO Rep. *11*, 45–51.

Okamoto, K., Kondo-Okamoto, N., and Ohsumi, Y. (2009). Mitochondria-Anchored Receptor Atg32 Mediates Degradation of Mitochondria via Selective Autophagy. Developmental Cell *17*, 87–97.

Okatsu, K., Iemura, S.-I., Koyano, F., Go, E., Kimura, M., Natsume, T., Tanaka, K., and Matsuda, N. (2012). Mitochondrial hexokinase HKI is a novel substrate of the Parkin ubiquitin ligase. Biochem Biophys Res Commun *428*, 197–202.

Ong, S.-B., Subrayan, S., Lim, S.Y., Yellon, D.M., Davidson, S.M., and Hausenloy, D.J. (2010). Inhibiting mitochondrial fission protects the heart against ischemia/reperfusion injury. Circulation *121*, 2012–2022.

Pankiv, S., Clausen, T.H., Lamark, T., Brech, A., Bruun, J.A., Outzen, H., Øvervatn, A., Bjørkøy, G., and Johansen, T. (2007). p62/SQSTM1 binds directly to Atg8/LC3 to facilitate degradation of ubiquitinated protein aggregates by autophagy. J Biol Chem *282*, 24131–24145.

Papanicolaou, K.N., Khairallah, R.J., Ngoh, G.A., Chikando, A., Luptak, I., O'Shea, K.M., Riley, D.D., Lugus, J.J., Colucci, W.S., Lederer, W.J., et al. (2011). Mitofusin-2 Maintains Mitochondrial Structure and Contributes to Stress-Induced Permeability Transition in Cardiac Myocytes. Molecular and Cellular Biology *31*, 1309.

Park, J., Lee, S.B., Lee, S., Kim, Y., Song, S., Kim, S., Bae, E., Kim, J., Shong, M., Kim, J.-M., et al. (2006). Mitochondrial dysfunction in Drosophila PINK1 mutants is complemented by parkin. Nature *441*, 1157–1161.

Parra, V., Eisner, V., Chiong, M., Criollo, A., Moraga, F., Garcia, A., Härtel, S., Jaimovich, E., Zorzano, A., Hidalgo, C., et al. (2008). Changes in mitochondrial dynamics during ceramide-induced cardiomyocyte early apoptosis. Cardiovascular Research *77*, 387–397.

Periquet, M., Latouche, M., Lohmann, E., Rawal, N., De Michele, G., Ricard, S., Teive, H., Fraix, V., Vidailhet, M., and Nicholl, D. (2003). Parkin mutations are frequent in patients with isolated early-onset parkinsonism. Brain *126*, 1271–1278.

Petrucelli, L., O'Farrell, C., Lockhart, P.J., Baptista, M., Kehoe, K., Vink, L., Choi, P., Wolozin, B., Farrer, M., Hardy, J., et al. (2002). Parkin protects against the toxicity associated with mutant alpha-synuclein: proteasome dysfunction selectively affects catecholaminergic neurons. Neuron *36*, 1007–1019.

Quinsay, M.N., Lee, Y., Rikka, S., Sayen, M.R., Molkentin, J.D., Gottlieb, R.A., and Gustafsson, A.B. (2010a). Bnip3 mediates permeabilization of mitochondria and release of cytochrome c via a novel mechanism. Journal of Molecular and Cellular Cardiology *48*, 1146–1156.

Quinsay, M.N., Thomas, R.L., Lee, Y., and Gustafsson, A.B. (2010b). Bnip3-mediated mitochondrial autophagy is independent of the mitochondrial permeability transition pore. Autophagy *6*, 855–862.

Rambold, A.S., Kostelecky, B., Elia, N., and Lippincott-Schwartz, J. (2011). Tubular network formation protects mitochondria from autophagosomal degradation during nutrient starvation. Proceedings of the National Academy of Sciences *108*, 10190–10195.

Ray, K.K., and Cannon, C.P. (2005). The potential relevance of the multiple lipid-independent (pleiotropic) effects of statins in the management of acute coronary syndromes. J. Am. Coll. Cardiol. *46*, 1425–1433.

Regula, K.M., Ens, K., and Kirshenbaum, L.A. (2002). Inducible expression of BNIP3 provokes mitochondrial defects and hypoxia-mediated cell death of ventricular myocytes. Circulation Research *91*, 226–231.

Reimer, K.A., and Jennings, R.B. (1979). The“ wavefront phenomenon” of myocardial ischemic cell death. II. Transmural progression of necrosis within the framework of ischemic bed size (myocardium at risk) and collateral flow. Lab. Invest. *40*, 633.

Rikka, S., Quinsay, M.N., Thomas, R.L., Kubli, D.A., Zhang, X., Murphy, A.N., and Gustafsson, A.B. (2011). Bnip3 impairs mitochondrial bioenergetics and stimulates mitochondrial turnover. Cell Death Differ *18*, 721–731.

Sandebring, A., and Mínguez, A.C. (2012). Parkin-An E3 Ubiquitin Ligase with Multiple Substrates. J Alzheimers Dis Parkinsonism S *10*, 2161–0460.

Sandoval, H., Thiagarajan, P., Dasgupta, S.K., Schumacher, A., Prchal, J.T., Chen, M., and Wang, J. (2008). Essential role for Nix in autophagic maturation of erythroid cells. Nature *454*, 232–235.

Sayen, M.R., Gustafsson, A.B., Sussman, M.A., Molkentin, J.D., and Gottlieb, R.A. (2003). Calcineurin transgenic mice have mitochondrial dysfunction and elevated superoxide production. Am J Physiol, Cell Physiol *284*, C562–C570.

Schips, T.G., Wietelmann, A., Höhn, K., Schimanski, S., Walther, P., Braun, T., Wirth, T., and Maier, H.J. (2011). FoxO3 induces reversible cardiac atrophy and autophagy in a transgenic mouse model. Cardiovascular Research *91*, 587–597.

Schweers, R.L., Zhang, J., Randall, M.S., Loyd, M.R., Li, W., Dorsey, F.C., Kundu, M., Opferman, J.T., Cleveland, J.L., Miller, J.L., et al. (2007). NIX is required for programmed mitochondrial clearance during reticulocyte maturation. Proceedings of the National Academy of Sciences *104*, 19500–19505.

Seibenhener, M.L., Babu, J.R., Geetha, T., Wong, H.C., Krishna, N.R., and Wooten, M.W. (2004). Sequestosome 1/p62 is a polyubiquitin chain binding protein involved in ubiquitin proteasome degradation. Molecular and Cellular Biology *24*, 8055–8068.

Sha, D., Chin, L.-S., and Li, L. (2010). Phosphorylation of parkin by Parkinson disease-linked kinase PINK1 activates parkin E3 ligase function and NF-kappaB signaling. Human Molecular Genetics *19*, 352–363.

Shin, J.-H., Ko, H.S., Kang, H., Lee, Y., Lee, Y.-I., Pletinkova, O., Troconso, J.C., Dawson, V.L., and Dawson, T.M. (2011). PARIS (ZNF746) Repression of PGC-1α Contributes to Neurodegeneration in Parkinson's Disease. Cell *144*, 689–702.

Simon, H.U., Haj-Yehia, A., and Levi-Schaffer, F. (2000). Role of reactive oxygen species (ROS) in apoptosis induction. Apoptosis *5*, 415–418.

Smirnova, E., Griparic, L., Shurland, D.L., and van der Bliek, A.M. (2001). Dynamin-related protein Drp1 is required for mitochondrial division in mammalian cells. Mol. Biol. Cell *12*, 2245–2256.

St-Pierre, J., Buckingham, J.A., Roebuck, S.J., and Brand, M.D. (2002). Topology of superoxide production from different sites in the mitochondrial electron transport chain. J Biol Chem *277*, 44784–44790.

Sterky, F.H., Lee, S., Wibom, R., Olson, L., and Larsson, N.-G. (2011). Impaired mitochondrial transport and Parkin-independent degeneration of respiratory chain-deficient dopamine neurons in vivo. Proceedings of the National Academy of Sciences *108*, 12937–12942.

Suen, D.-F., Narendra, D.P., Tanaka, A., Manfredi, G., and Youle, R.J. (2010). Parkin overexpression selects against a deleterious mtDNA mutation in heteroplasmic cybrid cells. Proceedings of the National Academy of Sciences *107*, 11835–11840.

Takagawa, J., Zhang, Y., Wong, M.L., Sievers, R.E., Kapasi, N.K., Wang, Y., Yeghiazarians, Y., Lee, R.J., Grossman, W., and Springer, M.L. (2007). Myocardial infarct size measurement in the mouse chronic infarction model: comparison of area- and length-based approaches. J. Appl. Physiol. *102*, 2104–2111.

Tanaka, A., Cleland, M.M., Xu, S., Narendra, D.P., Suen, D.-F., Karbowski, M., and Youle, R.J. (2010). Proteasome and p97 mediate mitophagy and degradation of mitofusins induced by Parkin. The Journal of Cell Biology *191*, 1367–1380.

Tang, D., Kang, R., Livesey, K.M., Kroemer, G., Billiar, T.R., Van Houten, B., Zeh, H.J., and Lotze, M.T. (2011). High-mobility group box 1 is essential for mitochondrial quality control. Cell Metab. *13*, 701–711.

Tannous, P., Zhu, H., Johnstone, J.L., Shelton, J.M., Rajasekaran, N.S., Benjamin, I.J., Nguyen, L., Gerard, R.D., Levine, B., Rothermel, B.A., et al. (2008). Autophagy is an adaptive response in desmin-related cardiomyopathy. Proceedings of the National Academy of Sciences *105*, 9745–9750.

Tompkins, A.J., Burwell, L.S., Digerness, S.B., Zaragoza, C., Holman, W.L., and Brookes, P.S. (2006). Mitochondrial dysfunction in cardiac ischemia-reperfusion injury: ROS from complex I, without inhibition. Biochimica Et Biophysica Acta *1762*, 223–231.

Tsai, Y.C., Fishman, P.S., Thakor, N.V., and Oyler, G.A. (2003). Parkin facilitates the elimination of expanded polyglutamine proteins and leads to preservation of proteasome function. J Biol Chem *278*, 22044–22055.

Twig, G., Elorza, A., Molina, A.J.A., Mohamed, H., Wikstrom, J.D., Walzer, G., Stiles, L., Haigh, S.E., Katz, S., Las, G., et al. (2008). Fission and selective fusion govern mitochondrial segregation and elimination by autophagy. Embo J. *27*, 433–446.

Wakabayashi, J., Zhang, Z., Wakabayashi, N., Tamura, Y., Fukaya, M., Kensler, T.W., Iijima, M., and Sesaki, H. (2009). The dynamin-related GTPase Drp1 is

required for embryonic and brain development in mice. The Journal of Cell Biology *186*, 805–816.

Wang, H., Song, P., Du, L., Tian, W., Yue, W., Liu, M., Li, D., Wang, B., Zhu, Y., Cao, C., et al. (2011a). Parkin ubiquitinates Drp1 for proteasome-dependent degradation: implication of dysregulated mitochondrial dynamics in Parkinson disease. J Biol Chem *286*, 11649–11658.

Wang, X., Winter, D., Ashrafi, G., Schlehe, J., Wong, Y.L., Selkoe, D., Rice, S., Steen, J., LaVoie, M.J., and Schwarz, T.L. (2011b). PINK1 and Parkin Target Miro for Phosphorylation and Degradation to Arrest Mitochondrial Motility. Cell *147*, 893–906.

Waterham, H.R., Koster, J., van Roermund, C.W.T., Mooyer, P.A.W., Wanders, R.J.A., and Leonard, J.V. (2007). A lethal defect of mitochondrial and peroxisomal fission. N. Engl. J. Med. *356*, 1736–1741.

Whitworth, A.J., Theodore, D.A., Greene, J.C., Benes, H., Wes, P.D., and Pallanck, L.J. (2005). Increased glutathione S-transferase activity rescues dopaminergic neuron loss in a Drosophila model of Parkinson's disease. Proc. Natl. Acad. Sci. U.S.a. *102*, 8024–8029.

Wu, J.J., Quijano, C., Chen, E., Liu, H., Cao, L., Fergusson, M.M., Rovira, I.I., Gutkind, S., Daniels, M.P., Komatsu, M., et al. (2009). Mitochondrial dysfunction and oxidative stress mediate the physiological impairment induced by the disruption of autophagy. Aging (Albany NY) *1*, 425–437.

Xie, Z., Lau, K., Eby, B., Lozano, P., He, C., Pennington, B., Li, H., Rathi, S., Dong, Y., Tian, R., et al. (2011). Improvement of cardiac functions by chronic metformin treatment is associated with enhanced cardiac autophagy in diabetic OVE26 mice. Diabetes *60*, 1770–1778.

Xiong, H., Wang, D., Chen, L., Choo, Y.S., Ma, H., Tang, C., Xia, K., Jiang, W., Ronai, Z., Zhuang, X., et al. (2009). Parkin, PINK1, and DJ-1 form a ubiquitin E3 ligase complex promoting unfolded protein degradation. J. Clin. Invest. *119*, 650–660.

Yan, L., Vatner, D.E., Kim, S.-J., Ge, H., Masurekar, M., Massover, W.H., Yang, G., Matsui, Y., Sadoshima, J., and Vatner, S.F. (2005). Autophagy in chronically ischemic myocardium. Proc. Natl. Acad. Sci. U.S.a. *102*, 13807–13812.

Yang, Y., Gehrke, S., Haque, M.E., Imai, Y., Kosek, J., Yang, L., Beal, M.F., Nishimura, I., Wakamatsu, K., Ito, S., et al. (2005). Inactivation of Drosophila DJ-1 leads to impairments of oxidative stress response and phosphatidylinositol 3-kinase/Akt signaling. Proc. Natl. Acad. Sci. U.S.a. *102*, 13670–13675.

Yitzhaki, S., Huang, C., Liu, W., Lee, Y., Gustafsson, A.B., Mentzer, R.M., and Gottlieb, R.A. (2009). Autophagy is required for preconditioning by the adenosine A1 receptor-selective agonist CCPA. Basic Res. Cardiol. *104*, 157–167.

Yoon, Y., Krueger, E.W., Oswald, B.J., and McNiven, M.A. (2003). The mitochondrial protein hFis1 regulates mitochondrial fission in mammalian cells through an interaction with the dynamin-like protein DLP1. Molecular and Cellular Biology *23*, 5409–5420.

Zhang, H., Bosch-Marce, M., Shimoda, L.A., Tan, Y.S., Baek, J.H., Wesley, J.B., Gonzalez, F.J., and Semenza, G.L. (2008). Mitochondrial autophagy is an HIF-1-dependent adaptive metabolic response to hypoxia. J Biol Chem *283*, 10892–10903.

Zhu, H., Tannous, P., Johnstone, J.L., Kong, Y., Shelton, J.M., Richardson, J.A., Le, V., Levine, B., Rothermel, B.A., and Hill, J.A. (2007). Cardiac autophagy is a maladaptive response to hemodynamic stress. J. Clin. Invest. *117*, 1782–1793.

Zoratti, M., and Szabò, I. (1995). The mitochondrial permeability transition. Biochimica Et Biophysica Acta *1241*, 139–176.